AD-A072 171 BRUNSWICK CORP DELAND FL TECHNETICS DIV F/G 21/5
DEVELOPMENT OF IMPROVED ABRADABLE COMPRESSOR GAS PATH SEAL.(U)
JUL 78 W P JARVI, A R ERICKSON F33615-76-C-5302
UNCLASSIFIED ER-382 AFML-TR-78-101 NL

1 OF 2
AD A072171

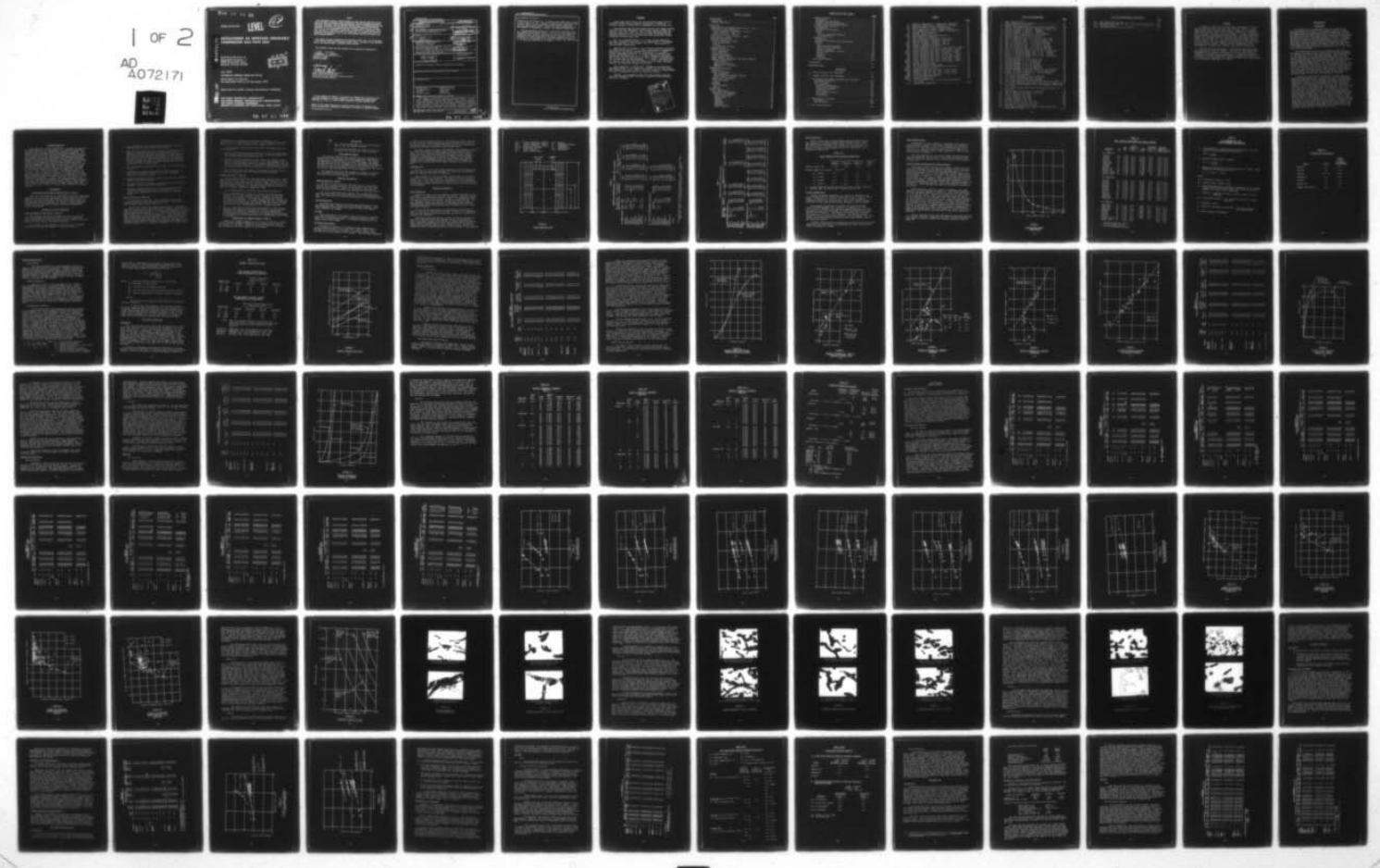

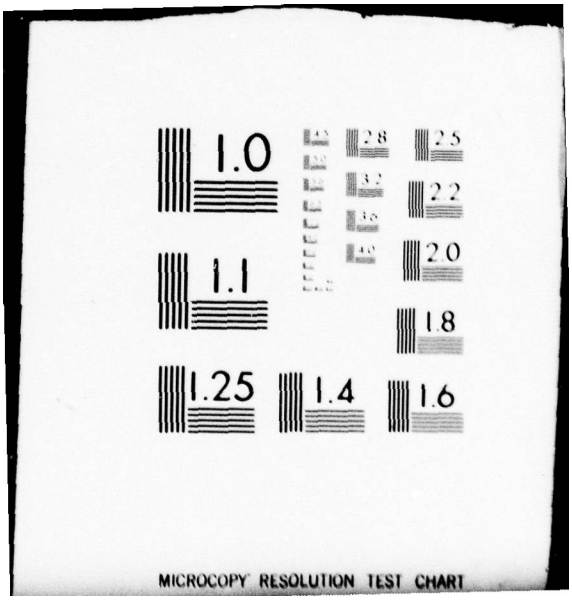
1.0
1.1
1.25
1.4
1.6
2.8
2.5
2.2
2.0
1.8
MICROCOPY RESOLUTION TEST CHART

AFML-TR-78-101

LEVEL

DEVELOPMENT OF IMPROVED ABRADABLE COMPRESSOR GAS PATH SEAL

Technetics Division of
Brunswick Corporation
2000 Brunswick Lane
DeLand, Florida 32720

July 1978

TECHNICAL REPORT AFML-TR-78-101

Final Report for Period
20 September 1976 to 15 December 1977

Approved for public release; distribution unlimited.

AIR FORCE MATERIALS LABORATORY
AIR FORCE WRIGHT AERONAUTICAL LABORATORIES
AIR FORCE SYSTEMS COMMAND
WRIGHT-PATTERSON AIR FORCE BASE, OHIO 45433

NOTICE

When Government drawings, specifications, or other data are used for any purpose other than in connection with a definitely related Government procurement operation, the United States Government thereby incurs no responsibility nor any obligation whatsoever; and the fact that the government may have formulated, furnished, or in any way supplied the said drawings, specifications, or other data, is not to be regarded by implication or otherwise as in any manner licensing the holder or any other person or corporation, or conveying any rights or permission to manufacture, use, or sell any patented invention that may in any way be related thereto.

This report has been reviewed by the Information Office (OI) and is releasable to the National Technical Information Service (NTIS). At NTIS, it will be available to the general public, including foreign nations.

This technical report has been reviewed and is approved for publication.

William T. O'Hara

WILLIAM T. O'HARA
PROJECT ENGINEER

FOR THE COMMANDER

Harold A. Lipsitt

HARRY A. LIPSITT, ACTING CHIEF
Processing and High Temperature Materials Branch
Metals and Ceramics Division

"If your address has changed, if you wish to be removed from our mailing list, or if the addressee is no longer employed by your organization please notify AFML/LLM ,W-PAFB, OH 45433 to help us maintain a current mailing list".

Copies of this report should not be returned unless return is required by security considerations, contractual obligations, or notice on a specific document.

AIR FORCE/56780/12 July 1979 — 250

UNCLASSIFIED

SECURITY CLASSIFICATION OF THIS PAGE (When Data Entered)

(19) REPORT DOCUMENTATION PAGE		READ INSTRUCTIONS BEFORE COMPLETING FORM
(18) 1. REPORT NUMBER: AFML-TR-78-181	2. GOVT ACCESSION NO.	3. RECIPIENT'S CATALOG NUMBER
(6) 4. TITLE (and Subtitle): DEVELOPMENT OF IMPROVED ABRADABLE COMPRESSOR GAS PATH SEAL		(9) 5. TYPE OF REPORT & PERIOD COVERED: Final Report 20 Sep 76 - 19 May 78
		(14) 6. PERFORMING ORG. REPORT NUMBER: ER-382
(10) 7. AUTHOR(s): W. P. Jarvi, A. R. Erickson		(15) 8. CONTRACT OR GRANT NUMBER(s): F33615-76-C-5302
9. PERFORMING ORGANIZATION NAME AND ADDRESS: Brunswick Corporation, Technetics Division, 2000 Brunswick Lane, DeLand, Fla 32720		(16) 10. PROGRAM ELEMENT, PROJECT, TASK AREA & WORK UNIT NUMBERS: 7312/01 38, 62102F
11. CONTROLLING OFFICE NAME AND ADDRESS: Air Force Materials Laboratory (AFML/LLM), Air Force Wright-Aeronautical Laboratories, Wrignt-Patterson AFB, OH 45433		(11) 12. REPORT DATE: July 1978; 13. NUMBER OF PAGES: 129
14. MONITORING AGENCY NAME & ADDRESS (if different from Controlling Office): (12) 140p.		15. SECURITY CLASS. (of this report): UNCLASSIFIED; 15a. DECLASSIFICATION/DOWNGRADING SCHEDULE

16. DISTRIBUTION STATEMENT (of this Report)

Approved for public release; distribution unlimited.

17. DISTRIBUTION STATEMENT (of the abstract entered in Block 20, if different from Report)

18. SUPPLEMENTARY NOTES

19. KEY WORDS (Continue on reverse side if necessary and identify by block number)

Abradability	FeNiCrAlY Alloys
Abradable Seals	Fiber Metal
Erosion	Oxidation
FeCrAlY Alloys	Rub Testing

20. ABSTRACT (Continue on reverse side if necessary and identify by block number)

A number of fiber metal systems were evaluated by rig testing in comparison with the base line material, FM-521 - a 19% dense, Haynes 188, 8 micron fiber metal - which is the standard production material used for the highest temperature compressor blade tip seals in the P & WA F-100 engine. A range of densities and strengths of alternative materials were evaluated including Haynes 188, FeCrAlY, NiCrAlY, and FeNiCrAlY employing fiber

DD FORM 1 JAN 73 1473 EDITION OF 1 NOV 65 IS OBSOLETE

UNCLASSIFIED

SECURITY CLASSIFICATION OF THIS PAGE (When Data Entered)

411 314

Continuation of Item 20.

diameters in the range of 8 - 23 microns with fiber aspect ratios in the range of 45 - 80. Rig tests employed were high speed rub testing, cyclic static oxidation, cyclic dynamic oxidation, and hot particulate erosion. These data were supplemented with measurements of mechanical, thermal, and chemical properties.

The best material tested was a 20.5% dense FeNiCrAlY fiber metal employing 17 micron fibers. This had at least equivalent abradability and improved oxidation and erosion resistance in comparison with the base line material. In addition to being a candidate for higher temperature advanced compressor seals, it is expected to be suitable for turbine abradable seal applications up to operating temperatures of 1600°F.

FOREWARD

This Final Report covers all work performed under Contract F33615-76-C-5302 by the Brunswick Corporation, Technetics Division, DeLand, Florida from 20 September 1976 to 19 May 1978.

This contract was initiated under Project 7312 "Metal Surface Deterioration and Protection", Task 731201, "Metal Surface Protection", Work Unit 73120138. The work was performed under the technical direction of Mr. William T. O'Hara of the Metals and Ceramics Division of the Air Force Materials Laboratory, Wright-Patterson Air Force Base, Ohio.

Mr. A. R. Erickson and Mr. W. P. Jarvi of the Technetics Division, Brunswick Corporation, were responsible for the management and execution of the program. Mr. W. P. Jarvi served as the principal investigator.

Appreciation is extended to the following Brunswick personnel for their participation: R. T. Frank, Group Leader of Mechanical Engineering, for overall program contributions; J. C. Nablo, Product Development Engineer, for assistance in mechanical properties determination; Dr. R. J. Donahue, Manager of Materials Evaluation, for SEM analysis; A. L. Geary, Materials Engineering, for contributions in data analysis; R. S. Cervero, Lab Technician, for rig test work and metallography; J. C. Viola, Lab Technician, for overall test work; and B. T. Dodge and W. B. Kuhn, Lab Technicians, for mechanical properties testing.

The guidance of P. Shilke and C. McComas in the Materials Technology Groups of the Commercial Products Division and Government Products Division of Pratt & Whitney Aircraft, is acknowledged for their consultation during the technical program.

Finally, the successful results of this program would not have been possible without the prior invention of the FeNiCrAlY alloy by C. Panzera.

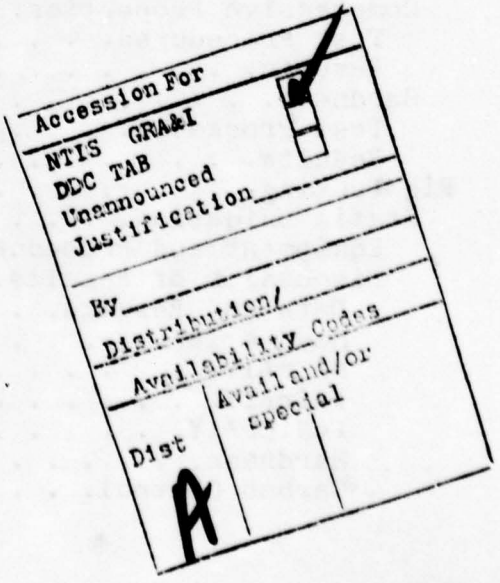

TABLE OF CONTENTS

Page

INTRODUCTION. 1
Background. 1
Program Objective. 2

DISCUSSION. 2
Consultation with Engine Manufacturer - Task I. 2
Selection of Seal Materials. 3
Initial Materials Selection - Task II. 3
First Iteration - Task III. 3
Second Iteration - Task IV. 4
Preparation of Sample Coupons - Task V. 4
Environmental Impact. 5
Material Preparation. 5
Baseline Material, FM-521. 5
Fiber Preparation. 5
Felting. 5
Sintering and Rolling. 5
Sampling Plan. 6
Material Properties. 6
Alloy Chemistry. 6
Alloy Densities. 10
Thermal Expansivity. 10
Fiber Aspect Ratio. 11
Sheet Density Uniformity and Fiber Diameter. 11
Thermal Conductivity. 16
Introduction. 16
Sample Preparation. 16
Experimental Procedure. 16
Results. 17
Mechanical Properties. 17
Background. 17
Tensile Properties. 20
Test Procedure. 20
Room Temperature Tensile Results. 20
1600°F Tensile Results. 22
Compressive Properties. 30
Test Procedures. 30
Results. 31
Hardness. 31
Test Procedure. 31
Results. 34
Rig Testing. 39
Static Oxidation. 39
Equipment and Procedure. 39
Discussion of Results. 39
Data and Results. 39
Haynes 188. 60
NiCrAlY. 60
FeCrAlY. 64
FeNiCrAlY. 64
Hardness. 68
Carbon Control. 68

TABLE OF CONTENTS (CONT.)

Page

Dynamic Oxidation. 71
Objectives. 71
Equipment and Procedures. 71
Oxidation and Erosion Results. 72
Thermal Shock and Fatigue Results. 72
Hot Particulate Erosion. 72
Introduction. 72
Equipment and Procedure. 76
Results. 77
Data. 77
Multiple Regression Analyses. 77
Alloy Evaluation. 81
Abradability. 81
Introduction. 81
Equipment, Procedures and Calculations. 82
Results. 83
Data. 83
Data Evaluation Methods. 83
Effect of Test Conditions. 97
Material Transfer. 98
Multiple Regression Analyses. 98
Haynes 188. 100
NiCrAlY. 100
FeCrAlY. 100
FeNiCrAlY. 102
Seal Specifications. 102

CONCLUSIONS. 104

RECOMMENDATIONS. 104

APPENDICES

A. Static Oxidation Test Equipment. 105

B. Dynamic Oxidation Test Equipment. 108

C. Hot Particulate Erosion Equipment and Procedure. 111
Equipment Description. 111
Test Conditions. 111
Test Procedure. 112
Specimen Preparation. 112
Particulate Preparation. 112
Combustion Apparatus. 114
Erosion Test. 114
Test Sample Evaluation. 114
Reiteration. 114
Calculations. 114

D. High Speed Rub Testing. 120
Equipment. 120
Test Procedure. 120

E. Seal Specifications. 126

TABLES

		Page
I.	Chemical Compositions - Haynes 188 & NiCrAlY.	8
II.	Chemical Compositions - FeNiCrAlY & FeCrAlY.	9
III.	Alloy Densities & Thermal Expansivity.	10
IV.	Sheet Density Uniformity & Fiber Diameter.	13
V.	Air Permeability & Fiber Diameter Calculations.	14
VI.	Average Fiber Diameters.	15
VII.	Thermal Conductivity Data.	18
VIII.	Room Temperature Tensile Properties.	21
IX.	1600°F Tensile Properties.	28
X.	Room Temperature Compressive Properties.	32
XI.	Tensile Strength & Hardness, Task II.	35
XII.	Tensile Strength & Hardness, Task III.	36
XIII.	Tensile Strength & Hardness, Task IV.	37
XIV.	Hardness Regression Analysis.	38
XV.	Static Oxidation Test Data, 4 Hrs Exposure, 1600°F.	40
XVI.	Static Oxidation Test Data, 68 Hrs Exp., 1600°F.	41
XVII.	Static Oxidation Test Data, 308 Hrs Exp., 1600°F.	42
XVIII.	Static Oxidation Test Data, 4 Hrs Exp., 1400°F.	43
XIX.	Static Oxidation Test Data, 68 Hrs Exp., 1400°F.	44
XX.	Static Oxidation Test Data, 308 Hrs Exp., 1400°F.	45
XXI.	Static Oxidation Test Data, 4 Hrs Exp., 1200°F.	46
XXII.	Static Oxidation Test Data, 68 Hrs Exp., 1200°F.	47
XXIII.	Static Oxidation Test Data, 308 Hrs Exp., 1200°F.	48
XXIV.	Dynamic Oxidation Data.	73
XXV.	Hot Particulate Erosion Data.	78
XXVI.	Hot Particulate Erosion Regression Analysis.	79
XXVII.	Calculated Erosion Rates.	80
XXVIII.	Waspaloy Blade Rub Test Data - 0.010 in/sec.	84
XXIX.	Waspaloy Blade Rub Test Data - 0.001 in/sec.	85
XXX.	Titanium Blade Rub Test Data - 0.001 in/sec.	86
XXXI.	Rub Test Regression Analyses.	99
XXXII.	Calculated Rub Energies.	101
XXXIII.	Product Properties.	103
C-I.	Flow Conditions for M = 0.35 and Exit Pressure 14.7 psia.	113
C-II.	Actual Flow Conditions.	113

LIST OF ILLUSTRATIONS

		Page
1.	Sheet Sampling Plan.	7
2.	Fiber Aspect Ratio Correlation.	12
3.	Thermal Conductivity Data.	19
4.	Typical Room Temperature Tensile Stress vs Strain.	23
5.	Tensile Strength vs Density - NiCrAlY & Haynes 188.	24
6.	Tensile Strength vs Density - FeCrAlY.	25
7.	Tensile Strength vs Density - FeNiCrAlY.	26
8.	Ultimate Tensile Strength vs Elastic Modulus.	27
9.	Typical 1600°F Tensile Stress vs Strain.	29
10.	Typical Compressive Stress vs Strain.	33
11.	Task II Oxidation Data - 7.7 Micron Haynes 188.	49
12.	Task II Oxidation Data - 20.8 Micron Haynes 188.	50
13.	Task II Oxidation Data - 11.1 Micron NiCrAlY.	51
14.	Task III Oxidation Data - 16.5 Micron FeCrAlY.	52
15.	Task III Oxidation Data - 12.6 Micron FeCrAlY.	53
16.	Task II Oxidation Data - 16.6 Micron FeNiCrAlY.	54
17.	Task III Oxidation Data - 16.6 Micron FeNiCrAlY.	55
18.	Effect of Oxidation Weight Gain on UTS - Haynes 188.	56
19.	Effect of Oxidation Weight Gain on UTS - NiCrAlY.	57
20.	Effect of Oxidation Weight Gain on UTS - FeCrAlY.	58
21.	Effect of Oxidation Weight Gain on UTS - FeNiCrAlY.	59
22.	Estimated Oxidation Lives.	61
23.	Photomicrographs of 7.7 µm Haynes 188.	62
24.	Photomicrographs of 20.8µ Haynes 188.	63
25.	Photomicrographs of 11.1 µm NiCrAlY.	65
26.	Photomicrographs of 16.5 µm FeCrAlY.	66
27.	Photomicrographs of 12.6 µm FeCrAlY.	67
28.	Photomicrographs of 16.6 µm FeNiCrAlY.	69
29.	Photomicrographs of Surface Fibers 16.6 µm FeNiCrAlY.	70
30.	Dynamic vs Static Oxidation 7.7 Micron Haynes 188.	74
31.	Dynamic vs Static Oxidation 11.1 Micron NiCrAlY.	75
32.	FM-521 Rub Test Specimen.	87
33.	16.6 Micron FeNiCrAlY Rub Test Specimen.	88
34.	12.6 Micron FeCrAlY Rub Test Specimen.	89
35.	23.4 Micron FeCrAlY Rub Test Specimen	90
36.	FM-521 Rub Groove with Waspaloy Blade Tips (Good Rub).	91
37.	16.6 Micron FeNiCrAlY Rub Groove with Waspaloy Blade Tips.	92
38.	12.6 Micron FeCrAlY (Rub Groove) with Waspaloy Blade Tips (Good Rub).	93
39.	23.4 Micron FeCrAlY Rub Groove with Waspaloy Blade Tips (Bad Rub).	94
40.	Typical Blade Tip Surfaces - Good Rubs.	95
41.	Typical Blade Tip Surfaces - Bad Rubs.	96
A-1.	Static Oxidation Test Stand.	106
A-2.	Static Oxidation Test Rig.	107
B-1.	Dynamic Oxidation Test Rig.	109
B-2.	Dynamic Oxidation Test Rig.	110
C-1.	Hot Particulate Erosion Test Rig.	116
C-2.	Hot Particulate Erosion Test Rig.	117
C-3.	Schematic of Erosion Test Setup.	118
C-4.	Test Sample Configuration Dynamic Oxidation and Hot Particulate Erosion.	119

LIST OF ILLUSTRATIONS (CONTINUED)

		Page
D-1.	High Speed Rub Test Rig.	122
D-2.	Brunswick High Speed Rub Rig - 360° Rub Configuration. .	123
D-3.	Rub Test Sample.	124
D-4.	Calculation of Rub Groove Volume.	125

SUMMARY

A number of fiber metal systems were evaluated by rig testing in comparison with the base line material, FM-521 - a 19% dense Haynes 188, 8 micron fiber metal - which is the standard production material used for the highest temperature compressor blade tip seals in the P & WA F-100 engine. A range of densities and strengths of alternative materials were evaluated including Haynes 188, FeCrAlY, NiCrAlY, and FeNiCrAlY employing fiber diameters in the range of 8 - 23 microns with fiber aspect ratios in the range of 45 - 80. Rig tests employed were high speed rub testing, cyclic static oxidation, cyclic dynamic oxidation, and hot particulate erosion. These data were supplemented with measurements of mechanical, thermal, and chemical properties.

The best material tested was a 20.5% dense FeNiCrAlY fiber metal employing 17 micron fibers. This had at least equivalent abradability and improved oxidation and erosion resistance in comparison with the base line material. In addition to being a candidate for higher temperature advanced compressor seals, it is expected to be suitable for turbine abradable seal applications up to operating temperatures of 1600°F.

INTRODUCTION

Background

The objective of an abradable seal is to permit the engine designer to install a rub tolerant material so that the engine operating clearance can be minimized with attendant maximization of engine efficiency by minimizing gas leakage past blade tips and between engine stages while minimizing aerodynamic losses in the high velocity gas path. As demand increases for improved engine performance, the use of abradable seals applied to the stationary engine parts becomes important to permit complete sealing of blade tips and interstage labyrinth seal knife edges through the full 360° arc of rotation while minimizing or eliminating wear on the expensive rotating hardware.

The design and selection of an abradable seal for any particular position in a gas turbine engine always represents a compromise of conflicting requirements. Each position has its own specific set of problems depending upon operating speed, temperature, pressure, pressure drop, gas velocity, fluctuating pressure and mechanical loadings, thermal cycling, gas impingement angle, size and quantity of particulates present, and gas composition. The seal material must be designed to withstand the rigors of the environment for the life of the engine while still fulfilling its basic abradable seal function. The material must be weak enough to abrade away when contacted by a high speed rotating part without wearing the part while, at the same time, being strong enough to withstand high velocity gas and particulate erosion.

A blade tip seal will be subjected to higher gas velocities and pressure drops in dirtier air than an interstage labyrinth seal and will be designed stronger to withstand the more severe erosion. An interstage knife edge seal will be subjected to more heat and friction due to the continuous rubbing of the knife edge in contrast with the intermittent cutting action of the blade tip. Consequently, the knife edge type seal must be designed weaker to eliminate knife edge wear with the more severe rubs. Gas erosion problems are minimal with the cleaner air and the low pressure drops and gas velocities experienced in compressor interstage labyrinth seals. However, these seals can be severely eroded by their own rub debris if the debris is too large so that it cannot be blown out of the sealing area by the gases leaking through. This type of erosion has been experienced in compressors with powder metal seals when the particles have been larger than 25 microns and in fiber metal seals when coarse debris from a powder metal (either an abradable or an abrasive coating) upstream has blown into a fiber metal seal.

Program Objective

The objective of this program was to develop an improved abradable material for operation in an advanced compressor gas path seal for high compression ratio gas turbines. The material must have seal surface temperature capability up to 1250°F for long life in the higher compression ratio engines. The abradable seal should have improved characteristics in both static and dynamic oxidation, thermal shock resistance, erosion resistance, and abradability by Waspaloy and titanium blade tips in comparison with available compressor seals. The best compressor seal material available is FM-521, a 19% density FELTMETAL product made from 8 micron Haynes Alloy 188 fibers, which is the blade tip seal material installed in the highest temperature compressor stages (10, 11, 12, and 13) of the P & WA F100 engine. The FM-521 would be expected to fail in advanced compressors by high velocity gas and particulate erosion as a result of weakening of the fiber metal caused by long term exposure of the fine fibers to high temperature oxidation. It was, therefore, decided to use FM-521 as the base line material for comparison and to evaluate other fiber metal systems employing larger fiber diameters, more oxidation resistant alloys, stronger fiber metal, and lower fiber aspect ratios to resolve this problem for advanced engines.

DISCUSSION

Consultation with Engine Manufacturer - Task I

Prior to the initiation of theprogram, Materials Technology personnel of P & WA were consulted to insure that the test program was relevant to the requirements for abradable seals in advanced gas turbine engines. In addition, several consultation meetings were held during the course of the program to review the test data and to assure continued relevancy to engine development.

Selection of Seal Materials

Initial Materials Selection - Task II -

Two strength and density extremes of each of five (5) fiber metal materials were selected to test in comparison with two densities of the base line material, FM-521 (8 micron, Haynes 188 fiber metal, 19% nominal density).

As a result of the testing on this task, the following decisions were made with regard to further testing:

1. Poor abradability and unsatisfactory oxidation resistance ruled out the 21 micron Haynes 188 system.

2. High cost and lower oxidation resistance of the 11 micron NiCrAlY system relative to the coarser FeCrAlY and FeNiCrAlY systems eliminated the NiCrAlY system from further testing, although the abradability of this system was satisfactory. An additional reason for eliminating NiCrAlY is that this alloy is sensitive to hot corrosion in the presence of sulfur in turbine applications operating in the 1500 - 1600°f range.

3. Poor abradability eliminated the coarser 23 micron FeCrAlY system.

4. FeNiCrAlY and FeCrAlY fiber metal at fiber diameters less than 18 microns were selected as the best candidate systems for further testing.

5. Improved abradability can be achieved by reducing strength, density, and fiber diameter.

6. Improved erosion resistance can be achieved by increasing strength, density, and fiber diameter.

7. Improved oxidation resistance can be obtained by using increased fiber diameters and using MCrAlY alloys to obtain thin, adherent, protective coatings of aluminum oxide.

First Iteration - Task III

For the first iteration, three densities each of four candidate materials were selected to evaluate in the low tensile strength range of 600 - 1500 psi.

The two best abradable materials from Task II, FeNiCrAlY and FeCrAlY, in the 15 - 18 micron fiber diameter range were selected for additional testing. To replace the high cost 11 micron NiCrAlY system from Task II, a 11 - 15 micron FeCrAlY system was used in Task III to evaluate the effect of fiber diameter and fiber aspect ratio, L/D, on abradability. Previous unpublished work at Brunswick had shown that very long fibers (L/D ≈1500) resulted in fiber metal systems with very poor abradability in comparison with typical fiber metal systems having aspect ratios in the vicinity of 75. In order to determine if an additional

shortening of the fibers could improve abradability. An 11 - 15 micron FeCrAlY fiber having a L/D of 45 was prepared to compare with the 11 - 15 micron FeCrAlY fiber having a L/D of 78.

The following conclusions and decisions were made after the first iteration:

1. The 15 - 18 micron FeNiCrAlY system was clearly the best abradable material and was selected for one of the two systems to test in the second iteration, Task IV.

2. Although the three FeCrAlY systems tested had similar abradability, the high aspect ratio (L/D = 78), fine diameter (11 -15 micron) FeCrAlY system resulted in better abradability than the other two FeCrAlY systems. Consequently, this system was chosen as the second best fiber metal system to evaluate in Task IV.

3. Both systems chosen had superior oxidation and erosion resistance in comparison with the baseline material, FM-521.

Second Iteration - Task IV

For the second iteration, four densities each of the 15 -18μm FeNiCrAlY system and the 11 - 15 micron FeCrAlY system (L/D = 78) were tested in the higher tensile strength range of 1900 - 2500 psi. Two additional samples of the baseline major material, FM-521, at tensile strength extremes of 1360 and 1660 psi were also tested in Task IV to obtain additional comparative data.

The following major conclusions were made after Task IV:

1. The 15-18μm FeNiCrAlY system was clearly the best material relative to the other systems tested including the baseline material with regard to abradability, oxidation resistance, and erosion resistance. Its only disadvantage was a higher air permeability; however, air leakage through this porous material is still low and the pores get plugged with dirt during normal operation, so this disadvantage is not a significant one.

2. The 11 - 15 micron FeCrAlY system was superior to the baseline material with regard to oxidation and erosion resistance but inferior with regard to abradability and air permeability. It should not be considered further for engine testing insomuch as the FeNiCrAlY system provides better abradability and erosion resistance.

Preparation of Sample Coupons - Task V

Twenty four sample coupons, 1 in. x 3 in. x 0.050 in. of each of the two best candidate materials were prepared after Task IV and shipped to the AFML of WPAFB for possible additional testing. The description of these samples is as follows:

ITEM	DESCRIPTION
1.	15 - 18 micron FeNiCrAlY, 20.9 to 26.1% density, 2299 to 3141 psi tensile strength
2.	11 - 15 micron FeCrAlY (L/D = 78), 23.1 to 25.2 % density, 2058 to 2310 psi tensile strength

Environmental Impact

The improved FeNiCrAlY seal product from this program will be manufactured using currently installed equipment at the DeLand, Florida plant of Technetics Div. of Brunswick Corp. The current abradable seal products using Hastelloy X and Haynes 188 fibers are manufactured on this equipment and no unfavorable environmental problems will be created by employing the new FeNiCrAlY alloy. The current plant and equipment conform to local, state, and federal regulations regarding protection of the environment.

The improved seals from the program are expected to improve the environment significantly by helping to increase the fuel efficiency of gas turbine engines.

Material Preparation

Baseline Material, FM-521

The FM-521 (8 micron Haynes 188 fiber metal at 19% nominal density) was standard production material made on the full scale manufacturing equipment. Sheets of the material were selected from inventory and cut into the test specimens as described below.

All of the other materials tested in this program were prepared on small scale pilot plant equipment in the Engineering Dept. that fully duplicates the processes and products in the Manufacturing Dept.

Fiber Preparation

The fibers were made with the same proprietary process used for making the Type A fibers used in the baseline material. Operating parameters were modified as needed to obtain the desired fiber diameters and lengths.

Felting

After inspection of the fibers, they are felted on a proprietary machine to provide a completely random and uniform array of fibers in the density range of 7 - 14% density depending upon the aspect ratio of the fibers.

Sintering and Rolling

The felts are sintered in a furnace at high temperatures to obtain diffusion bonds at all of the fiber contact sites. The sintered felts are rolled or pressed to a density slightly below the desired finished density of the product. They are then resintered

to obtain diffusion bonds at all of the new contact sites obtained by the pressing. After resintering, the felts are given a small additional compaction to achieve flatness as well as to obtain the desired density and thickness in the finished sheet.

Sintering conditions (time, temperature, and atmosphere quality) are varied as needed to achieve good sintering depending upon the alloy and fiber diameter being diffusion bonded. The standard Haynes 188 seals are sintered in dry hydrogen; however, vacuum sintering at extremely low pressures is required for the MCrAlY alloys. Some improvements in the felt processing and sintering parameters were developed during the course of the program to achieve more uniform sheets and higher strengths at a given density.

Sampling Plan

The 12 x 12 x 0.125 inch sheets prepared for this program were inspected and cut into test specimens on a band saw in accordance with the sampling plan shown in Figure 1.

Extra samples for rub and tensile testing were cut and saved for possible retest on any sheet. The average tensile strength on samples D, H, and I was considered representative of the strength of the sheet. After the sheet was sectioned, all test samples were individually measured and weighed to obtain actual percent densities of the samples.

Material Properties

Alloy Chemistry

Samples of each of the six material variants from Task II were submitted to an independent chemical laboratory. Duplicated analyses of each material were obtained in Task II by submitting samples from both the high and low density variants of each material. In the subsequent tasks, III and IV, only the high density sheet of each material variant was analyzed. Each material was analyzed quantitatively by the X-ray fluorescence technique plus the standard carbon analyses.

The results for the Haynes 188 and NiCrAlY are presented in Table I and for the FeNiCrAlY and FeCrAlY in Table II in comparison with the raw material specifications and raw material analyses provided by the suppliers.

There were some problems with control of carbon content with some of the MCrAlY alloys and aluminum content of the FeCrAlY. This is discussed later in the section on static oxidation testing. Also, there was a problem with iron contamination in the coarse Haynes 188 and NiCrAlY fiber metals. None of these problems are believed to have a significant effect on the outcome of this program.

A-C:	Static Oxidation, 1600°F	Q-S:	Erosion
E-G:	Static Oxidation, 1400°F	T:	Dynamic Oxidation
J-L:	Static Oxidation, 1200°F	U:	Chemistry
D,H,I:	Room Temp. Tensile	V:	Compression
M:	1600°F Tensile	W-Z:	Rub Tests
N-P:	Spare Tensile Bars		

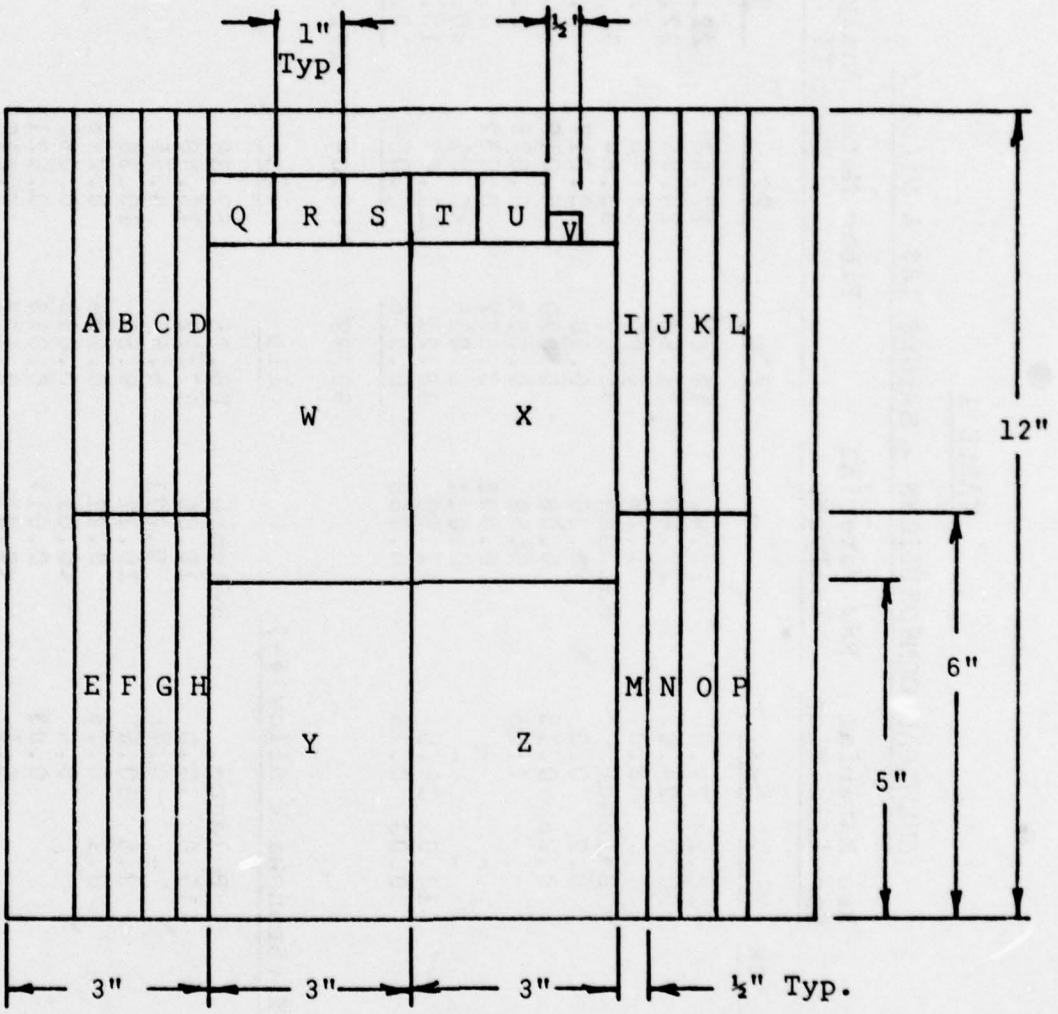

FIGURE 1

SHEET SAMPLING PLAN

TABLE I

CHEMICAL COMPOSITIONS - HAYNES 188 & NiCrAlY

	Raw Material Specification		Raw Material Analyses	Fiber Metal Analyses[1] Task II			
A. Haynes 188	Min.	Max.		20μ	22μ	8μ	8μ
Nickel	20.2	24.0	22.42	19.65	17.63	22.68	22.99
Chromium	20.0	24.0	22.48	21.88	24.85	22.96	23.05
Iron		3.0	1.78	8.66	11.75	2.60	2.07
Cobalt	Balance		Balance	35.49	33.64	37.08	37.41
Silicon	0.2	0.5	0.36	0.90	0.317	0.398	0.460
Carbon	0.05	0.15	0.08	0.023	0.010	0.263	0.283
Manganese		1.25	0.69	0.063	0.078	0.64	0.62
Sulfur	-	-	0.006	0.022	0.032	0.01	0.01
Phosphorus	-	-	0.011	0.016	<0.01	<0.01	<0.01
Tungsten	13.0	16.0	13.99	13.21	11.67	13.68	13.35
Lanthanum	0.03	0.15	0.058	0.076	0.064	0.045	0.045
Total				99.99	100.04	100.35	100.28
B. NiCrAlY (Brunswick Alloy #4)				11μ	12μ		
Nickel	Balance		Balance	66.25	67.38		
Chromium	15.0	17.0	15.68	17.22	16.40		
Iron	-	0.75	0.071	5.59	4.55		
Aluminum	9.5	10.5	10.12	9.51	10.36		
Yttrium	0.1	0.25	0.21	0.264	0.243		
Silicon		0.4	<0.01	0.096	0.082		
Carbon		0.03	0.017	0.013	0.021		
Manganese		0.5	<0.01	0.177	0.210		
Sulfur		0.015	0.001	<0.005	<0.005		
Boron		0.003	<0.001	<0.0001	<0.0001		
Phosphorus		0.015	0.006	<0.005	<0.005		
Total				99.12	99.25		

(1) X-ray fluorescense technique performed by Dirat Laboratories, Westfield, Mass. All constituents reported in weight %.

TABLE II

CHEMICAL COMPOSITIONS - FeNiCrAlY & FeCrAlY

	Raw Material Specification		Raw Material Analyses	Fiber Metal Analyses(1)							
				Task II				Task III			Task IV
	Min.	Max.		17μ	18μ			13μ			16μ
C. FeNiCrAlY (Brunswick Alloy #5)											
Nickel	24.0	26.0	25.42	25.03	27.85			21.91			24.85
Chromium	18.0	19.0	18.24	17.42	15.13			17.95			18.19
Iron	Balance		Balance	48.05	47.28			49.43			46.23
Aluminum	9.5	10.5	9.03	9.24	9.59			10.58			10.61
Cobalt		0.5	0.02	0.182	0.079			0.059			0.060
Yttrium	0.01	0.03	0.02	0.016	0.020			0.015			0.017
Silicon	-	0.1	0.01	0.051	0.044			0.053			0.069
Carbon	-	0.03	0.013	0.017	0.072			0.659			0.184
Manganese		0.5	0.01	0.013	<0.010			0.021			0.023
Sulfur		0.015	0.001	0.001	0.001			0.001			0.003
Boron		0.003	<0.001	0.0002	0.0001			<0.0001			0.0004
Phosphorus		0.015	0.005	0.002	0.002			0.002			0.002
Nitrogen		0.003	0.002								
Total				100.18	100.07			100.68			100.24
D. FeCrAlY (Brunswick Alloy #23)				17μ	15μ	24μ	23μ	L/D = 50 16μ	L/D = 78 11μ	L/D = 45 12μ	L/D = 78 11μ
Nickel	-	-	-	<0.005	<0.005	<0.005	<0.005	<0.005	<0.005	<0.005	<0.005
Chromium	19.5	20.5	19.95	22.96	21.11	22.37	20.39	22.65	20.73	22.23	20.40
Iron	Balance		Balance	72.33	71.42	72.33	72.90	68.80	69.96	66.58	67.67
Aluminum	5.75	6.25	6.07	4.41	7.19	5.03	6.42	8.31	9.06	10.96	11.74
Cobalt	-	-	<0.005	<0.005	<0.005	<0.005	<0.005	<0.005	<0.005	<0.005	<0.005
Yttrium	0.01	0.03	0.03	0.021	0.018	0.018	0.020	0.014	0.020	0.035	0.021
Silicon	-	-	<0.005	0.085	0.097	0.085	0.127	0.061	0.064	0.057	0.077
Carbon		0.01	0.005	0.185	0.525	0.027	0.032	0.302	0.471	0.404	0.153
Manganese	-	-	<0.005	0.162	0.140	0.146	0.128	0.167	0.175	0.184	0.136
Sulfur		0.005	<0.005	<0.005	<0.005	<0.005	<0.005	<0.005	<0.005	<0.005	<0.005
Boron		0.003	0.0015	0.0022	0.0018	0.0026	0.0012	0.0010	0.0023	0.0022	0.0013
Phosphorus		0.005	<0.005	<0.005	<0.005	<0.005	<0.005	<0.005	<0.005	<0.005	<0.005
Nitrogen		0.003	-	-	-	-	-	-	-	-	-
Total				100.15	100.50	100.01	100.02	100.2800	100.5023	100.4722	100.2183

(1) X-ray fluorescence technique performed by Dirats Laboratories, Westfield, Ma. All constituents reported in weight %.

Alloy Densities

Prior to the start of the program, Brunswick measured the true density of the three MCrAlY alloys employed here. These were measured by weighing known volumes of the solid alloys. The results were confirmed with theoretical calculations. The results, as well as the published value for Haynes 188, are presented in Table III.

TABLE III

ALLOY DENSITIES AND THERMAL EXPANSIVITY

	NiCrAlY[1] Alloy 4	FeNiCrAlY[1] Alloy 5	FeCrAlY[1] Alloy 23	Haynes[2] 188
Density, gm/cu. cm.	7.45	7.02	7.13	9.13
Thermal Expansivity, (in/in - °F) x 10^{-6}:				
72 - 800°F	7.6	7.6	7.1	7.8
72 - 1200°F	9.0	8.0	8.3	8.6
72 - 1600°F	9.6	9.0	8.7	9.4
72 - 1832°F	10.9	10.1	9.2	

1. Thermal Expansivity Data measured at Orton Ceramic Foundation
2. Stellite Div. of Cabot Corp. - Bulletin F-30, 494

Thermal Expansivity

Thermal expansion properties are useful in compressor and turbine design and for brazing fiber metal seals to their support rings. In early 1976, prior to the start of this program, Brunswick obtained at an independent laboratory thermal expansivity data on the three MCrAlY alloys employed in this program.

An automatic recording dilatometer was used to measure linear thermal expansion as a function of temperature. The 1 x 0.5 x 0.1 (±0.0001) inch machined samples were placed on the dilatometer such that the change in length measurement was along the one inch direction. The samples were purged with nitrogen and heated at a rate of 3°C per minute. The results are presented in Table II along with published data for Haynes 188. The results are reasonable and consistent with other similar nickel and iron base alloys.

Previous data obtained by Brunswick has shown that the thermal expansivity of fiber metal is essentially the same as the solid alloy from which it is made.

Fiber Aspect Ratio

Measurement of fiber lengths of extremely fine fibers by normal optical methods is very time consuming and expensive. Brunswick has developed a method for estimating fiber aspect ratio (L/D). This was done by measuring the bulk density of precision cut lengths of known fiber diameters. This correlation is shown in Figure 2.

The bulk densities of all of the fibers used in this program were measured and the correlation shown in Figure 2 was used to obtain the aspect ratios. These results are presented in Table IV.

Sheet Density Uniformity and Fiber Diameter

The length, width, thickness and weight of each 12" x 12" sheet were measured and the apparent densities were calculated. Each sheet was then divided into an imaginary grid of 4" x 4" squares and tested by the air permeability method using a one inch diameter test area at 2360 ft/hr (20 cm/sec) flow velocity in the center of each 4" x 4" square. The average permeability coefficient, K_1, and apparent fiber diameter were then calculated for each sheet. Using the average fiber diameter for the sheet, the minimum and maximum density were calculated using the permeability extremes from the 9 test spots and the equations in Table V. This indicates the density uniformity or runout of each sheet.

Sheet thickness, density, density uniformity, and fiber diameter data are presented in Table IV. The normal specification for allowable density gradients in production seal sheets is ±1.5% for all spots. This is equivalent to a range of 17.5 to 20.5% density for the 19% dense baseline material, FM-521. At low densities in the vicinity of 19 - 20%, this specification was more difficult to maintain with the coarser fibers because of the nature of the felting process. At higher densities in the vicinity of 30%, the specification was even more difficult because it represents a tighter specification in terms of variation in weight per unit area. With the process improvements made in the preparation of Task IV materials, the ±1.5% density uniformity specification was achieved on all sheets tested on Task IV.

For the purposes of the data correlations presented later in this report, the fiber diameters from Table IV were averaged for each batch of fibers to obtain the average diameters shown in Table VI.

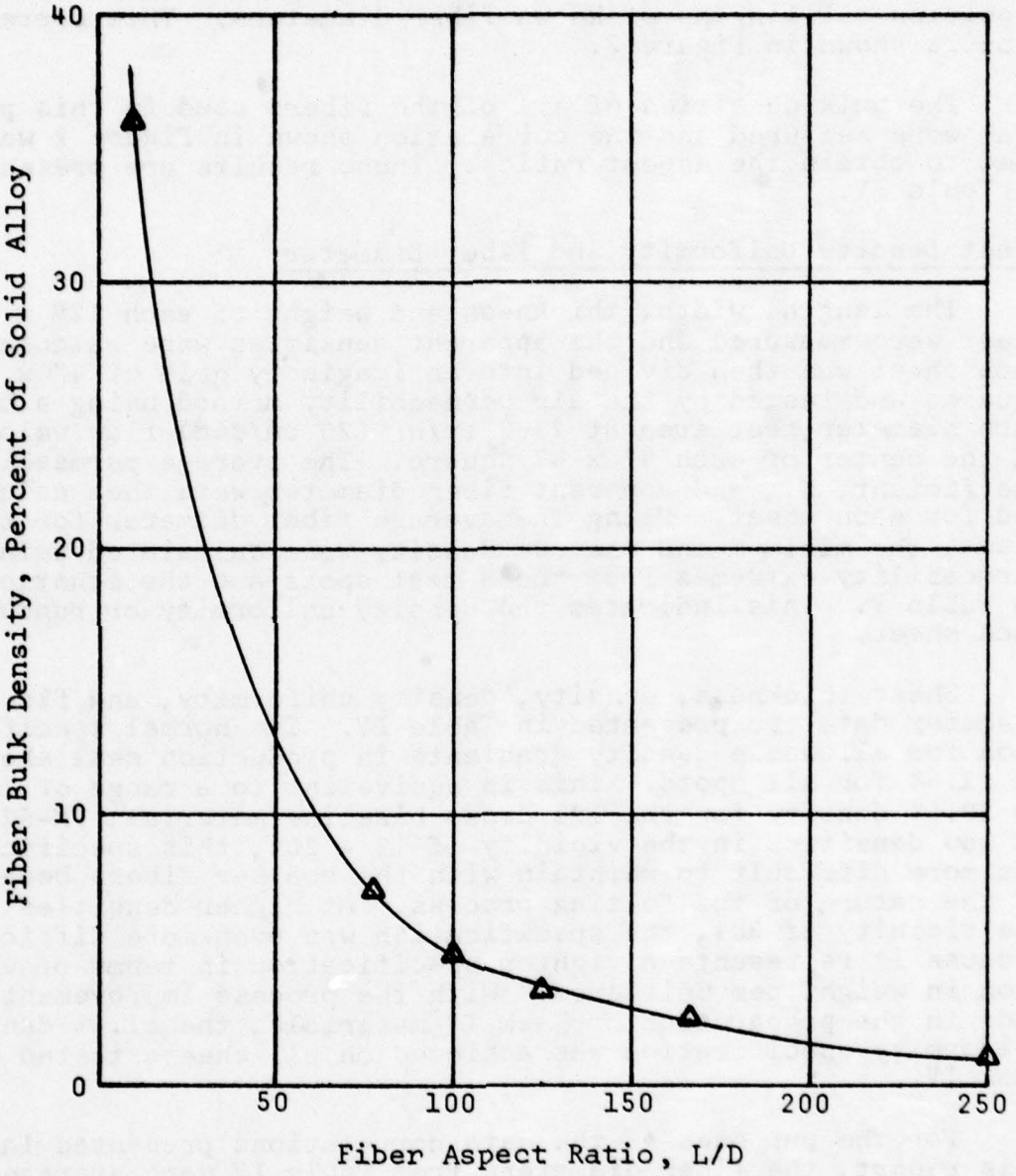

FIGURE 2

FIBER ASPECT RATIO
CORRELATION

TABLE IV

SHEET DENSITY UNIFORMITY AND FIBER DIAMETER

MATERIAL	L/D	THK. IN.	SHEET DENSITY[2] (%)	AVG. K_1[3]	APPARENT FIBER DIA. (μ)	DENSITY GRADIENT[3] (MIN & MAX %)
A. Task II						
FeCrAlY	50	0.109	18.5	9,230	16.6	18.0 - 19.1
FeCrAlY	50	0.128	27.4	2,370	15.3	25.4 - 29.7
FeCrAlY	40	0.114	18.8	18,236	23.8	17.3 - 20.5
FeCrAlY	40	0.114	30.0	3,940	23.1	28.4 - 31.4
FeNiCrAlY	64	0.092	24.7	4,142	17.1	23.8 - 26.3
FeNiCrAlY	64	0.141	26.2	3,749	17.9	25.5 - 27.1
NiCrAlY	47	0.121	19.5	3,185	10.5	18.8 - 20.5
NiCrAlY	47	0.120	30.7	934	11.7	29.7 - 31.6
Haynes 188	58	0.086	18.5	13,301	19.9	16.9 - 19.9
Haynes 188	58	0.086	30.0	3,443	21.6	27.9 - 32.9
Haynes 188[1]	80	0.124	18.9	1,869	7.7	18.4 - 19.3
Haynes 188[1]	80	0.126	18.9	1,847	7.6	18.5 - 19.3
B. Task III						
FeCrAlY	50	0.109	21.7	6,672	17.8	20.8 - 23.1
FeCrAlY	50	0.115	23.6	4,845	17.2	22.5 - 25.6
FeCrAlY	50	0.112	25.5	3,091	15.5	23.3 - 27.4
FeCrAlY	78	0.131	19.6	5,798	14.3	18.2 - 21.1
FeCrAlY	78	0.128	21.6	3,575	12.9	19.6 - 23.0
FeCrAlY	78	0.123	23.4	2,196	11.4	22.0 - 24.9
FeCrAlY	45	0.127	20.1	5,145	13.9	19.6 - 20.8
FeCrAlY	45	0.130	21.7	3,789	13.4	21.0 - 23.0
FeCrAlY	45	0.129	23.6	2,177	11.5	22.7 - 25.3
FeNiCrAlY	64	0.125	20.6	7,063	16.9	19.9 - 21.6
FeNiCrAlY	64	0.127	22.0	4,957	15.6	20.8 - 24.1
FeNiCrAlY	64	0.128	23.6	2,800	13.1	22.9 - 24.7
C. Task IV						
FeNiCrAlY	64	0.127	20.8	7,851	18.1	20.4 - 21.3
FeNiCrAlY	64	0.123	22.6	5,546	17.2	21.6 - 23.6
FeNiCrAlY	64	0.129	22.3	5,675	17.1	21.5 - 23.2
FeNiCrAlY	64	0.128	23.5	4,230	16.0	22.0 - 25.0
FeCrAlY	78	0.125	22.1	3,336	12.9	21.6 - 22.6
FeCrAlY	78	0.130	22.2	2,878	12.1	21.4 - 23.0
FeCrAlY	78	0.128	23.1	2,605	12.2	22.3 - 23.9
FeCrAlY	78	0.131	22.7	2,380	11.4	22.3 - 23.8
Haynes 188[1]	80	0.128	18.8	-	-	18.4 - 19.5
Haynes 188[1]	80	0.123	19.0	-	-	18.8 - 19.3

1 Baseline Material, FM-521
2 By Gravimetric method
3 By Air Permeability method

TABLE V

AIR PERMEABILITY AND FIBER DIAMETER CALCULATIONS

1. Air permeability through porous media (Darcy's law for laminar flow through porous materials):

$$V/\Delta P = \frac{K_1}{9.5\ L\ \mu}$$

2. Modified Kozeny-Carmen equation:

$$K_1 = 1.7\ \frac{\varepsilon^3\ D^2}{(1-\varepsilon)^2}\ \gamma$$

3. Empirical corrections to Kozeny constant for Type A fiber variations above porosity of .55:

$$\gamma = 1 + 0.95\ (\varepsilon - 0.55)$$

Where:

Va = Average gas velocity, ft/hr

ΔP = Pressure drop, inches of H_2O

K_1 = Laminar permeability coefficient determined by air permeability test at velocities below 3,000 ft/hr in units of CFH/ft^2 - in. H_2O - 1/16" thickness

ε = Porosity = fraction of voids in total volume of porous material

$1-\varepsilon$ = Fractional density = vol. fraction of solids in porous material

L = Thickness, inches

μ = Viscosity, centipoise (typically = .0175 cp for air at room temperature)

D = Fiber diameter, micrometers

TABLE VI

AVERAGE FIBER DIAMETERS

ALLOY	L/D	AVERAGE FIBER DIAMETER (MICROMETERS)
FeCrAlY	40	23.4
FeCrAlY	50	16.5
FeCrAlY	45 & 78	12.6
FeNiCrAlY	64	16.6
NiCrAlY	47	11.1
Haynes 188	58	20.8
Haynes 188 (FM-521)	80	7.7

Thermal Conductivity

Introduction

The thermal conductivity of an abradable seal is an important property needed by the engine designer to predict the amount of rub that will be experienced. A thermal insulating material is especially helpful in reducing the rub that occurs on a deceleration because the insulation effect will slow the thermal response of the case. Because fiber metal is so low in density, it is an excellent insulator and is the best abradable material available for this purpose.

Sample Preparation

Two 2.5" x 2.5" x 0.125" specimens each of FeCrAlY and FeNiCrAlY were tested for thermal conductivity. These samples were the two best candidate materials developed under the program. One sample of each material was at the low percent density range tested and one sample of each material was tested at the high percent density range that was tested in the program. The fiber metal samples were brazed with 3 mil Nicrobraze® LM tape (AMS 4777) to 2.5" x 2.5" x 0.080" Waspaloy (AMS 5544) plates at 1950°F for 15 minutes in a vacuum furnace. Groves (2.5" x 0.030" x 0.030") were machined on the top and bottom Waspaloy reference plates for thermocouple instrumentation.

Experimental Procedure

The Dynatech Model TCFCM comparative thermal conductivity instrument was used to determine the thermal conductivity of the samples over a wide temperature range. The comparative method was chosen as the test method. The sample with thermocouple instrumentation was placed between two Inconel 702 standards of known thermal conductivity with the thermocouples at the interfaces. The composite stack was placed between the plates of an upper heater, and auxiliary heater and a lower heat sink. A reproducible load was applied to the top of the complete system. A guard tube which could be heated or cooled was placed around the system and the interspace and surroundings were filled with an insulating powder. By means of adjustments to the power in the various heaters and of the heat sink temperature, a steady temperature distribution was maintained in the system and undue radial heat loss was prevented by keeping the guard tube at a temperature close to the average temperature of the sample. At equilibrium conditions, the temperatures at various points in the system were evaluated from the thermocouple readings. The thermal conductance of the composite was calculated from:

$$C_s = \left[\frac{1}{2}\right]\left[\frac{1}{\Delta T}\right]_s\left[\left[\frac{\lambda \Delta T}{x}\right]_R + \left[\frac{\lambda \Delta T}{x}\right]_r\right]$$

where R = top reference parameters
C_s = thermal conductance
ΔT = Temperature difference across mat'l
s = sample parameters
r = bottom reference parameters
x = distance between thermocouples
λ = thermal conductivity of standard

The results of temperatures of 200, 800, 1200 and 1600°F are shown in Table VII. After subtracting the conductivity of the Waspaloy backing plates, the apparent thermal conductivities of the fiber metal samples were calculated from:

$$\lambda_f = \frac{X_f}{C_s^{-1} - \frac{X_p - X_t}{\lambda_p}}$$

where λ_f = apparent thermal conductivity of fiber metal

X_f = thickness of fiber metal

X_p = thickness of both Waspaloy plates

X_t = half the depth of both thermocouple grooves, 0.035"

λ_p = thermal conductivity of Waspaloy given by Brunswick

Results

The results are included in Table VII and the data are plotted in Figure 3.

As can be seen from Figure 3, the 13 micron FeCrAlY system has lower thermal conductivities and lower slopes than the 17 micron FeNiCrAlY system at equivalent percent densities; although both systems are good insulators because of high porosities, Thermal conductivites at other densities in the 15 - 30% range can be estimated by a linear interpolation or extrapolation from the two densities measured for each alloy system.

Mechanical Properties

Background

Prior work has shown that the mechanical properties of fiber metal are a function of the % density, the strength of the solid alloy from which it is made, the sintering conditions, and the fiber aspect ratio. Fiber metal is completely isotropic in the plane of the sheet but is always weaker perpendicular to the plane of the sheet because of fiber orientation effects. Fiber metal made from very long fibers (L/D = 1500) will have a strength perpendicular to the plane of the felt of about 5 - 10% of its in-plane strength. Fiber metal made from the short Type A fibers used in this program (L/D = 40 - 80) have strengths perpendicular to the plane of the felt in the range of 20 - 40% of the in-plane strengths.

In order to ultimately understand the mechanisms of abradability and erosion resistance of abradable seals to permit optimum designs, it will be necessary to develop mathematical models of

TABLE VII

THERMAL CONDUCTIVITY DATA

THE THERMAL CONDUCTANCE OF FIBER METAL/WASPALOY COMPOSITE

Temperature C	Temperature F	Thermal Conductance BTU $h^{-1}ft^{-2}F^{-1}$ 14110-4	13479-6C	14149-7	14110-10
93	200	20	34	28	24
427	800	27	44	36	35
649	1200	32	50	42	42
871	1600	36	56	48	49

THE CALCULATED APPARENT THERMAL CONDUCTIVITY OF FIBER METAL

Temperature C	Temperature F	Apparent Thermal Conductivity BTU in $h^{-1}ft^{-2}F^{-1}$ 14110-4	13479-6C	14149-7	14110-10
93	200	2.8	5.1	3.7	3.2
427	800	3.7	6.4	4.9	4.7
649	1200	4.4	7.3	5.6	5.7
871	1600	5.0	8.2	6.4	6.6

NOTE: When the apparent thermal conductivity was calculated, 0.0175 inch was subtracted from each plate to account for the temperature sensor position.

#13479-6C - FeNiCrAlY, 17μ, 25.3% density @ 0.141" thk.
#14110-10 - FeNiCrAlY, 17μ, 18.3% density @ 0.132" thk.
#14110-4 - FeCrAlY, 13μ, 18.1% density @ 0.134" thk.
#14149-7 - FeCrAlY, 13μ, 22.4% density @ 0.130" thk.

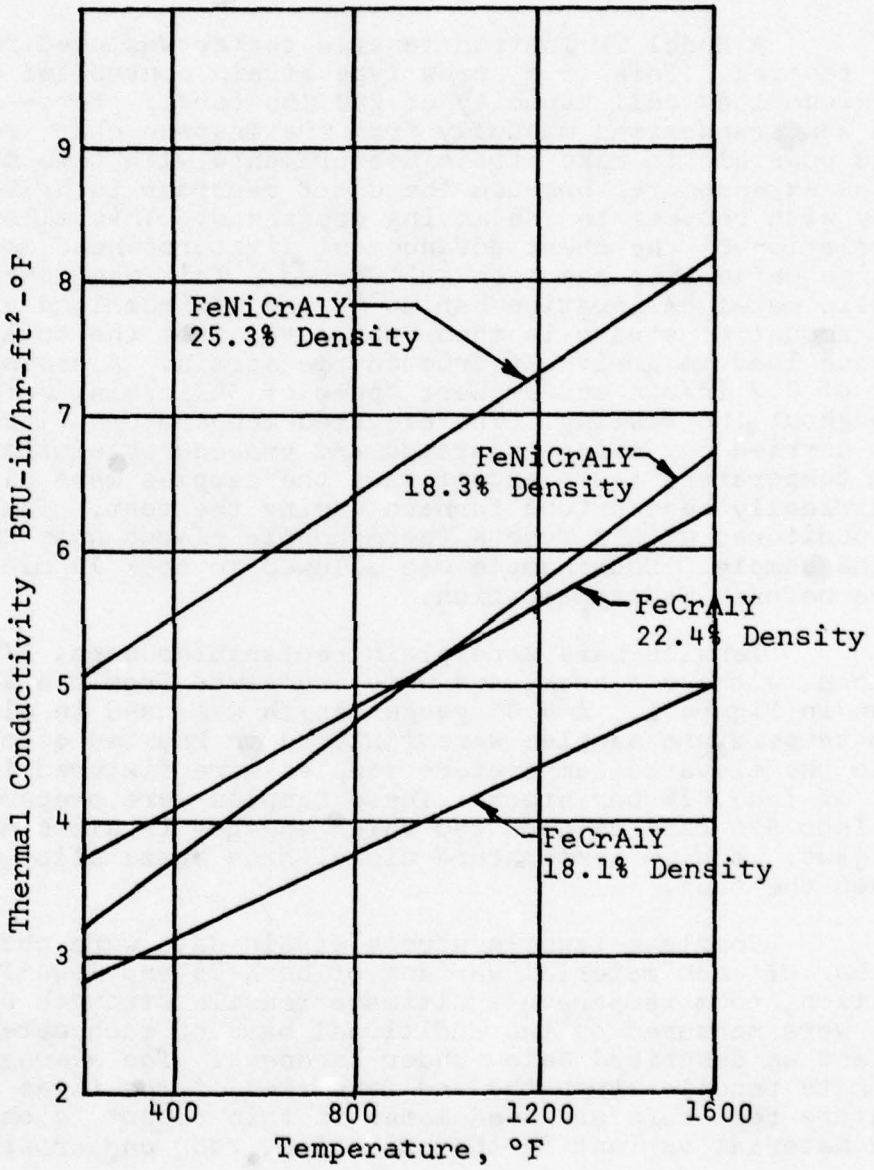

FIGURE 3

THERMAL CONDUCTIVITY DATA

these mechanical processes in terms of the mechanical and thermal properties of the abradables. The properties measurements made in this program on each material variant were a first step in that direction.

Tensile Properties

Test Procedures

A Model TM Instron tensile tester was used for all tensile testing. This is a screw type strain controlled machine with a maximum load cell capacity of 200 lbs force. Force and strain data was transcribed manually from the Instron chart recorder. It is possible to make strain measurements with this machine without an extensometer because the chart recorder is driven synchronously with respect to the moving crosshead. This allows direct correlation of the chart advancement with crosshead movement after machine deflection has been subtracted. This was done by pulling a solid metal calibration bar up to the maximum load anticipated. This amount of strain is then subtracted from the total strain at each load to arrive at true sample strain. A crosshead velocity of 0.2 in/min and a chart speed of 50 in/min. were used throughout the testing. The elevated temperature (1600°F) tests were carried out using apparatus and procedures similar to the room temperature tests except that the samples were placed in an electrically heated tube furnace during the test. Temperature was monitored with a Type K thermocouple placed near the center of the sample. Each sample was allowed to soak 10 min. at temperature before load application.

Tensile bars were plain rectangular bars, 1/2" wide by 6" long, without a neck, and were bandsawed from the sheets as shown in Figure 1. A 4.0" gauge length was used in all tests. Room temperature samples were fixtured in knurled quick grip jaws while the elevated temperature samples were fixtured in solid jaws of Inco 625 bar stock. These samples were prepared by brazing Inco 625 tabs to each end which engaged in slots machined in the jaws. A high temperature nickel base braze alloy was used to attach the tabs.

Complete tensile stress/strain data were obtained on one bar of each material variant of both 75 and 1600°F. In addition, room temperature ultimate tensile strength and hardness were measured on two additional bars of each material variant as described below under hardness. The averages of the ultimate tensile strengths and densities of the three room temperature test bars are used later in this report to characterize each material variant in the oxidation, rub, and erosion testing.

Room Temperature Tensile Results

The results from the room temperature tensile stress/strain measurements are presented in Table VIII. Typical tensile stress/strain curves are shown in Figure 4 for the 18.6% density Haynes 188 (7.7 micron) and for the 20.1% density FeNiCrAlY specimens.

TABLE VIII
ROOM TEMPERATURE TENSILE PROPERTIES

Alloy	Avg. Fiber Diam. μm	Fiber L/D	Density %	Ultimate Tensile Strength psi	Elastic Modulus psi x 10^3	Elongation @ Break %	Mod. of Toughness psi
Task II:							
NiCrAlY	11.1	47	19.8	1610	32.4	6.8	49.9
			30.9	3010	94.1	4.8	50.4
FeNiCrAlY	16.6	64	23.4	1160	34.7	4.4	21.0
			24.8	2600	80.0	5.0	48.8
FeCrAlY	16.5	50	18.0	610	14.1	5.8	18.4
			26.5	1390	38.1	5.6	23.2
	23.4	40	17.7	570	14.5	4.5	14.1
			28.9	2180	59.0	5.4	54.9
Haynes 188	20.8	68	16.7	770	14.9	11.8	69.3
			28.7	3400	64.7	12.8	163.2
	7.7	80	18.6	1660	20.8	10.8	97.4
			18.7	1330	15.6	11.3	81.7
Task III							
FeCrAlY	16.5	50	20.3	1020	26.5	6.1	25.2
			22.6	1320	34.4	6.4	37.4
			24.4	1480	36.6	6.2	39.0
	12.6	78	18.2	1270	25.1	6.5	40.0
			21.6	1700	40.3	7.0	51.4
			22.0	1060	23.0	5.7	27.6
	12.6	45	18.9	1060	21.1	7.0	31.8
			20.3	1180	29.7	6.3	35.0
			21.8	1080	24.3	5.9	30.6
FeNiCrAlY	16.6	64	19.4	1600	35.5	6.8	44.0
			20.2	1330	31.7	5.2	28.6
			21.7	640	17.5	4.1	12.4
Task IV							
FeNiCrAlY	16.6	64	20.1	1820	50.3	6.4	42.5
			22.4	2235	63.0	6.5	51.9
			22.0	2340	58.3	7.0	58.5
			23.3	2220	75.2	5.4	40.8
FeCrAlY	12.6	78	22.8	2320	50.4	7.7	73.2
			22.5	2090	57.8	7.2	53.8
			22.8	1870	49.1	6.0	48.4
			22.8	1720	48.3	6.4	46.2

Nearly all the material variants acted alike at room temperature when subjected to tensile stress. After an initial amount of strain, the materials tend to stiffen and respond nearly linearly to stress to near the ultimate. The material then yields slightly and fails abruptly. A good example of this behavior is the 18.6% dense Haynes 188 sample in Fig. 4. Because these materials lack a distinct yield point, no yield strength values have been shown. The elastic modulus values reported are taken from the most linear portion of the stress/strain curve. In some cases, the materials show no yield point at all. Tensile elongation to failure is an indication of the ductility of the material; the higher the elongation, the more ductile the material. Modulus of toughness is a measure of the energy needed to fail the sample and is defined as the area under the S/S curve in psi.

Characteristically, fiber metal made from a given alloy and fiber L/D will have a good correlation of tensile strength with density that is independent of fiber diameter. Variations from the typical curve are usually below the curve and result from variations in sintering and rolling procedures. The tensile strengths for each of the three tensile bars of each material variant tested in the program are plotted as a function of density in Figure 5, 6, and 7. The typical curve for Haynes 188 fiber metal is shown on all three figures for reference. There were some processing problems in Task II with the MCrAlY materials resulting in lower than expected tensile strengths. Processing improvements made in Tasks III and IV resulted in higher strengths for these materials.

Elastic modulus appears to be a linear function of ultimate tensile strength as shown in Fig. 8 for FeCrAlY and FeNiCrAlY alloys. This has been observed previously with other fiber metal systems. Modulus was determined graphically by placing the best straight line through the linear portion of the S/S curve.

Tensile elongation ranged from 4.1 to 7.0% for FeNiCrAlY and from 4.5 to 7.7% for FeCrAlY. Haynes 188 was most ductile ranging from 10.8 to 12.8% elongation. Nearly all the materials failed abruptly after yielding only slightly as a very brittle material would fail.

Modulus of toughness is the area under the stress strain curve so it considers both strength and tensile elongation. Strong ductile materials such as the 28.7% dense Haynes 188 sample had high toughness while weak materials with low elongation to failure like the 17.7% dense FeCrAlY sample had low values of toughness. There were no substantial differences in the toughness of the Task IV materials (FeCrAlY and FeNiCrAlY) at room temperature.

1600°F Tensile Results

The results from the 1600°F tensile testing are presented in Table IX. Typical 1600°F tensile stress/strain curves are presented in Figure 9 for the same materials shown in Figure 4 at room temperature.

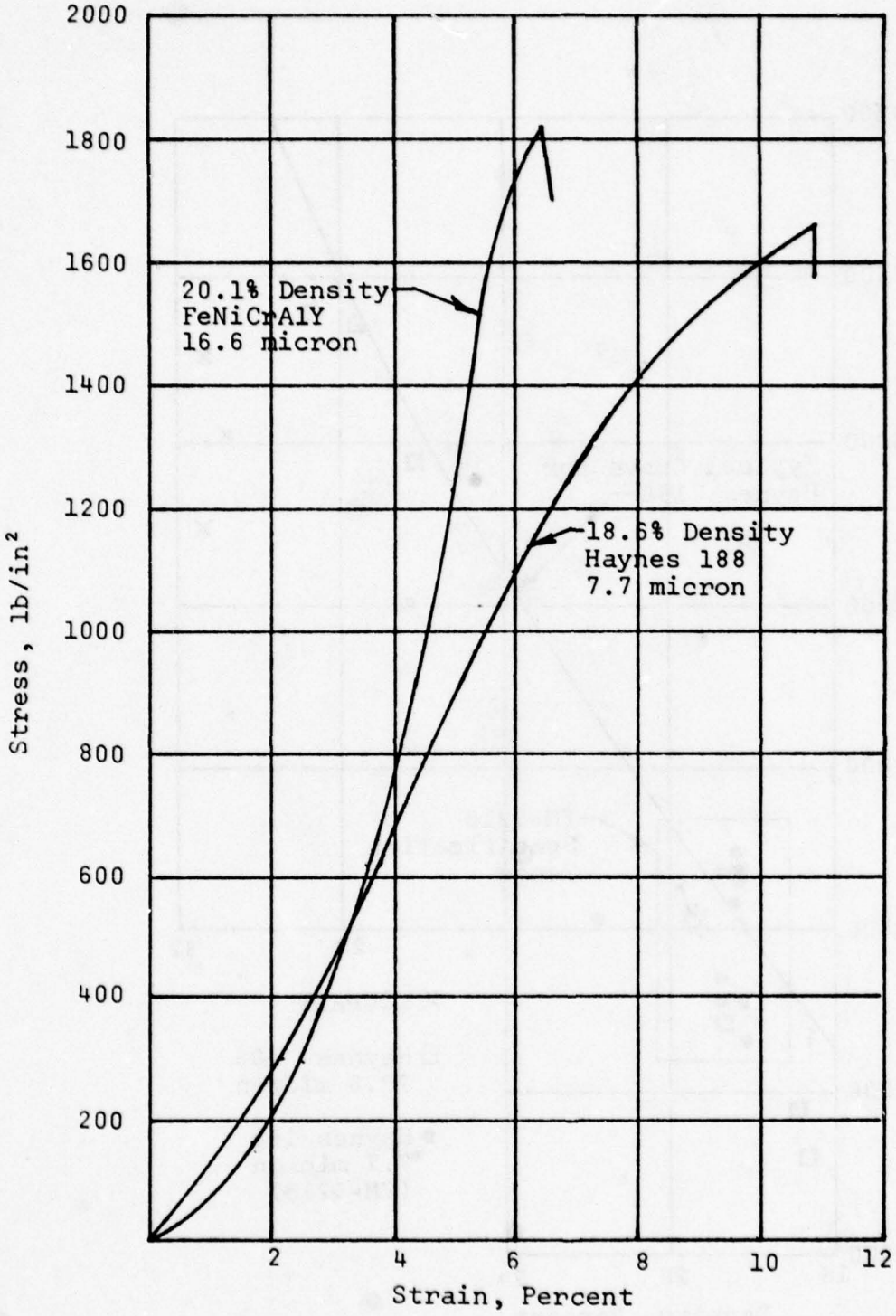

FIGURE 4
TYPICAL ROOM TEMPERATURE
TENSILE STRESS VS. STRAIN

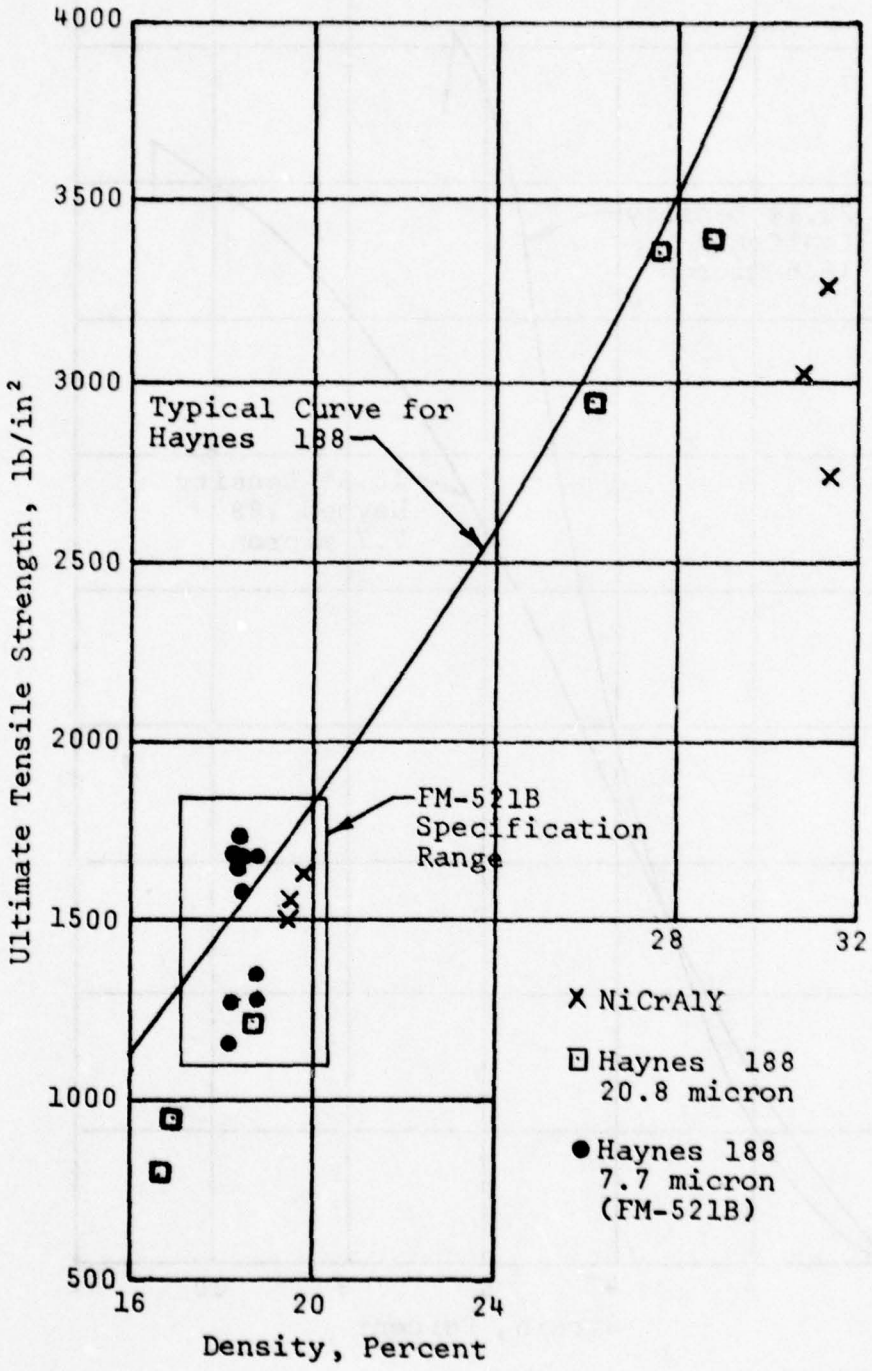

FIGURE 5

TENSILE STRENGTH VS. DENSITY
NiCrAlY & HAYNES 188

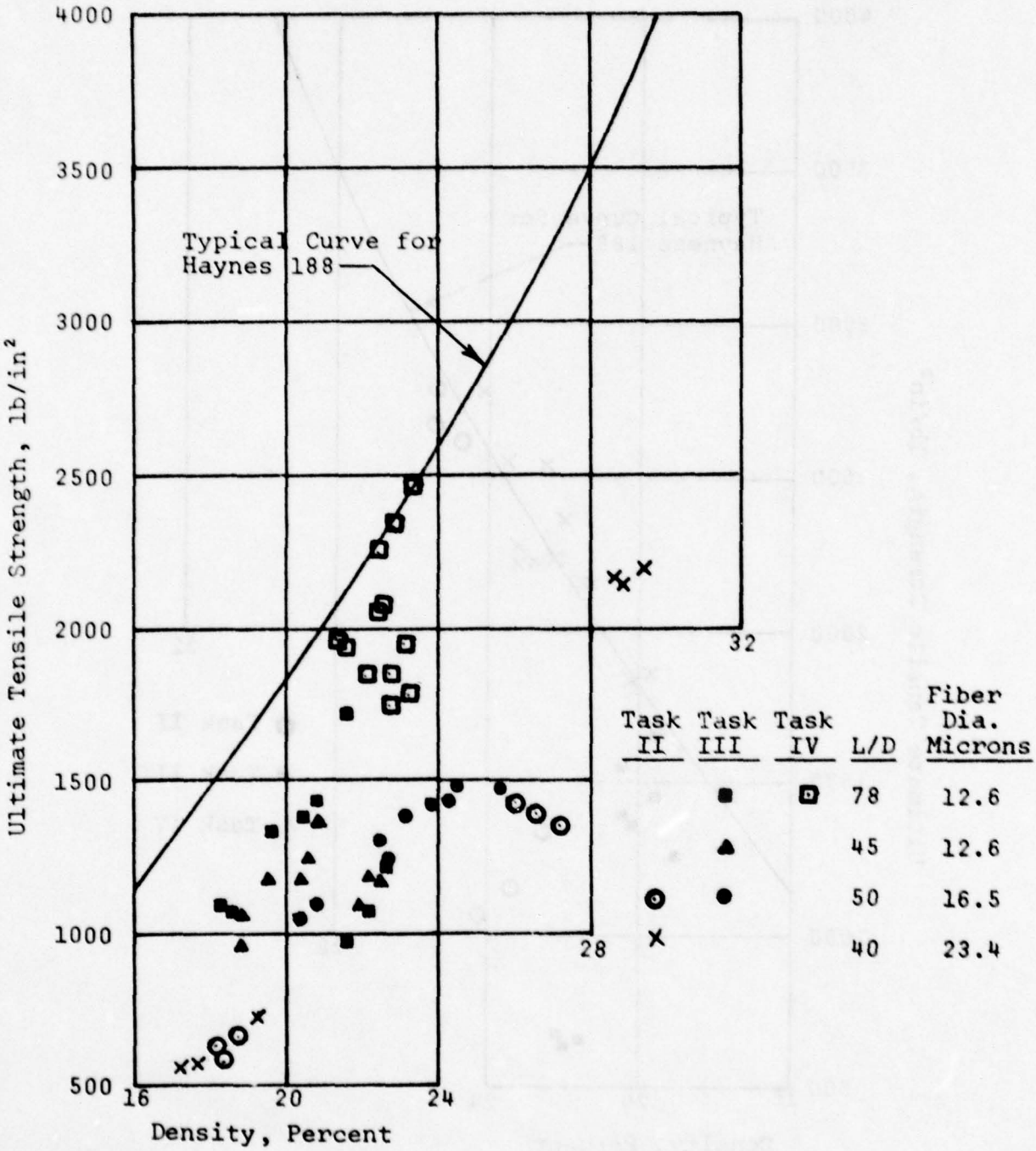

FIGURE 6

TENSILE STRENGTH VS. DENSITY
FeCrAlY

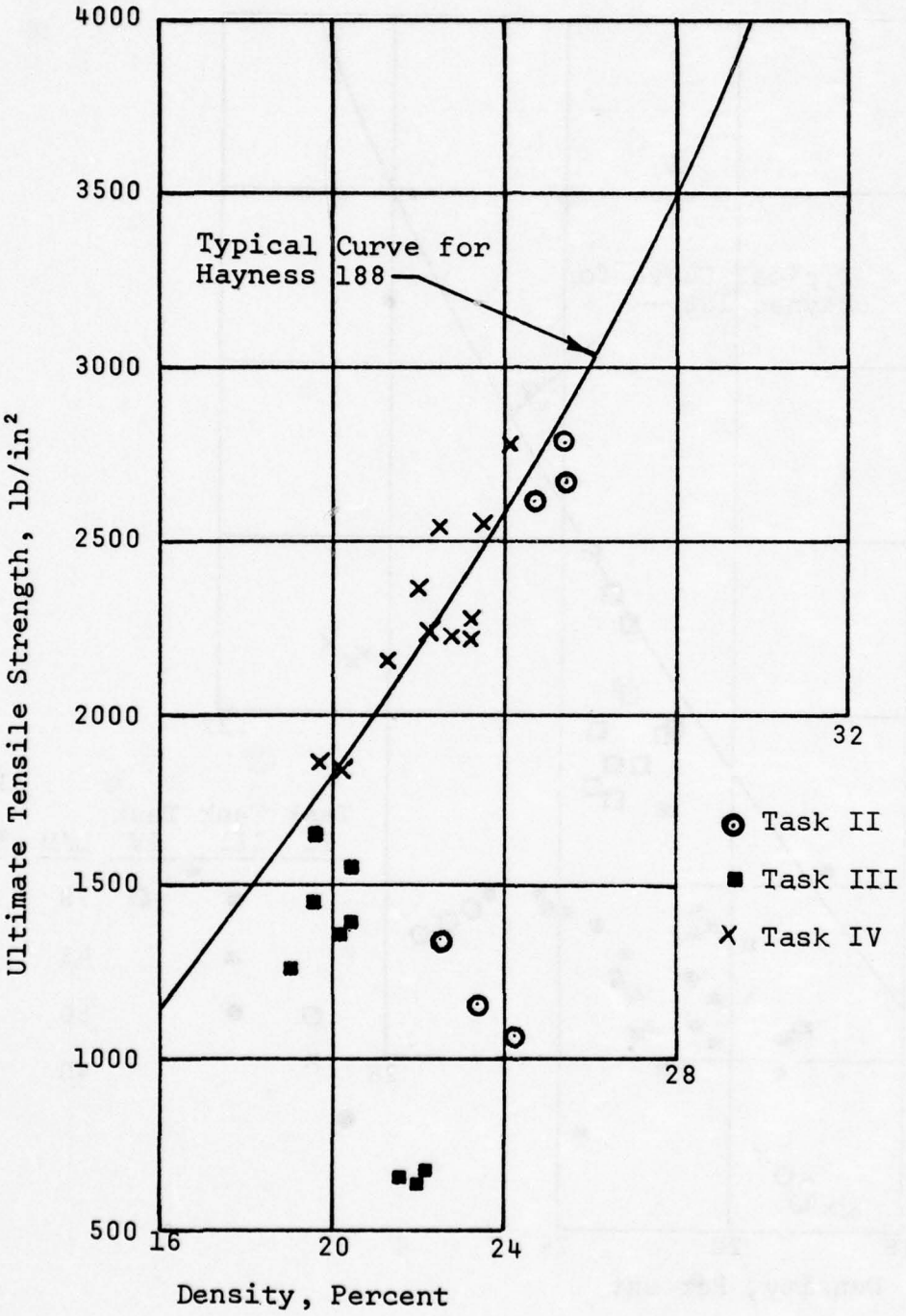

FIGURE 7

TENSILE STRENGTH VS. DENSITY
FeNiCrAlY

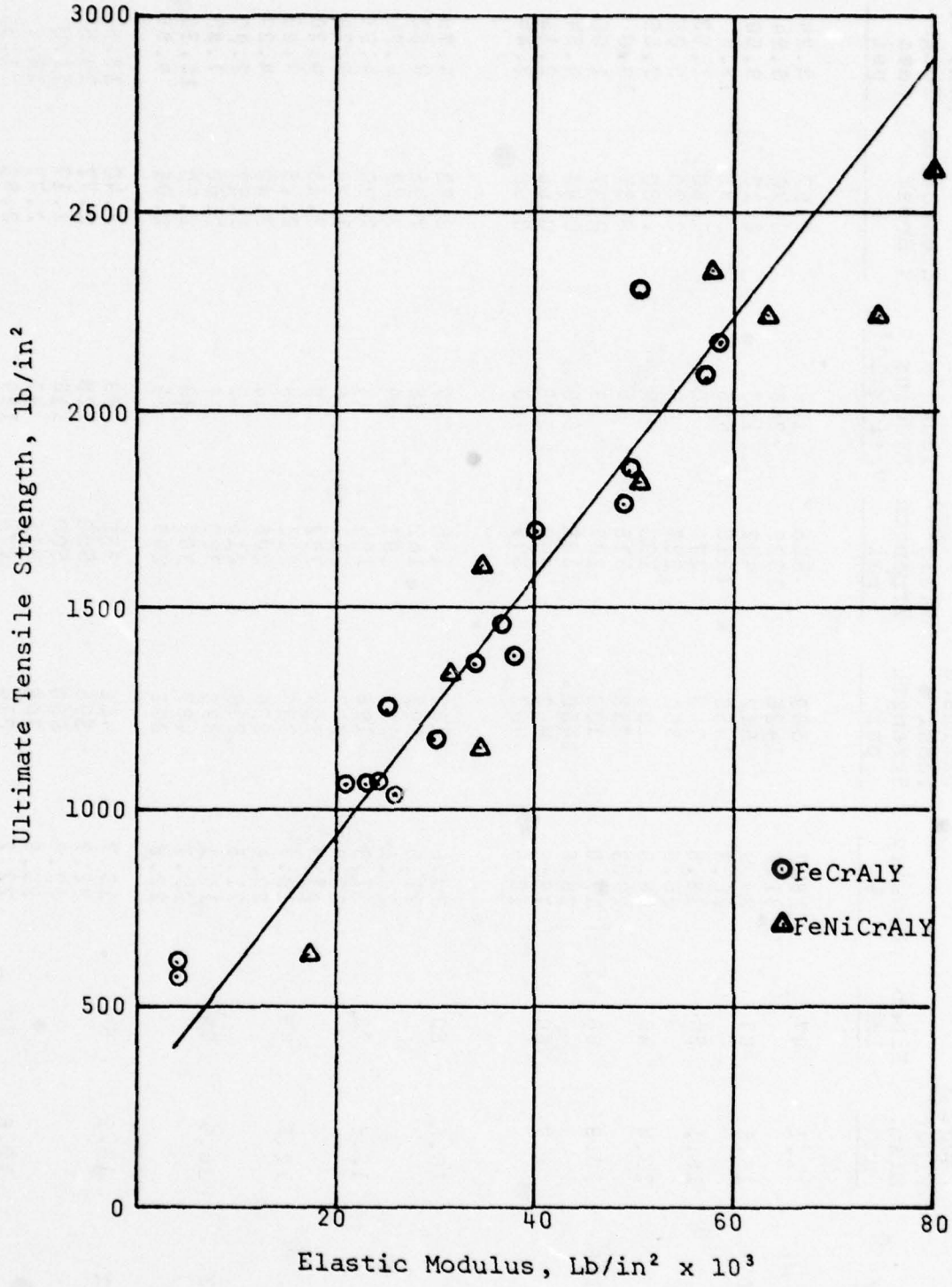

FIGURE 8

ULTIMATE TENSILE STRENGTH
VS. ELASTIC MODULUS

TABLE IX
1600°F TENSILE PROPERTIES

Alloy	Avg. Fiber Diam. µm	Fiber L/D	Density %	Ultimate Tensile Strength psi	Yield(1) Strength psi	Young's Modulus psi x 10^3	Elongation @ Break %	Mod. of Toughness psi
Task II:								
NiCrAlY	11.1	47	18.7	580	565	113	0.97	3.24
			31.2	1425	1395	266	0.70	5.94
FeNiCrAlY	16.6	64	23.9	542	432	133	2.10	9.60
			26.3	1458	1216	405	2.82	18.6
FeCrAlY	16.5	50	18.5	142	121	30	1.60	1.83
			26.8	300	237	79	2.20	5.05
	23.4	40	18.6	125	100	32	2.80	2.55
			28.9	353	315	44	3.37	10.0
Haynes 188	20.8	68	17.6	308	297	63	0.97	1.06
			28.6	1450	1388	509	0.47	4.54
	7.7	80	18.8	462	440	128	0.68	2.15
			18.5	402	397	60	0.96	2.44
Task III:								
FeCrAlY	16.5	50	20.6	182	156	52	2.88	4.75
			21.9	192	162	38	2.45	3.82
			24.1	229	191	59	3.03	6.20
	12.6	78	17.9	198	164	44	2.90	4.91
			20.7	247	211	68	1.79	3.74
			21.7	224	182	56	2.18	4.26
	12.6	45	19.3	236	211	33	2.15	3.93
			20.4	230	206	38	2.30	4.37
			21.5	239	215	45	1.57	2.90
FeNiCrAlY	16.6	64	19.1	393	320	67	2.68	7.85
			20.7	457	368	88	2.70	10.30
			22.8	298	243	55	2.05	4.88
Task IV:								
FeNiCrAlY	16.6	64	19.7	452	350	83	3.40	13.8
			22.7	595	500	128	2.77	14.6
			22.3	600	500	118	2.17	11.0
			23.8	708	615	97	2.77	16.2
FeCrAlY	12.6	78	22.2	310	278	139	0.81	1.82
			22.1	350	284	172	2.44	7.67
			26.9	473	408	155	2.88	12.3
			22.4	386	343	81	2.32	7.6

(1) At 0.2% offset

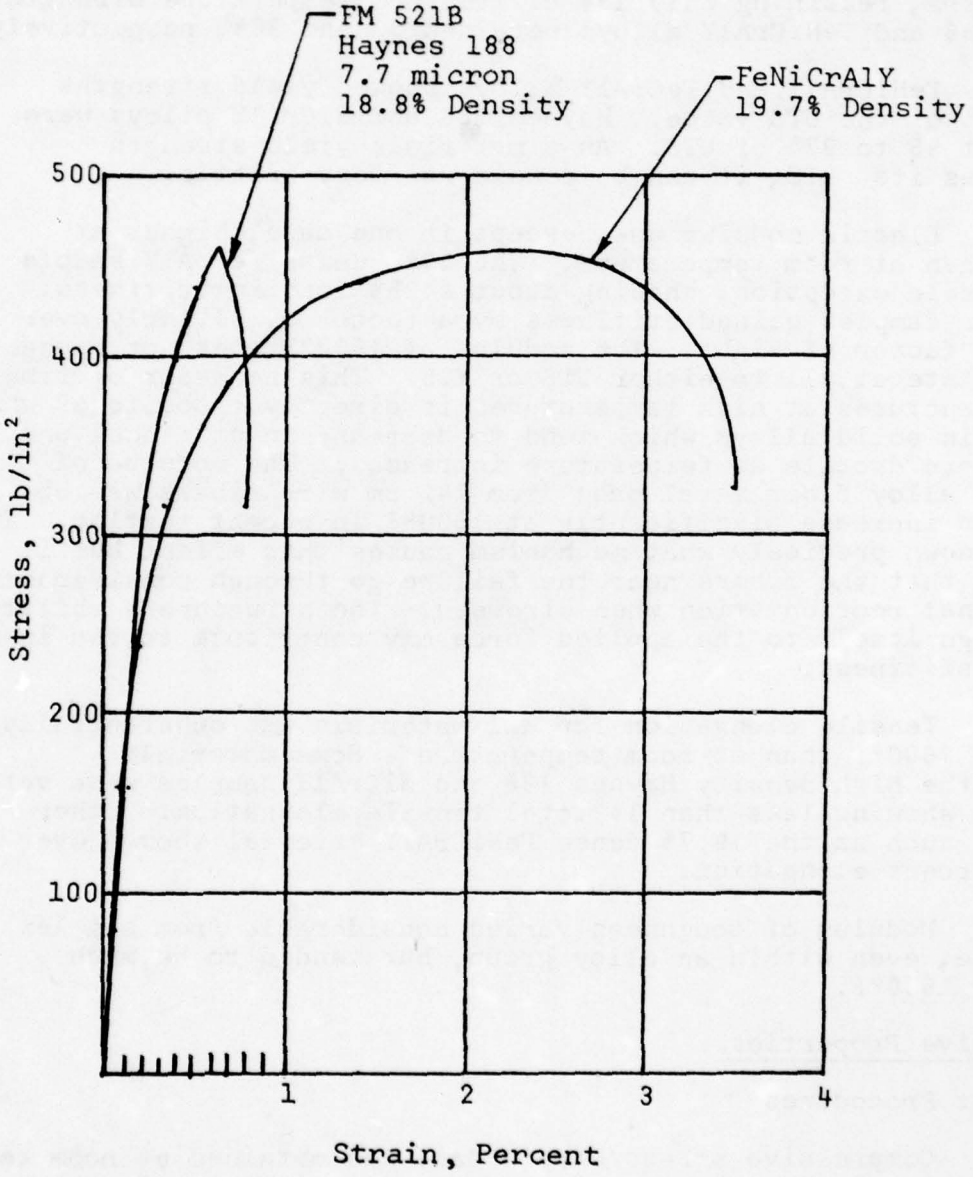

FIGURE 9

TYPICAL 1600°F TENSILE
STRESS VS. STRAIN

In contrast to the room temperature behavior of these materials, at 1600°F a distinct yield point is seen in the S/S plot of most variants. The yielding seen at the start of the S/S curve at room temperature is absent, in most cases, at 1600°F. Finally, though the materials appear more ductile just prior to failure, total elongation to failure is generally much less than at room temperature. The nickel base NiCrAlY materials showed the highest strength retention at 1600°F, averaging 42% of the room temperature strength. FeCrAlY was the weakest at elevated temperature, retaining only 19% of its room temperature strength. Haynes 188 and FeNiCrAlY alloys retained 33 and 36%, respectively.

FeNiCrAlY and FeCrAlY alloys showed yield strengths about 88% of the UTS value. Haynes 188 and NiCrAlY alloys were higher at 95 to 97% of UTS. As a materials yield strength approaches its UTS, it can be considered very brittle.

Elastic modulus was, except in one case, higher at 1600°F than at room temperature. The 29% dense FeCrAlY sample was the sole exception, showing about a 25% loss in stiffness. All other samples gained stiffness by a factor of slightly over one to a factor of eight. The modulus at 1600°F does not appear to correlate at all to either UTS or Y.S. This behavior of fiber metal structures at high temperatures is directly opposite of what is seen in solid alloys which tend to decrease in stiffness and become more ductile as temperature increases. The modulus of FeCrAlSi alloy fiber metal made from 142 μm wire fibers was observed to increase significantly at 1600°F in recent testing. It is not known precisely what mechanism causes this effect but it is known that the fibers near the failure go through considerable directional reorientation when stressed. The structure's ability to realign itself to the applied force may contribute to the increased stiffness.

Tensile elongation for all materials was substantially lower at 1600°F than at room temperature. Some materials such as the high density Haynes 188 and NiCrAlY samples were very brittle, showing less than 1% total tensile elongation. Other examples such as the 19.7% dense FeNiCrAlY material showed over three percent elongation.

Modulus of toughness varied considerable from sample to sample, even within an alloy group, but tended to be much lower at 1600°F.

Compressive Properties

Test Procedures

Compressive stress/strain data was obtained at room temperature up to 350 psi for each material variant. Testing was carried out in a dead weight type test apparatus especially designed to test fiber metal. The apparatus consists of two accurately manufactured hydraulic cylinders connected to each other by

suitable lines. Accurate weights are placed on the platform of one cylinder to yield an exact pressure within the test cylinder. This pressure transmits a known force to the 1/2 x 1/2 inch square test sample. A strain gauge type linear displacement transducer was used with an accurate digital readout ohmmeter to measure strain to the nearest ten thousandth of an inch. Strain was measured as a function of stress on both the loading and unloading portions of one cycle. Sample thickness was measured before and after the test to determine permanent set. Sample weight and dimensions were measured before the test to determine apparent density.

Results

The results are presented in Table X. Typical compressive stress/strain curves are shown in Figure 10 for the same two materials presented in Figures 4 and 9.

The majority of samples tended to deform a large amount at stress levels below 25 psi, then stiffened and reacted nearly linearly to increasing stress. Sample out-of-flat will contribute a large amount of apparent strain at low stress levels. If the sample does not lie completely flat on the test rig, its effective area of contact is actually much smaller than expected. Fiber metal structures tend to act like springs with a continuously decreasing pitch rather than conventional constant pitch springs. This may explain why the modulus generally tends to increase as the sample is compressed. Compressive moduli were estimated by taking the slope of the steepest portion of the loading portion of the cycle. The elastic modulus does not correlate well with sample density for these materials. Hardness tests were not run on these same samples so it is not known whether a good correlation exists between compressive elastic modulus and hardness.

Permanent set of each sample was measured after complete load release while the sample was still in the test fixture. The samples tend to spring back gradually after a period of hours to a thickness greater than that reported in the table.

For the Task IV materials, FeNiCrAlY samples had an average elastic modulus of 55.4×10^3 psi as compared to FeCrAlY which averaged 38.8×10^3 psi. FeNiCrAlY samples also showed less permanent set than FeCrAlY variants.

Hardness

Test Procedure

Three samples of each material variant were hardness tested at room temperature using a modified Rockwell superficial test procedure designated R_{5Z}. These were the same samples on which the tensile tests discussed previously were made. Soft, porous structures like fiber metal are best hardness tested using a large diameter ball indenter so that a large area is tested.

TABLE X

ROOM TEMPERATURE COMPRESSIVE PROPERTIES

Alloy	Avg. Fiber Diam. µm	Fiber L/D	Density %	Compr. Modulus psi x 10^3	Strain @ 50 psi %	Strain @ 350 psi %	Permanent Set @ 350 psi %
Task II:							
NiCrAlY	11.1	47	21.1	28.0	1.05	2.66	1.4
			31.8	23.0	1.64	4.40	3.4
FeNiCrAlY	16.6	64	24.6	33.3	2.10	3.55	0.9
			25.0	82.4	0.43	0.95	0.2
FeCrAlY	16.5	50	18.0	15.5	0.50	2.80	1.6
			26.2	33.3	2.46	4.02	2.2
	23.4	40	19.6	36.8	1.95	3.50	2.2
			31.6	90.9	1.95	3.31	2.5
Hayness 188	20.8	68	18.9	14.6	3.30	6.60	4.2
			31.2	14.9	2.86	4.55	2.5
	7.7	80	19.2	23.3	3.60	5.50	2.9
			19.1	15.9	2.67	5.70	2.3
Task III:							
FeCrAlY	16.5	50	20.8	36.4	0.01	0.70	0.3
			22.5	41.7	0.60	1.48	0.6
			24.0	41.7	0.63	1.44	0.4
	12.6	78	18.6	25.6	0.57	1.82	0.8
			20.5	31.8	0.49	1.54	0.6
			22.0	20.0	0.78	2.45	1.2
	12.6	45	19.7	25.9	0.44	1.63	0.6
			21.4	29.7	0.67	1.81	0.8
			21.8	19.4	1.10	2.77	0.4
FeNiCrAlY	16.6	64	19.8	14.4	1.00	3.28	2.0
			20.0	35.0	0.93	2.14	0.5
			24.9	42.2	0.62	1.64	0.8
Task IV:							
FeNiCrAlY	16.6	64	19.3	43.2	0.50	1.40	0.6
			22.6	72.9	0.28	0.86	0.3
			21.6	36.1	0.46	1.53	0.6
			24.4	69.3	0.30	0.91	0.2
FeCrAlY	12.6	78	20.2	25.5	0.83	2.35	1.5
			22.8	35.0	0.64	1.86	1.0
			24.5	53.8	0.50	1.31	0.8
			23.2	40.7	0.71	1.65	0.8

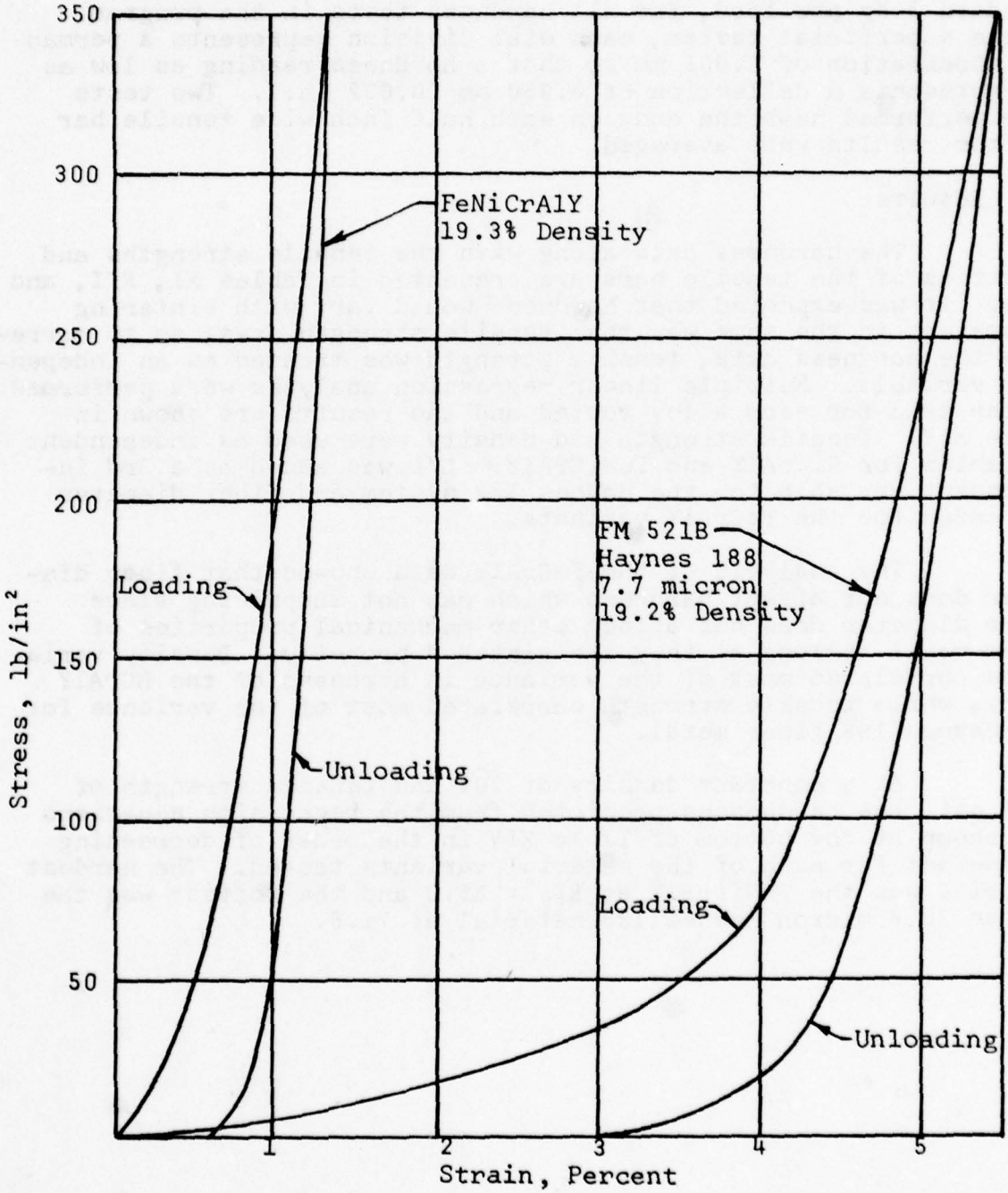

FIGURE 10

TYPICAL COMPRESSIVE
STRESS VS. STRAIN

A relatively small major load is used to avoid excessive penetration into the sample. For these reasons, a 0.750" dia. steel ball is used with a 5 kilogram major load in the R_{5Z} test. A Wilson superficial hardness testing machine was used, with the standard 3 Kg pre-load, for all hardness tests in the program. On the superficial tester, each dial division represents a permanent indentation of 0.001 mm so that a hardness reading as low as 50 represents a deflection of 0.050 mm (0.002 in.). Two tests were performed near the ends on each half inch wide tensile bar and the results were averaged.

Results

The hardness data along with the tensile strengths and densities of the tensile bars are presented in Tables XI, XII, and XIII. It was expected that hardness would vary with sintering parameters in the same way that tensile strength does; so to correlate the hardness data, tensile strength was treated as an independent variable. Multiple linear regression analyses were performed on the data for each alloy tested and the results are shown in Table XIV. Tensile strength and density were used as independent variables for NiCrAlY and FeNiCrAlY. L/D was added as a 3rd independent variable for the Haynes 188 system and fiber diameter was added for the FeCrAlY variants.

The analysis of the FeCrAlY data showed that fiber diameter does not affect hardness which was not surprising since fiber diameter does not affect other mechanical properties of fiber metal as long as they are sintered properly. Density variations correlated most of the variance in hardness of the MCrAlY alloys while tensile strength correlated most of the variance for the Haynes 188 fiber metal.

At a constant density of 20% and tensile strength of 1800 psi, the hardnesses predicted from the regression equations are shown at the bottom of Table XIV in the order of decreasing hardnesses for each of the material variants tested. The hardest material was the FeNiCrAlY at $R_{5Z} = 85.0$ and the softest was the coarse 20.8 micron Haynes 188 material at 71.8.

TABLE XI

TENSILE STRENGTH & HARDNESS
TASK II

Material	Fiber Dia. (μ)	Fiber L/D	Sample Thk. (in.)	Density (%)	Hardness R_{5Z}	UTS (psi)
NiCrAlY	11.1	47	0.123	19.2	81	1550
		47	0.120	19.8	82	1610
		47	0.122	19.1	79	1500
		47	0.122	31.4	97	2710
		47	0.122	31.2	98	3240
		47	0.122	30.9	97	3010
FeNiCrAlY	16.6	64	0.095	24.1	90	1060
		64	0.095	23.4	94	1160
		64	0.093	22.7	92	1330
		64	0.142	24.8	95	2600
		64	0.141	25.4	97	2680
		64	0.142	25.5	96	2790
FeCrAlY	16.5	50	0.107	18.8	67	660
		50	0.107	18.0	60	610
		50	0.108	18.3	73	560
		50	0.128	26.0	86	1410
		50	0.127	26.5	85	1390
		50	0.128	27.2	88	1340
	23.4	40	0.113	17.1	57	540
		40	0.113	17.7	61	570
		40	0.114	19.2	70	710
		40	0.113	29.0	94	2140
		40	0.113	28.9	92	2180
		40	0.114	29.8	91	2200
Haynes 188	20.8	68	0.088	16.7	59	770
		68	0.088	18.9	69	1200
		68	0.087	27.5	87	3360
		68	0.088	28.7	85	3390
		68	0.088	26.2	86	2950
	7.7	80	0.124	18.6	75	1540
		80	0.126	18.6	78	1660
		80	0.124	18.9	77	1660
		80	0.126	18.9	75	1250
		80	0.127	18.7	76	1330
		80	0.127	18.1	72	1140

TABLE XII

TENSILE STRENGTH & HARDNESS
TASK III

Material	Fiber Dia. (μ)	Fiber L/D	Sample Thk. (in.)	Density (%)	Hardness R_{5Z}	UTS (psi)
FeCrAlY	16.5	50	0.111	22.3	75	1280
			0.111	20.3	79	1020
			0.110	20.9	75	1070
			0.115	23.1	79	1390
			0.116	23.8	85	1440
			0.115	22.6	80	1320
			0.113	24.2	83	1430
			0.112	24.4	83	1480
			0.114	25.6	88	1450
	12.6	78	0.133	19.7	76	1320
			0.132	18.2	70	1070
			0.134	18.6	71	1060
			0.130	21.6	81	1700
			0.130	20.5	79	1380
			0.130	20.9	82	1420
			0.130	22.0	77	1060
			0.129	22.6	80	1230
			0.129	21.5	76	980
		45	0.129	18.8	66	980
			0.130	18.9	66	1060
			0.128	19.7	70	1180
			0.131	20.6	77	1240
			0.132	20.9	77	1350
			0.133	20.3	76	1190
			0.133	22.0	77	1180
			0.133	22.3	73	1190
			0.135	21.8	73	1090
FeNiCrAlY	16.6	64	0.129	19.0	79	1260
			0.126	19.5	78	1610
			0.130	19.5	82	1460
			0.129	20.2	86	1330
			0.130	20.4	86	1360
			0.133	20.4	85	1530
			0.133	21.7	78	640
			0.132	22.1	77	660
			0.132	22.0	76	620

TABLE XIII

TENSILE STRENGTH & HARDNESS
TASK IV

Material	Fiber Dia. (μ)	Fiber L/D	Sample Thk. (in.)	Density (%)	Hardness R_{5Z}	UTS (psi)
FeNiCrAlY	16.6	64	0.127	19.8	87	1850
			0.128	20.1	90	1820
			0.126	21.3	88	2150
			0.115	22.9	92	2320
			0.114	23.4	92	2290
			0.127	22.4	90	2230
			0.127	24.1	93	2790
			0.124	22.0	91	2370
			0.126	22.0	90	2240
			0.131	23.7	94	2540
			0.124	22.8	92	2310
↓	↓	↓	0.124	23.3	93	2220
FeCrAlY	12.6	78	0.125	21.6	82	1930
			0.124	21.3	86	1970
			0.122	22.8	88	2320
			0.127	22.5	83	2090
			0.128	22.4	84	2070
			0.136	22.0	85	1860
			0.127	23.1	85	1970
			0.126	22.8	86	1860
			0.121	23.4	79	2470
			0.127	22.8	81	1720
			0.130	23.1	85	1780
↓	↓	↓	0.129	22.4	85	2260
Haynes 188	7.7	80	0.128	18.5	76	1700
			0.128	18.4	74	1660
			0.128	18.6	76	1630
			0.124	18.5	70	1370
			0.124	18.4	71	1370
↓	↓	↓	0.124	18.3	70	1340

TABLE XIV

HARDNESS REGRESSION ANALYSIS

Alloy	Multiple Correlation Coeff.	Independent Variables Used(1)	Variation Explained	Significance Level Percent
FeNiCrAlY:		X_1	13.6	99.84
		X_2	60.6	99.99
	0.861		74.2	
Equation: $Y = 47.1 + 0.00522X_1 + 1.426X_2$				
FeCrAlY:		X_1	1.7	98.17
		X_2	72.3	100.00
		X_3	12.7	99.82
		X_4	-	insign.
	0.931		86.7	
Equation: $Y = 20.4 + 0.00381X_1 + 2.06X_2 + 0.123X_3$				
NiCrAlY:		X_1	-	insign.
		X_2	99.2	100.00
	0.996		99.2	
Equation: $Y = 53.3 + 1.414X_2$				
Haynes 188		X_1	78.6	100.00
		X_2	-	insign.
		X_3	11.9	99.94
		X_4	-	insign.
	0.951		90.5	
Equation: $Y = 22.1 + 0.00987X_1 + 0.469X_3$				

Results @ 1800 psi & 20% density:

Alloy	L/D	Fiber Dia. µm	Calculated Hardness, R_{5Z}
FeNiCrAlY	64	16.6	85.0
NiCrAlY	47	11.1	81.6
FeCrAlY	78	12.6	78.1
Haynes 188	80	7.7	77.4
FeCrAlY	50	16.5	74.6
FeCrAlY	45	12.6	74.0
FeCrAlY	40	23.4	73.4
Haynes 188	68	20.8	71.8

(1) Y = Hardness, R_{5Z}
X_1 = Ultimate tensile strength, psi
X_2 = % Density
X_3 = L/D
X_4 = Fiber Diameter, micrometers

Rig Testing
Static Oxidation

Equipment and Procedure

All material variants were tested by cyclic oxidation in a static air environment at each of three temperatures - 1200, 1400, and 1600°F. Details of the equipment are described in Appendix A.

On each isotherm, twelve specimens, 6" x 0.5" x 0.125", were attached to the sample holder rods and automatically cycled into the furnace for one hour of soak at the specified temperature and then removed for 1 minute each hour for convection air cooling to approximately 300°F. Spall was collected in quartz thimbles in the furnace and in alumina crucibles during the cooling period. The specimens and spall were cooled in a desiccator and weighed after initial test intervals of 4 and 8 hours and then daily after 20 hour exposure intervals in order to obtain differential weight gain data. In order to obtain strength loss data as a function of oxidation weight gain, the oxidized specimens were used as tensile bars and removed for tensile testing after cumulative times of 4, 68, and 308 hours. Hardnesses (Rockwell 5Z) were measured at the ends of the specimens before and after exposure to determine the effect of oxidation on material hardness.

Discussion of Results

Data and Results

The data for each isotherm and each of the three exposure times are presented in Tables XV through XXIII. Cumulative weight gains as a function of time for several of the material variants are shown in Figures 11 through 17.

The percent weight gains shown in the tables include any spall that was collected during exposure. All MCrAlY specimens had a negligible spall representing less than 0.01% wt. gain. The only material that had any significant spallation was the 7.7 micron Haynes 188 baseline material, FM-521. With this material, the maximum spall observed represented less than 0.10% of the specimen weights. Consequently, spallation is an insignificant factor in oxidation testing of fiber metal seal materials up to 1600°F.

For each of the alloy systems tested, the percent reduction in tensile strength was plotted against percent oxidation weight gain as shown in Figures 18 to 21. The observed tensile strengths on the oxidized specimens were corrected for the effect of density on tensile strength in order to relate their strength loss to the unoxidized tensile bars from the same sheet. Although there is some scatter, the percent strength loss on this basis appears to be independent of the fiber diameter, test temperature, or initial tensile strength. The MCrAlY alloys showed greater strength retentions for a given oxidation level than the Haynes 188 alloy. Engine operating experience with the FM-521 material has shown the vane

TABLE XV
STATIC OXIDATION TEST DATA
4 HOURS EXPOSURE, 1600 °F

Material	L/D	Fiber Dia. (μm)	Sheet Average Tens. Strength psi @	% Dens.	Oxidation Specimen Data: % Dens.	Pre-oxid. Wt. Gain %	Total Wt. Gain %	% Change in UTS	UTS (psi)	Hardness R_{5Z} Before	After
TASK II											
NiCrAlY	47	11.1	1550	19.4	19.8		3.7	+1.6	1640	86	86
			2990	31.2	34.9		2.5	+2.0	3820	96	96
FeNiCrAlY	64	16.6	1180	23.4							
			2690	25.2							
FeCrAlY	50	16.5	610	18.4	17.2		0.9	-5.5	450	61	60
			1380	26.6	25.9		0.8	+32.3	1730	86	87
	40	23.4	610	18.0	18.3		0.5	+28.4	810	74	67
			2170	29.2	28.2		0.6	+22.6	2480	91	89
Haynes 188	68	20.8	980	17.5	15.6		2.0	-28.0	560	65	67
			3240	27.5	28.6		1.4	-14.4	3000	75	89
(1)	80	7.7	1240	18.6	18.9		2.2	-22.7	990	81	84
(1)			1620	18.7	18.5		2.6	-27.5	1150	80	87
TASK III											
FeCrAlY	50	16.5	1120	21.3	24.3		0.7	+24.7	1820	81	83
			1380	23.2	25.5		0.8	+18.1	1970	85	83
			1460	24.7	25.2		0.5	+21.7	1850	87	82
	78	12.6	1150	18.8	21.9		1.2	+20.3	1880	83	78
			1500	21.0	23.1		1.3	+0.2	1820	82	81
			1090	22.0	23.0		1.6	+33.4	1590	83	88
	45		1070	19.1	20.4		1.8	-17.3	1010	78	75
			1260	20.5	22.1		1.7	+6.8	1550	81	78
			1150	22.0	24.0		2.2	+25.6	1720	82	86
FeNiCrAlY	64	16.6	1440	19.3	20.6	2.2	2.3	+7.2	1760	81	72
			1410	20.3	23.1	2.6	2.7	+25.3	2290	89	87
			640	21.9	25.1	3.2	3.4	+110.3	1770	89	91
TASK IV											
FeNiCrAlY	64	16.6	1940	20.1	19.8	2.1	2.9	-6.5	1760		84
			2280	22.9	23.7	2.5	3.6	-3.4	2360		89
			2460	22.7	24.8	2.3	2.7	+8.9	3200		90
			2350	23.3	26.4	2.3	2.9	+9.9	3320		93
FeCrAlY	78	12.6	2070	21.9	21.7		1.7	-19.8	1630		84
			2010	22.9	22.0		2.0	-14.6	1670		88
			2100	23.1	24.0		1.7	-1.2	2240		89
			1920	22.8	24.0		1.6	+16.5	2480		87

(1) - Base line material, FM-521

TABLE XVI
STATIC OXIDATION TEST DATA
68 HOURS EXPOSURE, 1600°F

Material	L/D	Fiber Dia. (μm)	Sheet Average Tens. Strength psi @ % Dens.		Oxidation Specimen Data % Dens.	Pre-oxid. Wt. Gain %	Total Wt. Gain %	% Change in UTS	UTS (psi)	Hardness Rc Before	Hardness Rc After
TASK II											
NiCrAlY	47	11.1	1550	19.4	19.4		6.7	-41.3	910	86	83
			2990	31.2	30.8		4.6	-7.6	2690	96	93
FeNiCrAlY	64	16.6	1180	23.4							
			2690	25.2							
FeCrAlY	50	16.5	610	18.4	18.9		2.8	-11.5	570	61	66
			1380	26.6	28.7		3.2	+13.8	1830	86	89
	40	23.4	610	18.0	19.5		1.5	+10.3	790	74	70
			2170	29.2	30.9		2.1	+15.2	2800	91	93
Haynes 188	68	20.8	980	17.5	18.1		7.2	-82.8	180	65	45
			3240	27.5	27.4		7.1	-73.0	870	75	91
(1)	80	7.7	1240	18.6	18.9		24.4	-93.8	80(2)	81	69
(1)			1620	18.7	19.1		27.6		N.A.(2)	80	36
TASK III											
FeCrAlY	50	16.5	1120	21.3	23.4		1.2	-0.2	1350	78	82
			1380	23.2	24.0		1.6	-1.2	1460	82	83
			1460	24.7	24.6		1.7	+9.1	1580	84	64
	78	12.6	1150	18.8	20.5		1.7	+8.9	1490	81	78
			1500	21.0	22.5		2.9	-3.1	1670	82	78
			1090	22.0	22.3		4.2	-3.6	1080	80	86
	45		1070	19.1	19.4		4.7	-33.0	740	69	77
			1260	20.6	21.2		4.6	-7.9	1230	79	84
			1150	22.0	22.8		5.6	+6.0	1310	78	84
FeNiCrAlY	64	16.6	1440	19.3	20.2	2.4	3.0	-3.7	1520	81	80
			1410	20.3	22.7	2.8	3.5	+7.7	1900	90	86
			640	21.9	24.2	3.7	4.9	+48.3	1160	85	88
TASK IV											
FeNiCrAlY	64	16.6	1940	20.1	20.2	2.3	4.4	-25.0	1470		89
			2280	22.9	23.2	2.3	5.0	-20.5	1860		92
			2460	22.7	25.1	2.3	3.7	-14.6	2570		91
			2350	23.3	26.6	2.6	4.1	-3.5	2960		94
FeCrAlY	78	12.6	2070	21.9	21.8		4.8	-32.7	1380		85
			2010	22.3	21.7		6.0	-32.3	1290		88
			2100	23.1	23.7		5.0	-21.8	1730		92
			1920	22.9	24.4		5.0	-9.6	1990		92

(1) Baseline Material, FM-521
(2) 48 hr. exposure.

TABLE XVII
STATIC OXIDATION TEST DATA
308 HOURS EXPOSURE, 1600°F

Material	L/D	Fiber Dia. (μm)	Sheet Tens. Strength psi @ % Dens.	Average Strength	Oxidation Specimen Data % Dens.	Pre-oxid. Wt. Gain %	Total Wt. Gain %	% Change in UTS	UTS (psi)	Hardness Before	Hardness After	Useful Oxidation Life, hrs(2)
TASK II												
NiCrAlY	47	11.1	1550	19.4	19.4		5.5	-21.9	1210	86	80	1200
			2990	31.2	31.7		5.3	-3.8	2970	96	90	1500
FeNiCrAlY	64	16.6	1180	23.4	24.6		12.7	-54.0	600(3)	93	96	56
			2690	25.2	24.8		14.2	-81.6	480(3)	94	94	40
FeCrAlY	50	16.5	610	18.4	18.6		2.4	-34.2	410	61	64	1.2×10^5
			1380	26.6	25.9		4.0	-4.4	1250	86	91	10400
	40	23.4	610	18.0	17.6		1.5	+14.9	670	74	72	1.5×10^6
			2170	29.2	28.7		2.6	-5.1	1990	91	84	88000
Haynes 188	68	20.6	980	17.5								24
			3240	27.5								29
(1)	80	7.7	1240	18.6								9
(1)			1620	18.7								6
TASK III												
FeCrAlY	50	16.5	1120	21.3	22.7		2.1	-1.8	1250	82	86	2.5×10^5
			1380	23.2	23.3		2.6	-15.9	1170	83	82	88000
			1460	24.7	24.5		3.1	-17.8	1180	85	89	33000
	78	12.6	1150	18.8	19.9		2.7	-4.6	1230	78	84	64000
			1500	21.0	22.1		4.3	-23.0	1280	80	86	7200
			1090	22.0	22.2		9.0	-39.6	670	78	89	200
	45		1070	19.1	19.1		7.2	-17.8	880	74	85	620
			1260	20.6	20.9		7.6	-2.1	1270	77	93	400
			1150	22.0	22.3		8.3	+6.6	1260	75	90	290
FeNiCrAlY	64	16.6	1440	19.3	19.9	2.5	4.0	-12.5	1340	83	78	31000
			1410	20.3	21.6	3.0	4.7	-18.0	1310	87	83	11000
			640	21.9	23.2	4.0	6.5	-1.2	710	82	84	1200
TASK IV												
FeNiCrAlY	64	16.6	1940	20.1	20.6	2.4	6.4	-38.2	1260		85	500
			2280	22.9	23.2	2.4	6.8	-26.5	1720		91	640
			2460	22.7	24.6	2.4	5.2	-24.6	2180		91	2000
			2350	23.3	25.7	2.3	5.9	-20.7	2270		93	920
FeCrAlY	78	12.6	2070	21.9	21.7		7.5	-52.8	960		92	380
			2010	22.3	22.2		11.8	-39.8	1200		94	170
			2100	23.1	22.4		8.8	-24.0	1500		93	260
			1920	22.8	23.4		8.4	-19.9	1620		94	280

(1) Baseline Mat'l, FM-521
(2) At 40% Strength Loss
(3) 240 Hr. Exposure

TABLE XVIII
STATIC OXIDATION TEST DATA
4 HOURS EXPOSURE, 1400°F

Material	L/D	Fiber Dia. (μm)	Sheet Tens. Average Strength psi @ % Dens.		Oxidation Specimen Data % Dens.	Pre-oxid. Wt. Gain %	Total Wt. Gain %	% Change in UTS	UTS (psi)	Hardness R_{5Z} Before	After
TASK II											
NiCrAlY	47	11.1	1550	19.4	20.3		0.8	+21.9	2070	86	87
			2990	31.2	33.2		0.6	+14.5	3880	96	95
FeNiCrAlY	64	16.6	1180	23.4	24.2		0.7	+80.6	2280	93	93
			2690	25.2	25.6		0.6	+15.6	3210	94	95
FeCrAlY	50	16.5	610	18.4	18.3		0.3	-0.6	600	61	64
			1380	26.6	27.7		0.3	+46.3	2190	86	85
	40	23.4	610	18.0	19.5		0.2	+35.4	970	74	71
			2170	29.2	29.3		0.3	+23.1	2690	91	84
Haynes 188	68	20.8	980	17.5	19.7		1.2	+5.4	1310	65	61
			3240	27.5	27.8		0.9	-7.0	3080	75	88
(1)	80	7.7	1240	18.6	19.4		1.3	-7.4	1250	81	77
(1)			1620	18.7	18.9		1.3	-10.6	1480	80	80
TASK III											
FeCrAlY	50	16.5	1120	21.3	21.1		0.3	+1.0	1110	78	73
			1380	23.2	25.9		0.3	+17.3	2020	86	88
			1460	24.7	25.3		0.3	+16.2	1780	86	89
	78	12.6	1150	18.8	20.0		0.3	+5.2	1370	76	84
			1500	21.0	21.7		0.3	+9.9	1760	80	81
			1090	22.0	23.5		0.4	+49.5	1860	82	88
	45		1070	19.1	19.9		0.5	+9.3	1270	73	77
			1260	20.6	22.8		0.4	+21.0	1870	85	84
			1150	22.0	24.0		0.5	+38.0	1890	84	84
FeNiCrAlY	64	16.6	1440	19.3	21.0	2.1	2.1	+9.0	1860	80	85
			1410	20.3	23.0	2.6	2.6	+16.4	2110	87	90
			640	21.9	25.0	3.1	3.1	+149.1	2080	90	88
TASK IV											
FeNiCrAlY	64	16.6	1940	20.1	21.0	2.3	2.4	-16.9	1760		85
			2280	22.9	24.9	2.1	2.7	+6.4	2870		93
			2460	22.7	23.2	2.6	2.7	-8.6	2350		86
			2350	23.3	24.9	2.5	2.9	+2.4	2750		91
FeCrAlY	78	12.6	2070	21.9	21.1		0.4	-8.9	1750		79
			2010	22.3	22.1		0.5	+3.9	2050		83
			2100	23.1	24.4		0.4	+1.5	2380		88
			1920	22.8	25.5		0.4	+23.5	2970		87

(1) Baseline material, FM-521

TABLE XIX
STATIC OXIDATION TEST DATA
68 HOURS EXPOSURE, 1400°F

Material	L/D	Fiber Dia. (μm)	Sheet Average Tens. Strength psi @ % Dens.		Oxidation Specimen Data % Dens.	Pre-oxid. Wt. Gain %	Total Wt. Gain %	% Change in UTS	UTS (psi)	Hardness R_{5Z} Before	Hardness R_{5Z} After
TASK II											
NiCrAlY	47	11.1	1550	19.4	19.7		2.7	+3.8	1660	87	87
			2990	31.2	32.3		1.3	+19.8	3840	90	91
FeNiCrAlY	64	16.6	1180	23.4	23.5		1.1	+52.1	1810	91	89
			2690	25.2	25.4		1.1	+14.5	3130	94	93
FeCrAlY	50	16.5	610	18.4	18.0		0.7	+4.5	610	60	64
			1380	26.6	26.9		0.5	+33.2	1880	88	84
	40	23.4	610	18.0	18.7		0.4	+29.1	850	72	65
			2170	29.2	28.5		0.5	+7.4	2220	92	93
Haynes 188	68	20.8	980	17.5	19.3		2.1	+21.2	940	73	74
			3240	27.5	28.4		1.9	-19.0	2800	89	87
(1)	80	7.7	1240	18.6	19.2		3.4	-32.7	890	81	77
(1)			1620	18.7	18.6		3.7	-39.5	970	79	83
TASK III											
FeCrAlY	50	16.5	1120	21.3	21.9		0.6	+7.2	1270	81	76
			1380	23.2	24.6		0.6	+8.2	1680	86	88
			1460	24.7	24.7		0.6	+9.6	1600	86	89
	78	12.6	1150	18.8	18.7		0.7	+2.8	1170	71	75
			1500	21.0	21.0		0.7	+2.7	1540	83	83
			1090	22.0	23.1		0.8	+23.1	1480	82	85
	45		1070	19.1	19.4		1.0	+5.1	1160	66	77
			1260	20.6	21.5		0.9	+15.1	1580	83	81
			1150	22.0	23.2		1.2	+23.5	1580	79	83
FeNiCrAlY	64	16.6	1440	19.3	21.0	2.3	2.5	+16.1	1980	83	81
			1410	20.3	22.4	2.7	3.0	+10.6	1900	84	84
			640	21.9	24.2	3.6	3.7	+41.9	1110	87	91
TASK IV											
FeNiCrAlY	64	16.6	1940	20.1	20.8	2.4	3.2	-24.5	1570		81
			2280	22.9	24.1	2.3	3.4	-7.4	2340		89
			2460	22.7	23.0	2.7	3.2	-14.1	2170		86
			2350	23.3	24.9	2.9	3.0	-0.2	2680		92
FeCrAlY	78	12.6	2070	21.9	21.3		0.7	-14.2	1680		77
			2010	22.3	22.0		0.9	-13.6	1690		82
			2100	23.1	23.5		0.8	-4.3	2080		88
			1920	22.8	24.6		0.8	+9.1	2440		88

(1) Baseline Material, FM-521

TABLE XX
STATIC OXIDATION TEST DATA
308 HOURS EXPOSURE, 1400°F

Material	L/D	Fiber Dia. (μm)	Sheet Tens. Strength psi @	% Dens.	Oxidation Specimen Data: % Dens.	Pre-oxid. Wt. Gain %	Total Wt. Gain %	% Change in UTS	UTS (psi)	Hardness R_{5Z} Before	Hardness R_{5Z} After	Useful Oxidation Life, Hrs(2)
TASK II												
NiCrAlY	47	11.1	1550	19.4	19.4		3.9	-14.8	1320	85	86	5900
			2990	31.2	32.3		2.0	-0.2	3200	93	94	1.7×10^5
FeNiCrAlY	64	16.6	1180	23.4	23.3		1.5	+10.3	1290	92	89	1.4×10^6
			2690	25.2	25.7		1.5	+10.4	3090	95	94	1.2×10^6
FeCrAlY	50	16.5	610	18.4	17.8		0.8	-0.1	570	64	72	2.6×10^7
			1380	26.6	26.6		0.7	+18.1	1630	80	78	5.6×10^7
	40	23.4	610	18.0	18.1		0.6	+21.6	750	70	67	1.4×10^6
			2170	29.2	28.2		0.7	+7.3	2170	86	84	7.5×10^7
Haynes 188	68	20.8	980	17.5	19.3		2.9	-30.4	830	70	77	1200
			3240	27.5	28.8		3.1	-27.1	2590	88	92	1500
(1)	80	7.7	1240	18.6	19.1		8.1	-49.5	660(3)	80	80	74
(1)			1620	18.7	18.5		11.8	-74.1	410(3)	79	78	66
TASK III												
FeCrAlY	50	16.5	1120	21.3	20.6		0.8	+2.6	1050	76	83	3.3×10^7
			1380	23.2	24.1		0.7	-1.3	1470	84	86	4.8×10^7
			1460	24.7	24.6		0.8	-0.6	1440	88	91	3.7×10^7
	78	12.6	1150	18.8	18.3		0.9	-6.4	1020	71	76	1.8×10^7
			1500	21.0	20.4		0.9	-0.4	1410	81	87	1.5×10^7
			1090	22.0	22.7		1.5	-13.9	1000	78	87	1.3×10^8
	45		1070	19.1	19.1		1.4	+0.9	1080	70	78	1.7×10^6
			1260	20.6	21.1		1.4	+2.1	1350	77	82	1.6×10^6
			1150	22.0	22.6		2.4	+7.1	1300	80	84	1.3×10^5
FeNiCrAlY	64	16.6	1440	19.3	20.6	2.5	2.6	-0.1	1640	81	83	>100000
			1410	20.3	21.9	2.8	3.1	-10.5	1470	84	88	"
			640	21.9	23.6	4.4	4.5	+7.6	800	83	86	"
TASK IV												
FeNiCrAlY	64	16.6	1940	20.1	21.1	2.6	2.8	-14.9	1820		87	>100000
			2280	22.9	24.1	2.9	3.1	-13.7	2180		89	"
			2460	22.7	22.8	2.7	2.9	-6.1	2330		87	"
			2350	23.3	23.9	2.9	3.1	-15.5	2090		91	"
FeCrAlY	78	12.6	2070	21.9	21.3		1.1	-18.3	1600		79	7.2×10^6
			2010	22.3	22.2		1.6	-16.7	1660		83	8.8×10^5
			2100	23.1	22.8		1.7	-4.2	1960		88	8.3×10^5
			1920	22.8	24.0		1.7	-6.5	1990		87	6.5×10^5

(1) Baseline Material, FM-521
(2) After 40% strength loss
(3) 128 Hr. Exposure

TABLE XXI
STATIC OXIDATION TEST DATA
4 HOURS EXPOSURE, 1200°F

Material	L/D	Fiber Dia. (μm)	Sheet Tens. Strength psi @ % Dens.		Oxidation Specimen Data: % Dens.	Pre-oxid. Wt. Gain %	Total Wt. Gain %	% Change in UTS	UTS (psi)	Hardness R_{5Z} Before	Hardness R_{5Z} After
TASK II											
NiCrAlY	47	11.1	1550	19.4	19.5		0.2	+1.5	1590	83	87
			2990	31.2	32.3		0.5	+20.7	3870	94	97
FeNiCrAlY	64	16.6	1180	23.4	24.1		0.2	+27.0	1590	90	88
			2690	25.2	27.8		0.2	+25.1	4100	95	95
FeCrAlY	50	16.5	610	18.4	20.0		0.1	+17.9	850	71	71
			1380	26.6	29.2		0.1	+44.2	2400	83	88
	40	23.4	610	18.0	20.1		0.1	+9.0	830	76	64
			2170	29.2	32.5		0.1	+28.6	3460	91	85
Haynes 188	68	20.8	980	17.5	18.8		0.2	+17.5	1330	63	63
			3240	27.5	32.6		0.2	+3.3	4710	88	89
(1)	80	7.7	1240	18.6	18.2		0.8	-15.8	1000	79	79
(1)			1620	18.7	19.2		0.8	-9.3	1550	82	84
TASK III											
FeCrAlY	50	16.5	1120	21.3	21.2		0.1	+1.9	1130	75	73
			1380	23.2	23.1		0.1	+6.0	1450	81	84
			1460	24.7	25.9		0.1	+6.5	1710	86	85
	78	12.6	1150	18.8	19.5		0.1	+3.4	1280	78	74
			1500	21.0	21.7		0.1	+4.2	1670	79	80
			1090	22.0	22.9		0.1	+54.9	1830	86	88
	45		1070	19.1	20.6		0.1	+5.2	1310	77	77
			1260	20.6	21.2		0.1	+4.1	1390	75	79
			1150	22.0	22.2		0.2	+20.4	1410	75	82
FeNiCrAlY	64	16.6	1440	19.3	21.3	2.6	2.6	-2.6	1710	79	90
			1410	20.3	22.0	2.4	2.4	+7.4	1780	86	90
			640	21.9	23.9	3.9	3.9	+69.1	1290	89	89
TASK IV											
FeNiCrAlY	64	16.6	1940	20.1	22.8	2.3	2.3	+6.0	2650		90
			2280	22.9	22.3	2.5	2.5	-7.9	1990		89
			2460	22.7	25.1	2.2	2.2	-14.3	2580		91
			2350	23.3	25.7	2.9	2.9	+4.5	2990		95
FeCrAlY	78	12.6	2070	21.9	22.6		0.1	-13.8	1990		85
			2010	22.3	23.3		0.1	+17.1	2570		85
			2100	23.1	23.5		0.1	-9.4	1970		86
			1920	22.8	22.8		0.1	+2.6	1970		82

(1) Baseline Material, FM-521

TABLE XXII
STATIC OXIDATION TEST DATA
68 HOURS EXPOSURE, 1200°F

Material	L/D	Fiber Dia. (μm)	Sheet Tens. Strength psi	Average % Dens.	Oxidation Specimen Data % Dens.	Pre-oxid. Wt. Gain %	Total Wt. Gain %	% Change in UTS	UTS (psi)	Hardness R_{5Z} Before	After
TASK II											
NiCrAlY	47	11.1	1550	19.4	19.3		0.6	-7.4	1420	84	81
			2990	31.2	32.6		0.6	+10.9	3620	91	96
FeNiCrAlY	64	16.6	1180	23.4	23.7		0.5	+26.4	1530	91	85
			2690	25.2	26.7		0.4	+19.5	3610	94	94
FeCrAlY	50	16.5	610	18.4	19.6		0.2	+17.0	810	70	71
			1380	26.6	28.2		0.2	+32.1	2050	91	86
	40	23.4	610	18.0	19.6		0.1	+6.4	770	71	75
			2170	29.2	31.6		0.1	+16.8	2970	90	83
Haynes 188	68	20.8	980	17.5	18.2		0.7	+8.5	1150	65	65
			3240	27.5	27.1		0.7	-3.1	3050	84	83
(1)	80	7.7	1240	18.6	18.6		1.2	-27.4	900	76	78
(1)			1620	18.7	18.7		1.6	-17.3	1340	82	82
TASK III											
FeCrAlY	50	16.5	1120	21.3	21.2		0.2	-3.6	1070	77	85
			1380	23.2	22.5		0.2	+1.0	1310	80	85
			1460	24.7	25.8		0.2	+0.4	1600	79	86
	78	12.6	1150	18.8	18.8		0.2	-11.3	1020	71	75
			1500	21.0	21.3		0.2	+3.7	1600	82	90
			1090	22.0	22.4		0.3	+27.4	1440	81	84
	45		1070	19.1	20.2		0.3	+5.2	1260	77	79
			1260	20.6	20.9		0.3	+6.4	1380	77	79
			1150	22.0	22.1		0.3	+12.9	1310	78	79
FeNiCrAlY	64	16.6	1440	19.3	20.8	2.6	2.6	+0.4	1680	78	80
			1410	20.3	21.6	2.7	2.7	+10.8	1770	85	84
			640	21.9	23.7	4.4	4.4	+28.0	960	85	88
TASK IV											
FeNiCrAlY	64	16.6	1940	20.1	22.6	2.4	2.4	+5.5	2590		88
			2280	22.9	22.5	2.5	2.5	-5.0	2090		91
			2460	22.7	22.9	2.4	2.4	+1.4	2540		90
			2350	23.3	24.8	2.7	2.7	+6.2	2830		94
FeCrAlY	78	12.6	2070	21.9	22.3		0.3	-8.2	1970		83
			2010	22.3	22.8		0.2	+9.0	2290		87
			2100	23.1	23.7		0.3	+6.3	2350		86
			1920	22.8	22.2		0.3	-6.6	1700		84

(1) Baseline Material, FM-521

TABLE XXIII
STATIC OXIDATION TEST DATA
308 HOURS EXPOSURE, 1200°F

Material	L/D	Fiber Dia. (μm)	Sheet Tens. Strength psi @ % Dens.		Oxidation Specimen Data: % Dens.	Pre-oxid. Wt. Gain %	Total Wt. Gain %	% Change in UTS	UTS (psi)	Hardness R_{5Z} Before	Hardness R_{5Z} After	Useful Oxidation Life, Hr(2)
TASK II												
NiCrAlY	47	11.1	1550	19.4	19.4		0.8	-5.8	1460	84	85	1.2×10^7
			2990	31.2	31.5		0.9	+7.0	3260	95	92	9.3×10^6
FeNiCrAlY	64	16.6	1180	23.4	22.9		0.6	+46.0	1650	92	86	6.9×10^7
			2690	25.2	26.1		0.5	+16.4	3360	95	94	4.4×10^8
FeCrAlY	50	16.5	610	18.4	19.0		0.2	+7.6	700	68	78	2.5×10^{10}
			1380	26.6	27.5		0.3	+14.5	1690	88	87	8.5×10^9
	40	23.4	610	18.0	19.5		0.1	+18.6	850	74	75	2.7×10^{11}
			2170	29.2	30.3		0.2	-2.0	2290	90	21	7.1×10^{10}
Haynes 188	68	20.8	980	17.5	17.6		1.1	-5.2	940	63	66	1.6×10^5
			3240	27.5	26.9		1.2	-9.3	2810	82	91	1.5×10^5
(1)	80	7.7	1240	18.6	18.2		1.7	-29.2	840	73	80	14,000
(1)			1620	18.7	19.0		1.8	-25.9	1240	81	80	20,000
TASK III												
FeCrAlY	50	16.5	1120	21.3	21.2		0.2	-3.6	1070	74	80	2.0×10^{10}
			1380	23.2	22.4		0.2	+1.1	1300	79	80	2.0×10^{10}
			1460	24.7	25.7		0.3	-5.1	1500	80	89	8.5×10^9
	78	12.6	1150	18.8	18.8		0.3	-7.0	1070	73	73	7.0×10^9
			1500	21.0	21.2		0.3	-1.6	1490	77	80	4.2×10^9
			1090	22.0	22.0		0.4	+7.3	1170	81	80	1.3×10^9
	45		1070	19.1	19.9		0.3	-6.2	1090	71	75	2.6×10^9
			1260	20.6	20.7		0.3	-1.0	1260	74	79	2.2×10^9
			1150	22.0	21.8		0.4	+2.7	1160	75	81	8.7×10^9
FeNiCrAlY	64	16.6	1440	19.3	20.5	2.8	3.6	-13.3	1410	80	82	>100,000
			1410	20.3	21.4	2.8	2.9	+14.8	1800	85	90	"
			640	21.9	23.7	4.6	4.6	+2.7	770	86	89	"
TASK IV												
FeNiCrAlY	64	16.6	1940	20.1	22.5	2.5	2.5	+1.1	2460		89	>100,000
			2280	22.9	22.8	2.5	2.5	+2.7	2320		92	"
			2460	22.7	22.4	2.6	2.6	+1.9	2440		92	"
			2350	23.3	24.4	2.9	2.9	+5.5	2720		92	"
FeCrAlY	78	12.6	2070	21.9	22.2		0.3	-7.9	1960		88	4.9×10^9
			2010	22.3	22.5		0.4	-8.6	1870		84	1.9×10^9
			2100	23.1	23.3		0.3	+2.5	2190		88	4.2×10^9
			1920	22.8	22.4		0.4	-19.0	1500		83	1.1×10^9

(1) Baseline Material, FM-521
(2) At 40% Strength Loss

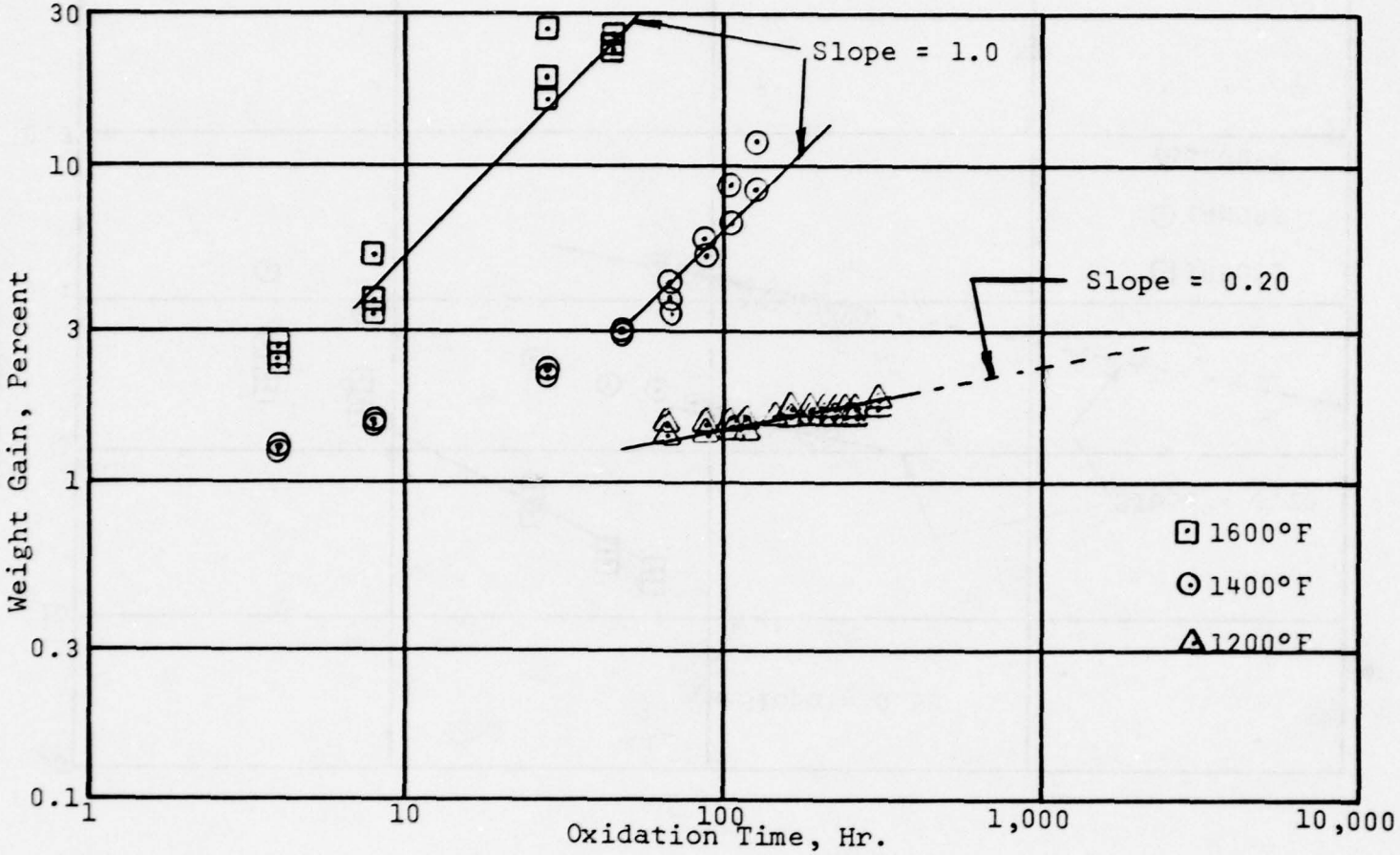

FIGURE 11

TASK II OXIDATION DATA
7.7 MICRON HAYNES 188

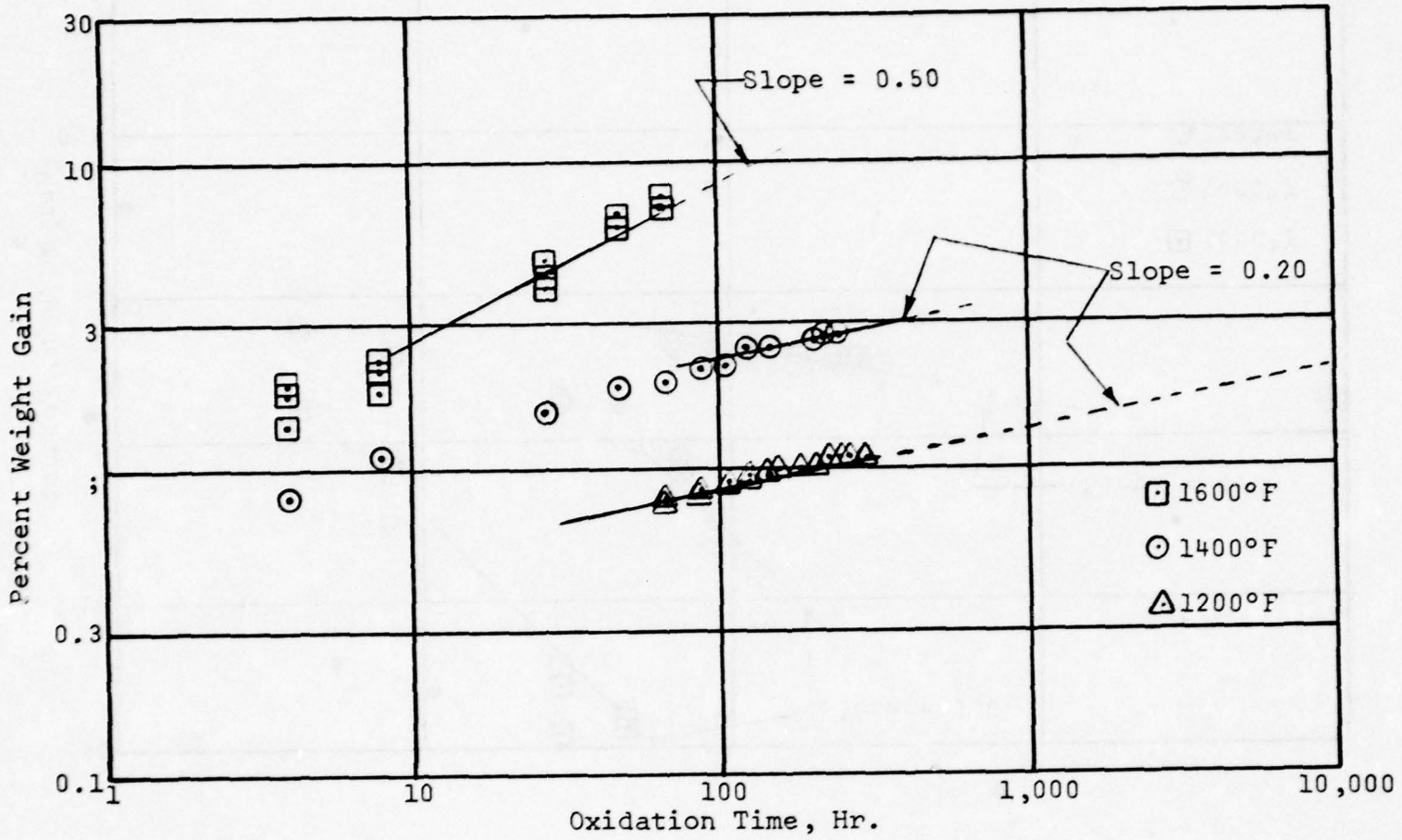

FIGURE 12

TASK II OXIDATION DATA
20.8 MICRON HAYNES 188

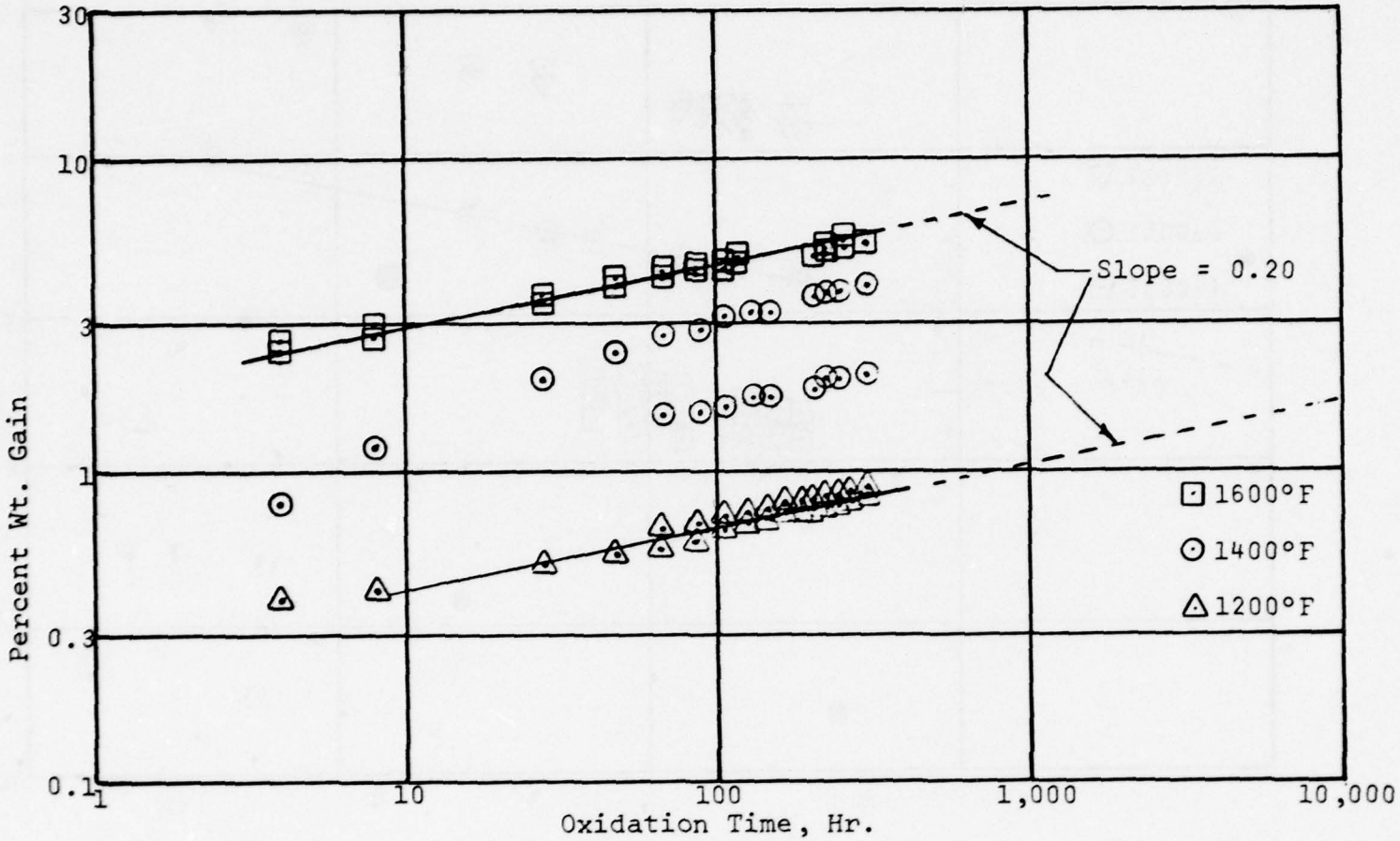

FIGURE 13

TASK II OXIDATION DATA
11.1 MICRON NiCrAlY

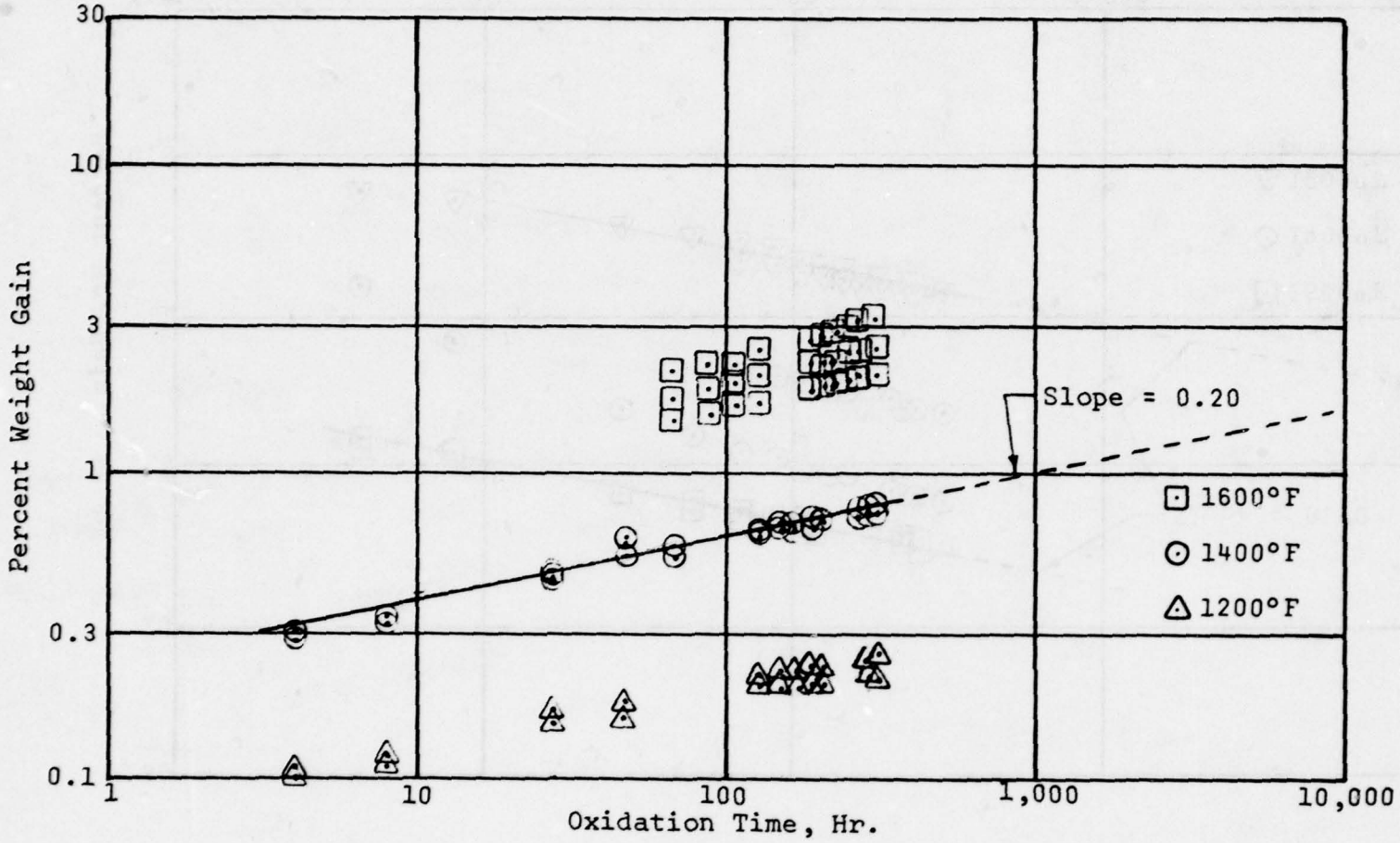

FIGURE 14

TASK III OXIDATION DATA
16.5 MICRON FeCrAlY

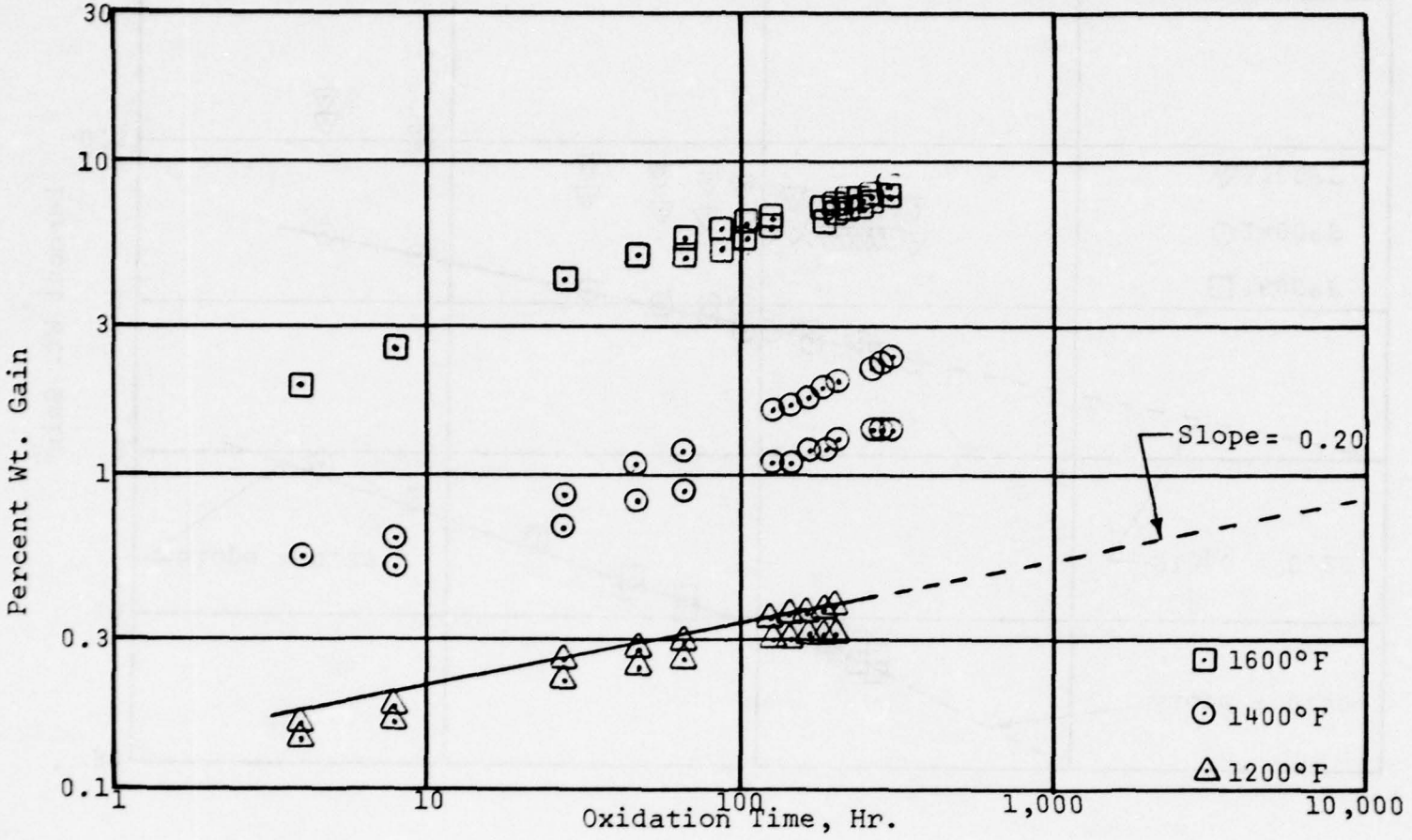

FIGURE 15

TASK III OXIDATION DATA
12.6 MICRON FeCrAlY

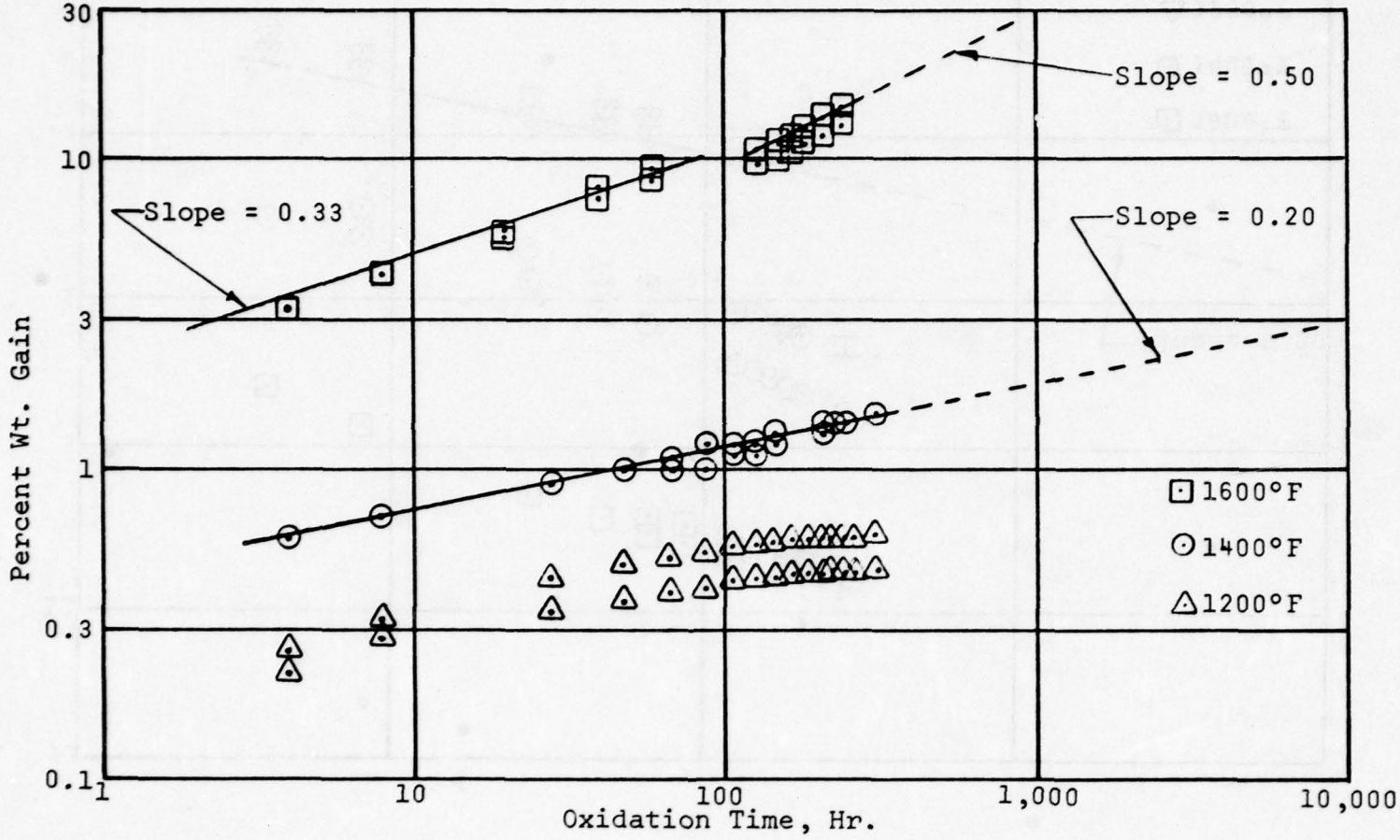

FIGURE 16

TASK II OXIDATION DATA
16.6 MICRON FeNiCrAlY

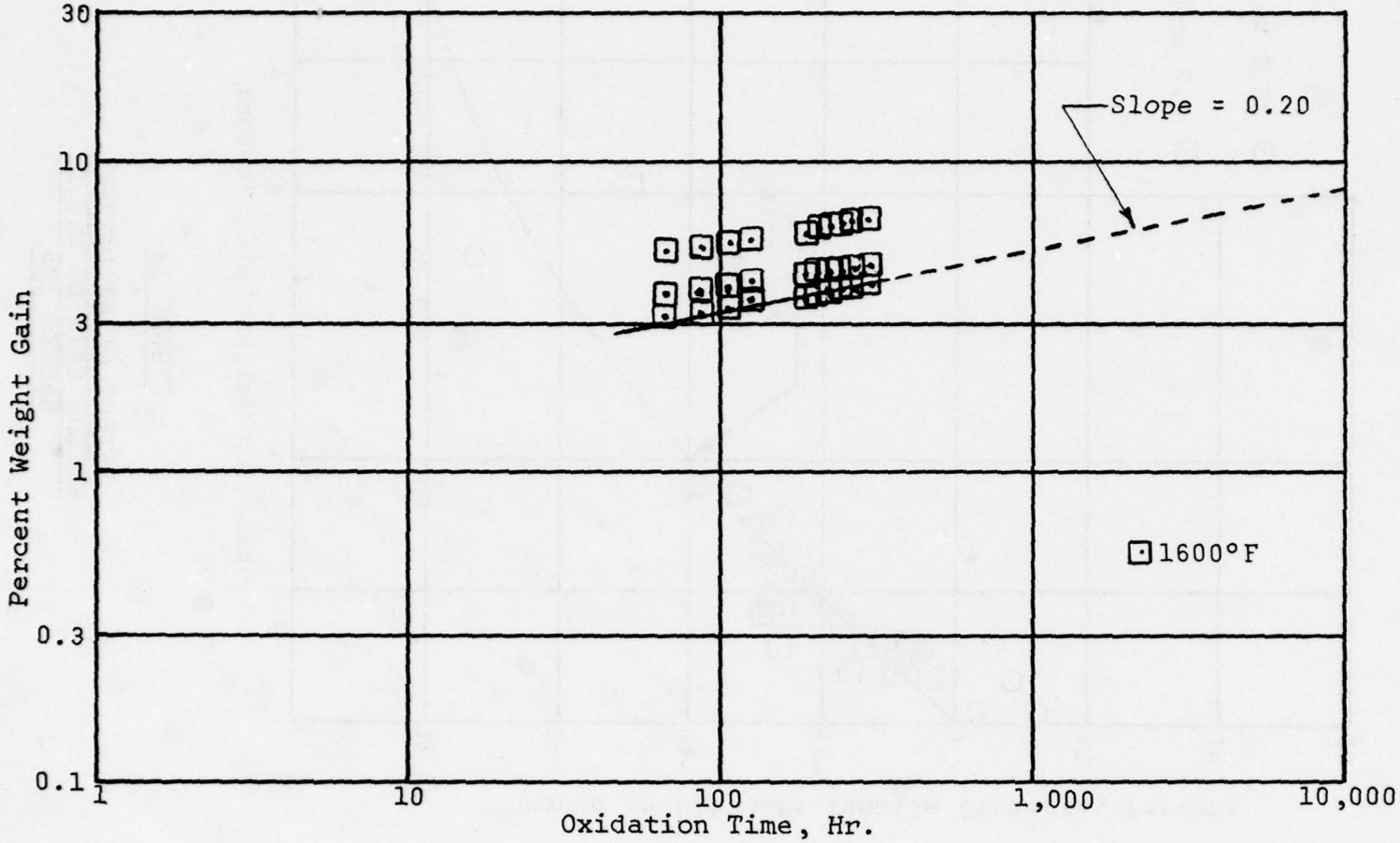

FIGURE 17

TASK III OXIDATION DATA
16.6 MICRON FeNiCrAlY

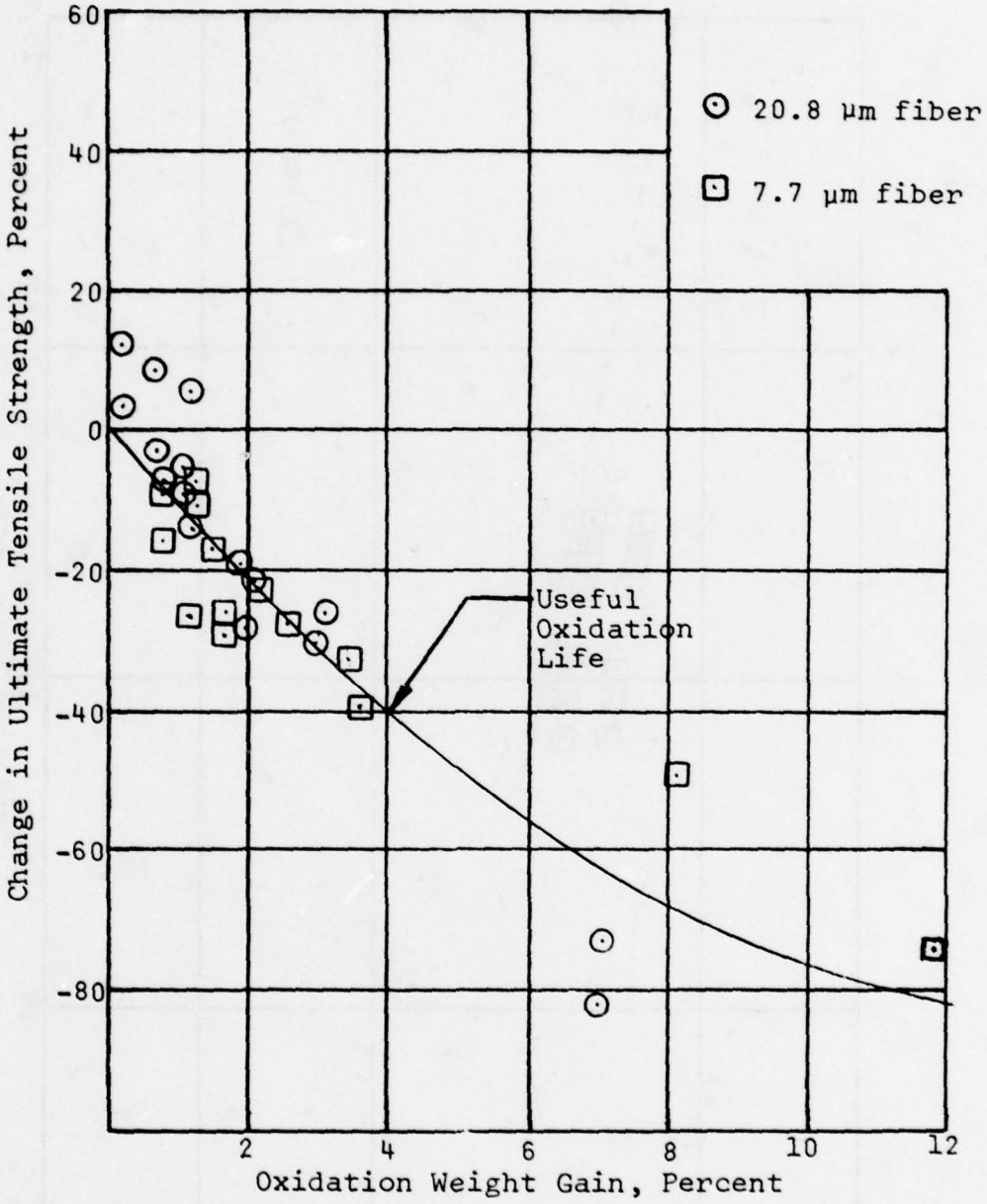

FIGURE 18

EFFECT OF OXIDATION
WEIGHT GAIN ON U.T.S.
HAYNES 188

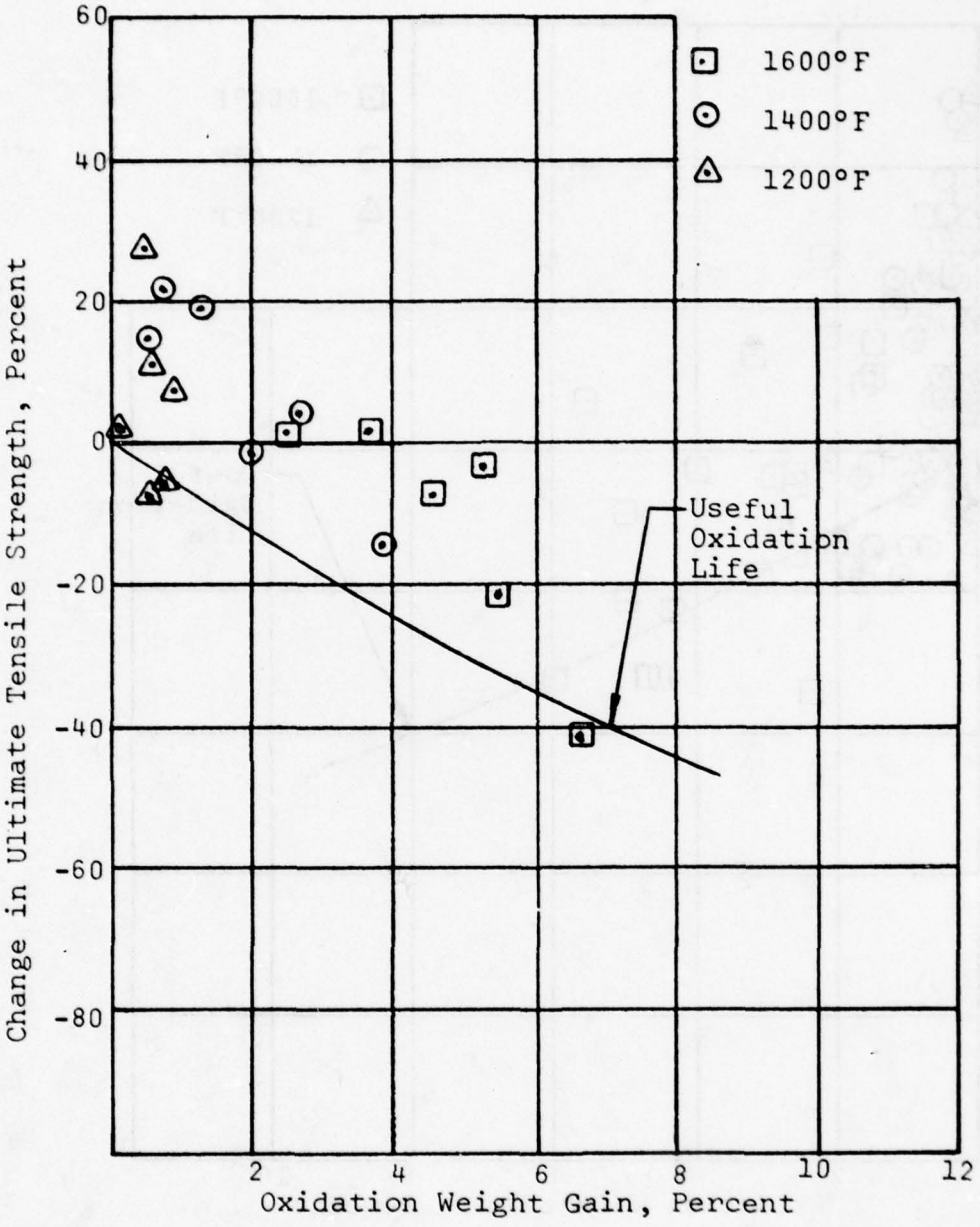

FIGURE 19

EFFECT OF OXIDATION
WEIGHT GAIN ON U.T.S.
NiCrAlY

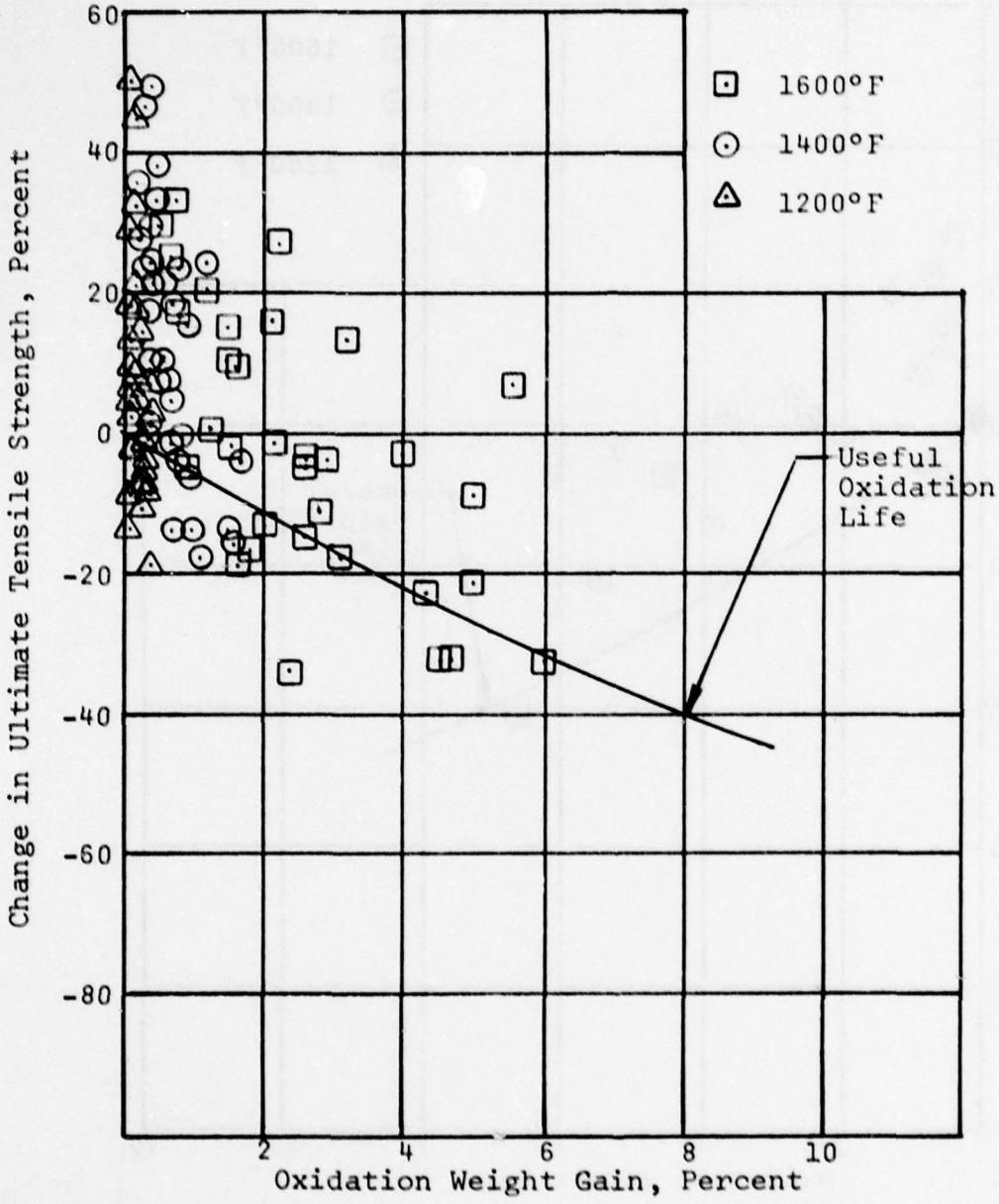

FIGURE 20

EFFECT OF OXIDATION
WEIGHT GAIN ON U.T.S.
FeCrAlY

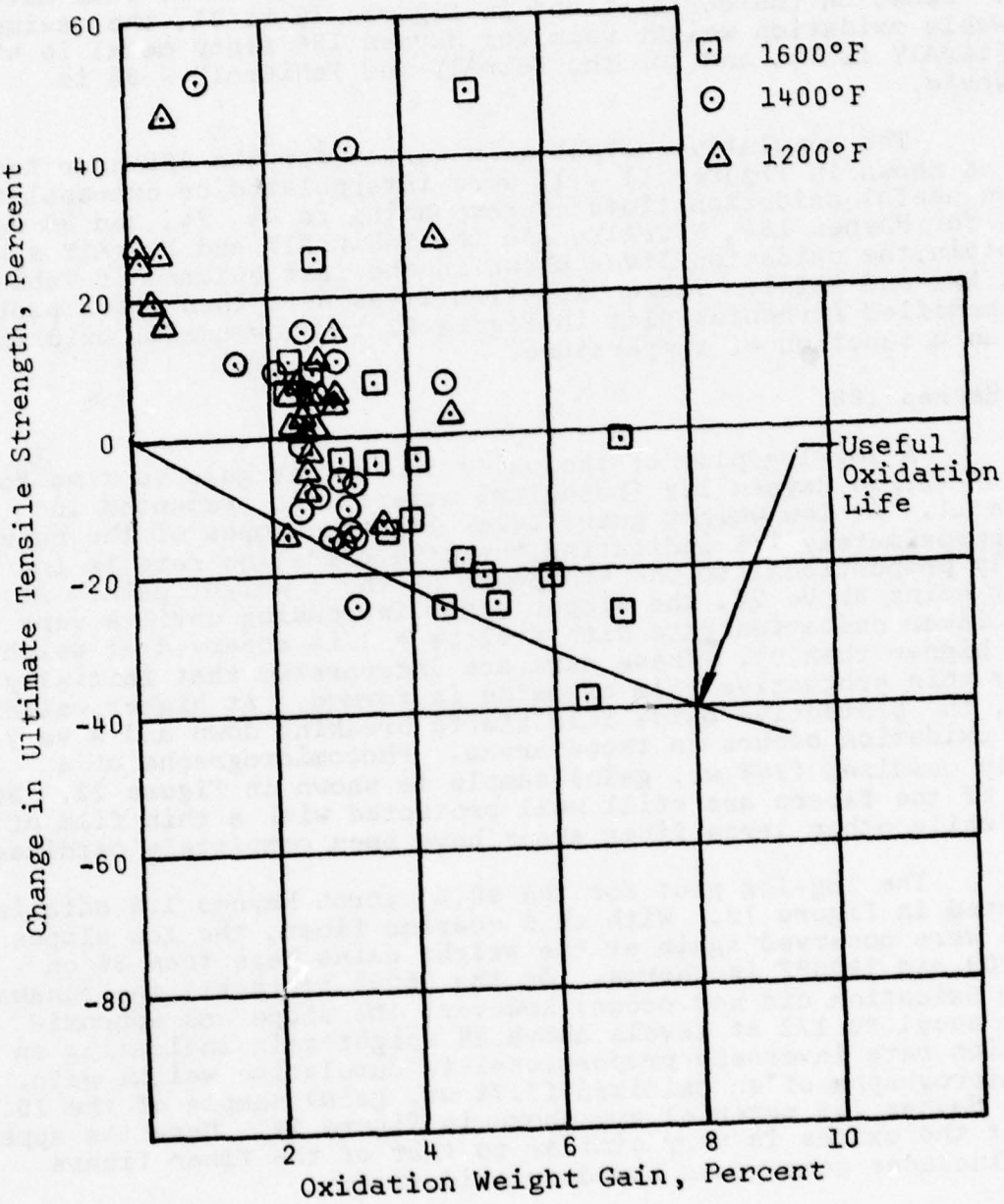

FIGURE 21

EFFECT OF OXIDATION
WEIGHT GAIN ON U.T.S.
FeNiCrAlY

wake erosion occurs on compressor seals installed at a 7° impingement angle when the material strength levels fall below 700 psi. Based on this and minimum strength levels of 1100 psi specified for compressor seal materials, a maximum allowable strength loss of 40% was defined as the oxidation life of these seal materials. Based on the correlations in Figures 18 to 21, the maximum allowable oxidation weight gain for Haynes 188 fiber metal is 4%, for NiCrAlY is 7%, and for the FeCrAlY and FeNiCrAlY - 8% is allowable.

The cumulative weight gain curves for the 308 hour tests such as shown in Figures 11 - 17 were interpolated or extrapolated to the useful oxidation times corresponding to 4%, 7%, and 8% weight gains for Haynes 188, NiCrAlY, and the FeNiCrAlY and FeCrAlY systems to obtain the oxidation lives shown in the last columns of Tables XVII, XX, and XXIII. These oxidation lives were then cross plotted on a modified Arrhenius plot in Figure 22 to show useful oxidation life as a function of temperature.

Haynes 188

A log-log plot of the oxidation weight gain vs time for the 7.7 micron Haynes 188 (baseline) material is presented in Figure 11. At low weight gains below 2%, the slopes of the curves are approximately 1/5 indicating that the oxidation rate is inversely proportional to the 4th power of the % weight gain. At weight gains above 2%, the slopes start increasing until a very high linear oxidation rate with a slope = 1 is observed at weight gains higher than 4%. These data are interpreted that initially a very thin protective film of oxide is formed. At higher weight gains, the protective oxide film starts breaking down and a very rapid oxidation occurs in those areas. Photomicrographs of a heavily oxidized (24% wt. gain) sample is shown in Figure 23. Some areas of the fibers are still well protected with a thin film of oxide while other large fiber areas have been completely oxidized.

The log-log plot for the 20.8 micron Haynes 188 data is presented in Figure 12. With this coarser fiber, the low slopes of 1/5 were observed again at the weight gains less than 3% on the 1200 and 1400°F isotherms. On the 1600° isotherm, the runaway linear oxidation did not occur; however, the slope was approximately equal to 1/2 at levels above 3% weight gain indicating an oxidation rate inversely proportional to cumulative weight gain. Photomicrographs of an oxidized (7.7% wt. gain) sample of the 20.8 micron Haynes 188 material are shown in Figure 24. Here the appearance of the oxides is very similar to that of the finer fibers which includes some grain boundary oxidation.

The weight gains observed for the coarser Haynes 188 material were lower than the 7.7 micron material as expected but they were not directly proportional to surface area.

NiCrAlY

The log-log plot of the incremental weight gain data for the 11.1 micron NiCrAlY system is shown in Figure 13. The slopes

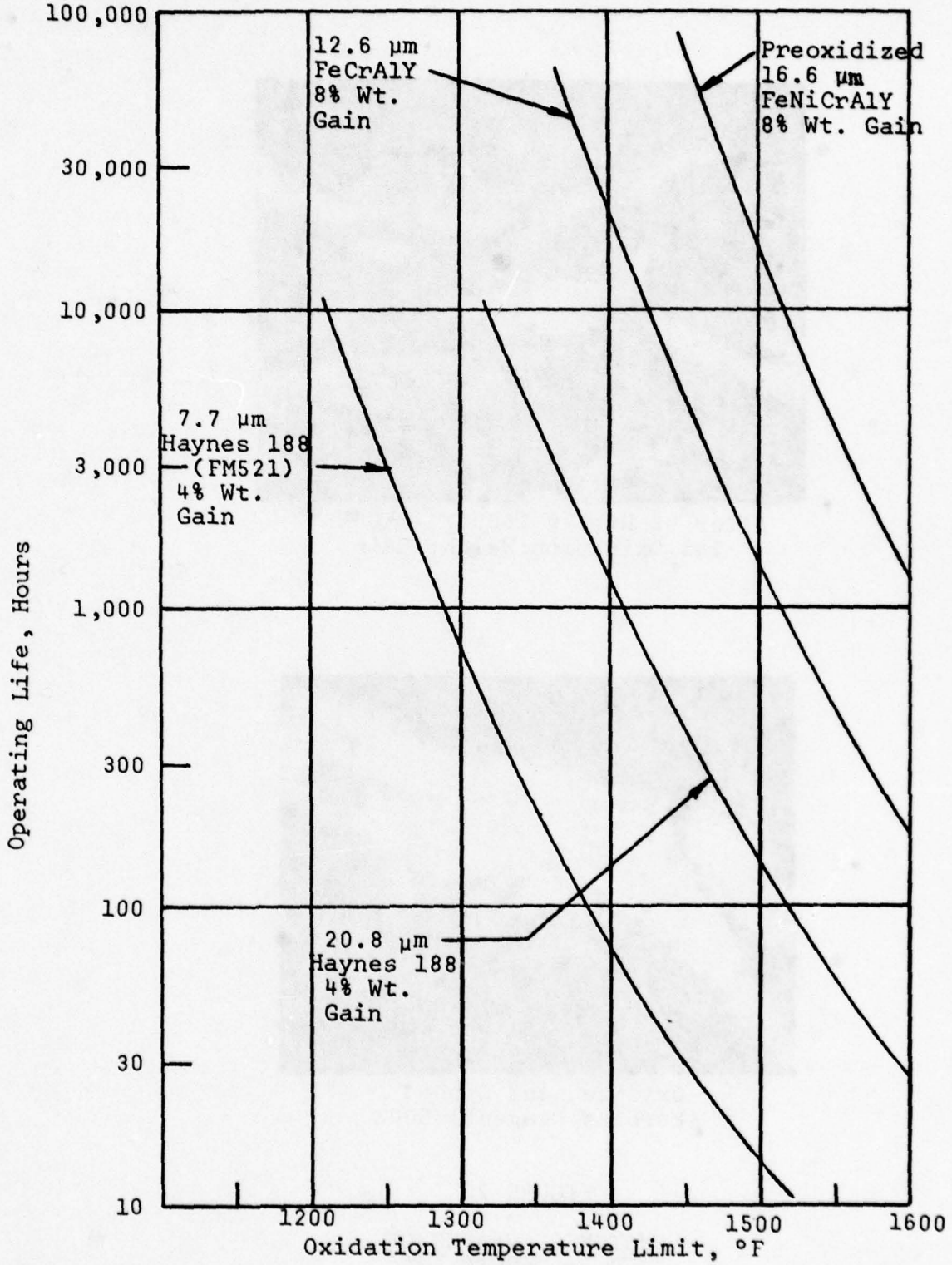

FIGURE 22

ESTIMATED OXIDATION LIVES

After 48 Hrs. @ 1600°F - 500X
24% Oxidation Weight Gain

Oxidized and Etched
(Marbles Reagent) 500X

FIGURE 23

PHOTOMICROGRAPHS OF
7.7 µm HAYNES 188

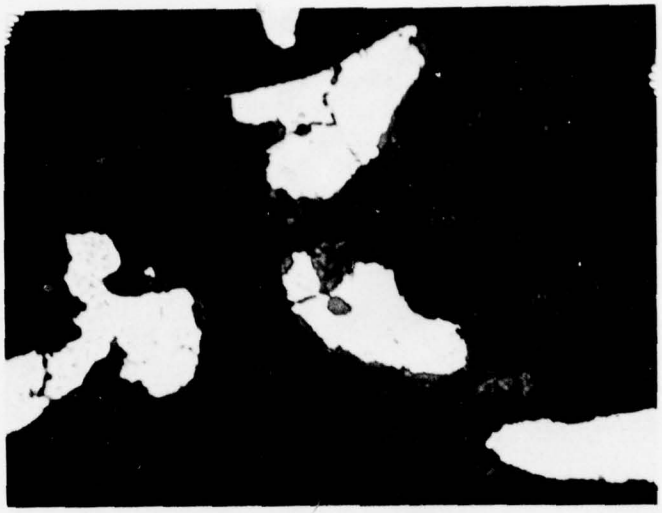

After 68 Hrs @ 1600°F - 500X
7.7% Oxidation Weight Gain

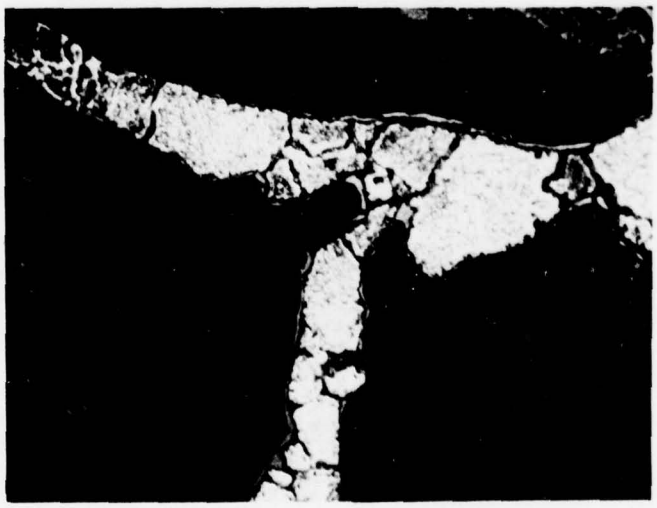

Oxidized and Etched - 500X
Marbles Reagent

FIGURE 24

PHOTOMICROGRAPHS OF 20.8μ HAYNES 188

of the curves are approximately equal to 1/5 indicating the oxidation rate is inversely proportional to the weight gain to the 4th power. One sample tested for 308 hrs at 1400°F had an initial high weight gain, however, the rate of weight change slowed to the 1/5th slope with time above 3% weight gain. Replicated specimens from this sheet that were tested at 4 and 68 hours at 1400 and 1600°F also had equivalent weight gains. It is believed that this sheet was contaminated with iron particles which oxidized completely early in testing. At higher oxidation levels, the contaminant was depleated, allowing the oxidation to proceed at the lower characteristic rates.

Photomicrographs of a moderately oxidized sample (5.3% weight gain) are shown in Figure 25. At this oxidation level, the theoretical oxide film thickness is too thin to be optically visible. However, careful search for the field chosen shows a few discontinuous oxide coatings on the fiber surface.

FeCrAlY

Log-log plots of the incremental weight gain vs. time oxidation data for 16.5 and 12.6 micron FeCrAlY fiber metal systems are shown in Figures 14 and 15. Here again these plots have a slope of 1/5 indicating the oxidation rate is inversely proportional to the 4th power of weight gain. An exception to this was the 22.6% dense sample of 12.6 micron (L/D = 45) oxidized for 308 hours at 1400°F in Task III where the slope increased to 1/2 after about 1% weight gain. This anomalous result could have been caused by contamination in sintering by some trace element, however, this could not be proved.

Photomicrographs of the 16.5 and 12.6 micron FeCrAlY materials are shown in Figures 26 and 27. This is a single phase alloy that has the same oxidation appearance as the NiCrAlY. The highly reflective grains observed in the etched samples are probably chromium carbides caused by a carbon control problem in the processing of these materials. There was no microscopic evidence on the oxidized samples to indicate that the presence of these carbides caused accelerated oxidation or grain boundary attack.

As with the Haynes 188, increased oxidation weight gains were measured with the smaller diameter FeCrAlY fibers but not in direct proportion with the surface areas.

FeNiCrAlY

Log-log plots of incremental oxidation weight gains vs. time are shown in Figure 16 for the FeNiCrAlY oxidation data from Task II. The slopes on the 1200°F and 1400°F isotherms were reasonably consistent with other MCrAlY alloys; however, the oxidation rates and slopes for the 1600°F data were surprisingly high. It was decided to try to develop a more dense, resistant protective Al_2O_3 oxide film by preoxidizing the material for 1 hour at 1800°F prior to oxidation testing in Tasks III and IV. The results for

After 308 Hrs @ 1600°F - 500X
5.3% Oxidation Weight Gain

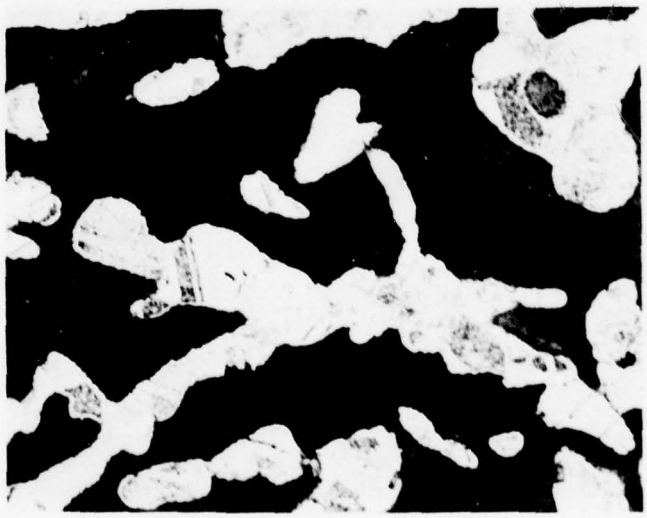

Oxidized and Etched - 500X
30 ml Lactic Acid, 30 ml HCL, & 10 ml HNO_3

FIGURE 25

PHOTOMICROGRAPHS OF 11.1μ NiCrAlY

After 308 Hrs @ 1600°F - 500X
2.1% Oxidation Weight Gain

Oxidized and Etched - 500X
20 ml glycerol; 20 ml HNO_3; 5 ml HF

FIGURE 26

PHOTOMICROGRAPHS OF 16.5μ FeCrAlY

After 308 Hrs @ 1600°F - 500X
11.8% Oxidation Weight Gain

Unoxidized and Etched - 500X
20 ml Glycerol; 20 ml HNO_3; 5 ml HF

FIGURE 27

PHOTOMICROGRAPHS OF 12.6μ FeCrAlY

Task III at 1600°F are shown in Figure 17. Rates of weight gain calculated from these data show they are inversely proportional to the 4th power of the cumulative weight gain. The preoxidation treatment resulted in significantly longer oxidation lives at 1600°F than for the Task II material. The measured incremental weight gains (after the preoxidation treatment) at 1200°F and 1400°F for oxidation times up to 308 hours were very small so that these data when plotted generate horizontal lines on the log-log plots.

A photomicrograph of a FeNiCrAlY specimen with 6.8% weight gain after 308 hours of oxidation at 1600°F in Task IV is shown in Figure 28 along with a photomicrograph of an etched but unoxidized specimen. The dark, small grains of a second phase are an aluminum rich phase that acts as an aluminum source to replenish the aluminum in the matrix after depletion of aluminum by oxidation. The highly reflective grains in the etched specimen are believed to be chromium carbides. There was no microscopic evidence in the oxidized specimens that the presence of these carbides caused accelerated oxidation or grain boundary attack. The field shown in the oxidized specimen shows some discontinuous surface oxides with some areas of penetration. In this same mount, the only completely oxidized fibers found were at the exposed surface. It is believed that the higher oxidation rate of these surface fibers was caused by depletion of aluminum in surface fibers as a result of evaporation during vacuum sintering. This is shown in the photomicrographs in Figure 29. The top photo shows the completely oxidized surface fibers. The bottom photo of an etched unoxidized FeNiCrAlY specimen shows the loss of the aluminum-rich phase in some surface fibers. This particular sheet was vacuum sintered adjacent to a FeCrAlY sheet where there appeared to be a vapor phase transfer of aluminum from the high to the low aluminum alloy. This is believed to be the reason for the variable but high aluminum contents measured in some of the FeCrAlY sheets. A revised processing technique is available to prevent this in future fabrication of FeNiCrAlY fiber metal.

Hardness

For the Haynes 188, NiCrAlY, and FeNiCrAlY systems, there was no apparent effect of oxidation on hardness (see Tables XV/XXIII) except for the samples of almost completely oxidized (20% weight gain) Haynes 188 materials at 1600°F which showed substantial reduction in hardness. The FeCrAlY materials showed higher hardnesses, on the average, after oxidation - particularly at the higher weight gains experienced after 308 hours of oxidation. Metallography indicated no significant changes in the grain structure of this alloy after oxidation, so this effect cannot be explained at the present. One possibility is that after oxidation, the unoxidized FeCr alloy remaining is depleted of aluminum and is stronger than the original FeCrAlY alloy.

Carbon Control

There was considerable variation in the carbon content of the sintered MCrAlY materials tested in the program. The carbon

After 308 Hrs @ 1600°F - 500X
6.8% Oxidation Weight Gain

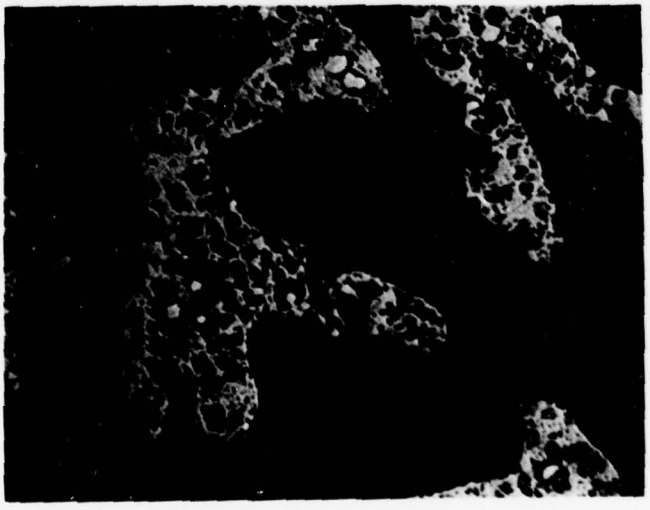

Unoxidized and Etched - 500X
Marbles Reagent

FIGURE 28

PHOTOMICROGRAPHS OF 16.6μ FeNiCrAlY

After 308 Hrs @ 1600°F - 200X
6.8% Oxidation Weight Gain

Unoxidized and Etched - 500X
Marbles Reagent

FIGURE 29

PHOTOMICROGRAPHS OF SURFACE FIBERS
16.6 MICRON FeNiCrAlY

content of the raw materials was low so the variability was introduced in the processing. High carbon results in precipitation of chromium carbides which results in a reduction of the chromium content of the surrounding matrix. There was no evidence that the higher carbon resulted in higher oxidation rates or grain boundary attack during air oxidation. However, this could cause sulfidation attack in turbine environments. Based on some partial success with carbon control in this program, additional work should result in control of carbon contents to the 0.03% level in future processing.

Dynamic Oxidation

Objectives

The objectives of the dynamic oxidation testing were twofold:

1. Evaluate the effect of a high velocity (Mach 0.8) jet of particulate-free hot gas (1400°F) on the erosion resistance of the candidate materials to determine the minimum strength at which hot gas erosion starts eroding surface fibers.

2. Evaluate the thermal shock and thermal cycling fatigue resistance of the candidate materials.

Equipment and Procedures

Details of the equipment are presented in Appendix B. One 1 in. x 1 in. coupon of each material variant was brazed to a 1 in. x 1.25 in x 0.090 in. Waspaloy (AMS 5544) backing plate with 0.003 in. thick Nicrobraze® LM braze tape. The twelve samples for each task (eight for Task IV) were attached to the rotary sample holder. The electrically heated furnace was brought to 1400°F with the holder in the "out" position. After the furnace was preheated, the propane-oxygen jet was ignited and adjusted with the secondary cooling air on to bring the hot gas jet to operating conditions of 1400°F and Mach 0.8 velocity. The temperature of the furnace and the jet exit were adjusted and recorded on a strip chart to hold the desired operating conditions throughout the exposure. Rotation of the sample holder was started at 175 rpm and the cycle timer was set to expose the samples to the direct (90°) impingement of the jet for 60 minutes and then to cool the samples surfaces to less than 200°F with four high velocity air jets during the one minute period with the sample holder rotating while out of the furnace.

The samples were weighed before exposure and then after 4, 8, 28 hour exposure intervals and then every 20 hours up to a total exposure time of 308 hours. In order to calculate percent weight gains, the oxidation of the backings and braze alloy was assumed to be negligible so the weight of the fiber metal only was used as the starting weight.

Since it is planned to preoxidize the FeNiCrAlY and FeCrAlY materials prior to actual engine service, both these materials were preoxidized in Task IV and the FeNiCrAlY was also preoxidized in Task III. One hour at 1800°F in static air was used for preoxidizing the FeNiCrAlY while one hour at 1600°F in static air was used for the FeCrAlY.

Oxidation and Erosion Results

The weight gains after 308 hours of dynamic oxidation exposure at 1400°F are shown in Table XXIV along with the equivalent results for the static oxidation at both 1200 and 1400°F.

Typically, the weight gains for dynamic oxidation at 1400°F were somewhere between the 1200 and 1400°F static oxidation weight gains. Since the sample holder shaft in the dynamic oxidation rig was water cooled and fiber metal is a good insulator, it is believed that the back sides of the fiber metal coupons were significantly below the temperatures of the exposed specimen surfaces so that the average temperature of the samples was somewhere between 1200° and 1400°F. Incremental weight gains as a function of time for the dynamic oxidation of the 7.7 micron Haynes 188 (baseline material) and 11.1 micron NiCrAlY are shown in Figures 30 and 31 in contrast with the comparable Task II static oxidation data previously presented in Figures 23 and 25. Here the slopes are similar but the weight gains fall between the 1200 and 1400°F static oxidation results.

Only three samples in the program showed evidence of hot gas erosion by giving lower slopes on weight gain vs. time plots or by showing incremental weight losses during the dynamic oxidation exposure. These results are underlined in Table XXIV. These three samples were the only samples in the program with strengths below 640 psi. Since the weight losses were so small, there was no visible sign of hot gas erosion on these specimens. As long as tensile strengths are maintained above the 700 psi level with fiber metal, hot gas erosion should be no problem.

Thermal Shock and Fatigue Results

There was no evidence of cracking or spallation on any of the specimens tested in the program after 308 thermal cycles between 200 and 1400°F. Although the MCrAlY materials are somewhat brittle, they have satisfactory thermal shock and fatigue resistance when braze bonded to Waspaloy backings. Thermal fatigue should be investigated for other bonding methods or for backings with thermal expansivities significantly different than Waspaloy.

Hot Particulate Erosion

Introduction

Particulate erosion can cause a serious problem of wear on blade tip seals, particularly if the engine is operating on short cycle times on dusty runways. Since there are no good bench marks

TABLE XXIV
DYNAMIC OXIDATION DATA

Material	L/D	Fiber Diam. (μm)	Sheet Avg. UTS (psi)	Dynamic Oxidation 308 Hr @ 1400°F Dens. %	Preox. Wt. Gain %	Total Wt. Gain %	Static Oxid. 308 Hr @ 1400°F Preox. Wt. Gain %	Total Wt. Gain %	Static Oxid. 308 Hr @ 1200°F Preox. Wt. Gain %	Total Wt. Gain %
Task II										
NiCrAlY	47	11.1	1550	20.2		1.2		3.9		0.8
			2990	28.7		1.3		2.0		0.9
FeNiCrAlY	64	16.6	1180	23.7		0.6		1.5		0.6
			2690	26.6		0.4		1.5		0.5
FeCrAlY	50	16.5	610	19.6		-0.1		0.8		0.2
			1380	27.6		0.3		0.7		0.3
	40	23.4	610	20.3		0.2(2)		0.6		0.1
			2170	32.3		0.4		0.7		0.2
Haynes 188	68	20.8	980	16.2		1.6		2.9		1.1
			3240	26.5		1.5		3.1		1.2
(1)	80	7.7	1240	18.5		2.3		8.1(3)		1.7
(1)			1620	18.8		2.3		11.8(3)		1.8
Task III										
FeCrAlY	50	16.5	1120	20.8		0.5		0.8		0.2
			1380	22.1		0.4		0.7		0.2
			1460	25.3		0.5		0.8		0.3
	78	12.6	1150	18.8		0.6		0.9		0.3
			1500	21.1		0.5		0.9		0.3
			1090	20.9		0.5		1.5		0.4
	45	16.6	1070	18.6		0.7		1.4		0.3
			1260	20.5		0.5		1.4		0.3
			1150	21.6		0.6		2.4		0.4
FeNiCrAlY	64	16.6	1440	18.7	3.8	4.9	2.5	2.6	2.8	3.6
			1410	20.0	4.4	6.3	2.8	3.1	2.8	2.9
			640	21.5	5.0	5.4(4)	4.4	4.5	4.6	4.6
Task IV										
FeNiCrAlY	64	16.6	1940	21.9	3.8	4.0	2.6	2.8	2.5	2.5
			2280	20.8	4.4	4.5	2.9	3.1	2.5	2.5
			2460	21.3	4.0	4.3	2.7	2.9	2.6	2.6
			2350	21.6	4.4	4.7	2.9	3.1	2.9	2.9
FeCrAlY	78	12.6	2070	23.2	1.9	2.1		1.1		0.3
			2010	20.5	1.9	2.1		1.6		0.4
			2100	22.4	1.9	2.1		1.7		0.3
			1920	22.1	1.9	2.1		1.7		0.4

(1) Baseline Material, FM-521
(2) Specimen lost weight in first 8 hrs.
(3) Wt. gain for 128 hr. exposure
(4) Total wt. gain was 5.6% after 200 hrs., then started losing weight.

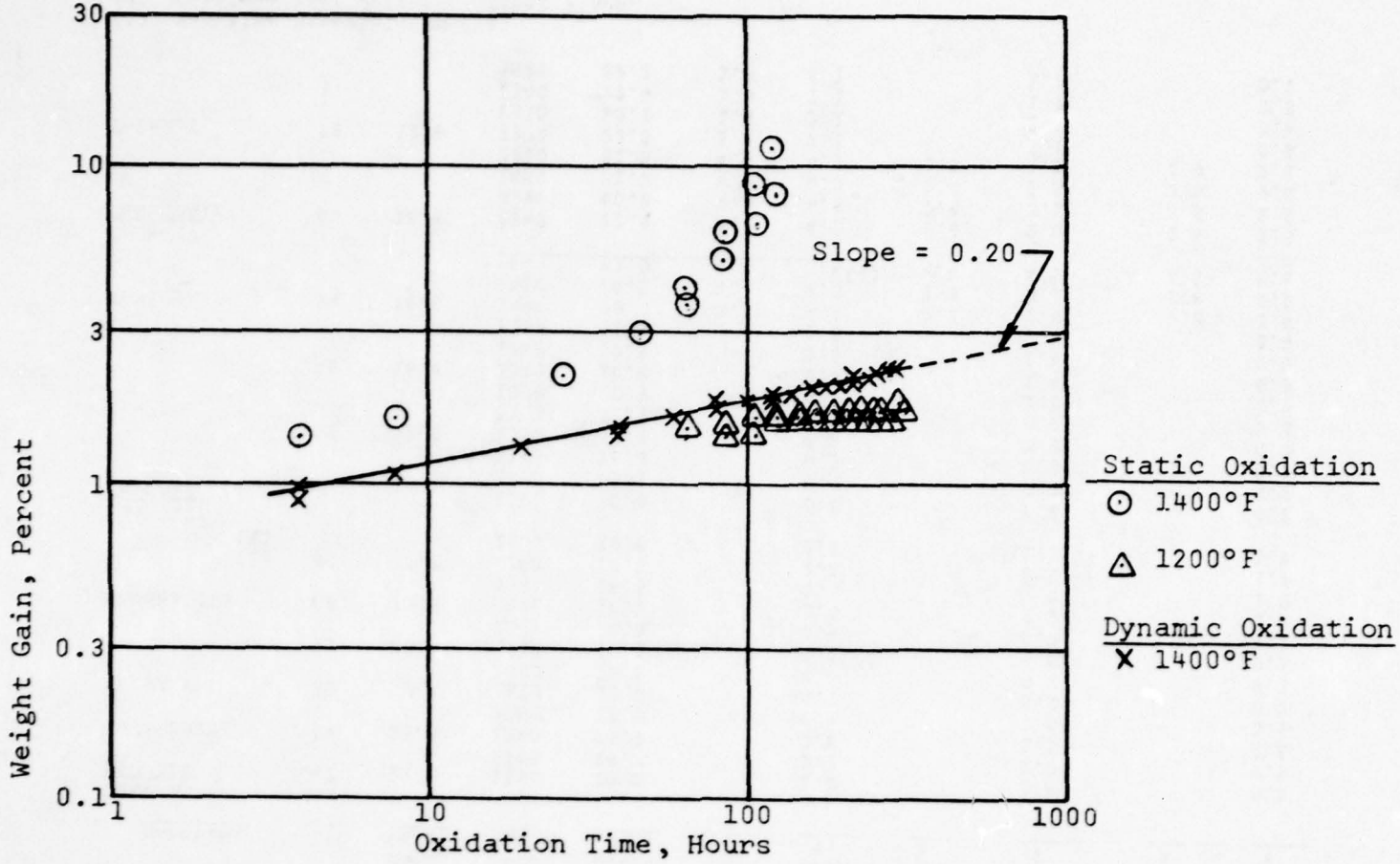

FIGURE 30

DYNAMIC VS. STATIC OXIDATION
7.7 MICRON HAYNES 188

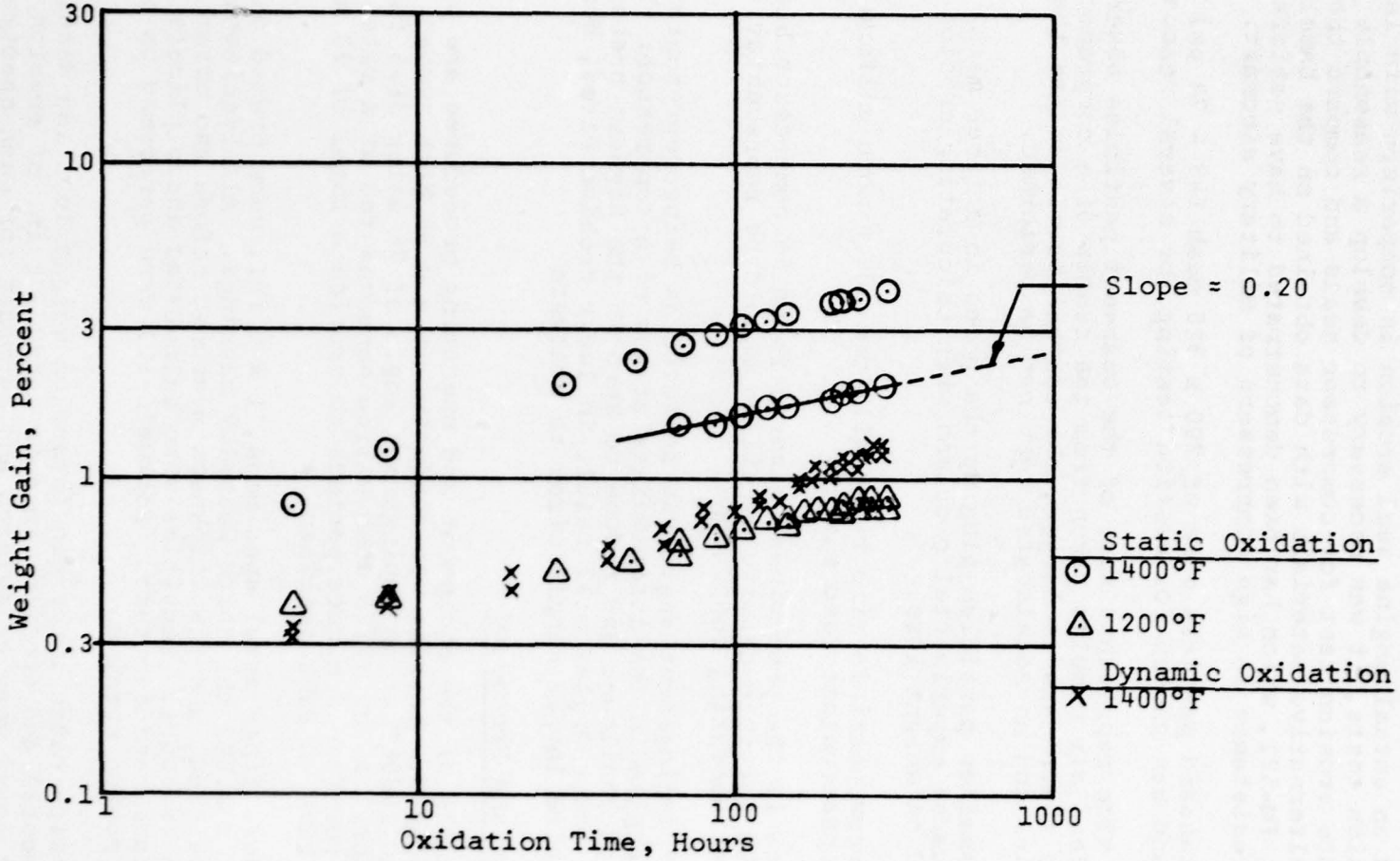

FIGURE 31

DYNAMIC VS. STATIC OXIDATION
11.1 MICRON NiCrAlY

published on actual engine seal erosion in comparison with laboratory erosion tests, it was necessary to develop a reasonable hot particulate erosion test for compressor seals and compare the test data of alternative materials with data obtained on the baseline material, FM-521, which has been demonstrated to have satisfactory erosion resistance in high compressors of military aircraft.

A standard particle size of 200 x 325 mesh (43 - 74 μm) sieved silica sand was chosen for erosion testing for several reasons:

1. This size represents some of the coarsest particles observed in bleed air samples taken from the center of a compressor. Since their mass is larger, the coarser particles are the most erosive and an accelerated test can be performed.

2. The smaller particles plug up the pores in a fiber metal material and cause experimental problems when calculating erosion rates based on weight loss.

3. A narrow particle size range will provide a more uniform flow in a particulate feed system.

4. Silica is the predominant mineral found in compressor bleed air, so the particle density of silica should be representative of actual operating conditions.

A 7° impingement angle was selected as being representative of seal angles in the intermediate stages of a compressor. These angles get shallower and reduce to zero in the highest pressure stages. Lower angles will result in lower erosion rates, however, they require larger sample sizes to evaluate.

Equipment and Procedure

Details of the equipment and operating procedures are presented in Appendix C. Testing was conducted at a 0.35 Mach number at 1200, 1400, and 1600°F at an impingement angle of 7° using JP-5 fuel in the burner. A 200 x 325 mesh silica sand was fed at a rate of 6 lb/hr for four 5 minute periods to provide a total of 20 minutes erosion time on each specimen.

Square fiber metal specimens, 1 x 1 in., were brazed onto 1.25 x 1 x 0.090 in. thick Waspaloy backings. All specimens were dried, weighed, and the thickness measured before and after each 5 minute exposure. Densities were calculated and duplicate room temperature hardness tests (Rockwell 5Z) were performed on each brazed erosion specimen.

Erosion rates in cc/min (based on weight loss and density measurements) and erosion times in sec/0.001 in. of erosion (based on depth loss) were calculated and recorded for each specimen since both measurements are used by materials investigators in the industry. Plots were made of erosion rates vs. the reciprocal of erosion times and it was found that a reasonable straight line

correlation resulted. Consequently, either measurement should be valid for quantifying and correlating erosion rates. For the purposes of the correlations in this report, only the volumetric erosion rates were employed, although both are reported.

Results

Data

The calculated results from all tests are presented in Table XXV along with the properties data.

Multiple Regression Analyses

General Electric's linear multiple regression and multiple correlation programs were used with a computer to evaluate statistically the effect of the variables on volumetric erosion rate. Since each material can be expected to have different properties, the data were separated into material groups for analysis. The results are presented in Table XXVI.

Although about 24% of the variance in erosion rates could not be explained with the independent variables evaluated, the analysis indicated a significant effect of three variables - fiber diameter, hardness, and test temperature. Fiber diameter was independently varied only with the FeCrAlY and Haynes 188 systems and in both systems this variable explained most of the variance with increasing fiber diameters resulting in lower erosion rates.

Fiber aspect ratio, L/D, was varied independently only with the FeCrAlY system and found to have no significant effect on erosion rate.

Hardness was the second most important variable with increasing hardness resulting in decreasing erosion rates. As was mentioned previously, hardness was found to be a function of density and degree of sintering as measured by tensile strength at a given density. The use of hardness in the regression analysis resulted in density and tensile strength being insignificant variables. However, had hardness been deleted from the analysis, tensile strength and density would probably have been significant.

The FeNiCrAlY and FeCrAlY erosion specimens were both preoxidized in Task IV. The analyses of these systems indicated that level of preoxidation had no independent effect on erosion rate.

Test temperature was also a significant variable with increasing temperature causing a small increase in erosion rates. At least a part of this effect is the result of increased velocities at the higher temperatures since these tests were run at a constant Mach no. of 0.35 rather than at a constant velocity. (see Appendix C).

TABLE XXV
HOT PARTICULATE EROSION[1] DATA

Material	Fiber Dia. μm	L/D	Avg. 3 Tensile Bar Dens. (%)	Avg. 3 Tensile Bar UTS (psi)	1200°F Erosion Sample Dens. %	1200°F Erosion Sample Hardness R_{45}	1200°F Erosion Rate[2] cc/min x 10^{-3}	1200°F Erosion Time[3] sec/mil	1400°F Erosion Sample Dens. %	1400°F Erosion Sample Hardness R_{45}	1400°F Erosion Rate[2] cc/min x 10^{-3}	1400°F Erosion Time[3] sec/mil	1600°F Erosion Sample Dens. %	1600°F Erosion Sample Hardness R_{45}	1600°F Erosion Rate[2] cc/min x 10^{-3}	1600°F Erosion Time[3] sec/mil
Task II:																
NiCrAlY:	11.1	47	19.4	1550	19.6	82	9.8	32	20.0	85	12.7	28	19.8	84	12.1	24
			31.2	2990	29.2	97	3.2	109	29.4	96	4.9	63	29.4	94	7.1	60
FeNiCrAlY:	16.6	64	23.4	1180	24.0	92	2.9	109	24.2	90	4.3	75	24.1	93	4.3	60
			25.2	2690	26.5	94	2.3	171	25.8	92	4.3	86	26.0	95	4.2	86
FeCrAlY:	16.5	50	18.4	610	19.4	70	8.1*	38	19.7	72	12.8*	23	19.5	70	11.6*	28
			26.6	1380	26.8	88	5.3	60	27.3	87	4.8	64	26.6	85	6.8	44
	23.4	40	18.0	610	19.1	68	4.2*	60	18.1	67	8.4*	33	17.9	66	10.1*	31
			29.2	2170	30.9	93	2.8	100	30.9	92	3.4	100	30.7	95	3.2	71
Haynes 188	20.8	68	17.5	980	16.4	58	10.5*	30	16.8	66	11.0*	21	16.6	64	12.0*	21
			27.5	3240	26.4	85	5.1	75	26.7	88	5.4	63	26.5	86	6.0	46
	7.7	80	18.6	1240	18.3	77	24.0	19	19.0	79	23.6	18	18.8	78	24.4	19
			18.7	1620	18.6	79	13.6	29	18.5	78	17.8	23	18.7	78	18.8	19
Task III:																
FeCrAlY:	16.5	50	21.3	1120	21.6	75	6.5	552	20.9	77	11.5	26	21.9	81	10.8	27
			23.2	1380	22.0	82	8.1	40	22.3	82	7.2	39	22.1	79	10.5	28
			24.7	1460	25.9	89	5.3	660	26.4	88	6.4	46	26.3	90	7.1	43
	12.6	78	18.8	1150	18.6	71	9.9	30	18.5	75	15.7	21	18.4	71	14.3	26
			21.0	1500	20.6	78	13.4	26	20.6	79	15.8	21	20.4	79	16.2	22
			22.0	1090	20.9	77	15.2	23	21.7	81	16.4	20	21.2	80	15.7	21
		45	19.1	1070	18.8	69	15.5	18	18.9	74	15.4	21	18.8	72	15.9	23
			20.6	1260	20.6	79	9.0	35	20.5	78	13.3	24	20.4	79	15.6	24
			22.0	1150	21.9	76	14.6	24	21.9	81	13.9	26	22.0	78	17.8	19
FeNiCrAlY	16.6	64	19.3	1440	18.6	79	8.7*	33	18.6	86	10.0	36	18.7	85	12.7	27
			20.3	1410	19.4	83	13.0	23	19.2	86	15.7	22	19.2	82	15.2	20
			21.9	640	21.4	76	25.1	15	22.2	81	25.6	15	21.9	78	25.0	12
Task IV:																
FeNiCrAlY:	16.6	64	20.1	1940	21.6	86	8.1	35	19.5	84	9.3	28	19.5	88	15.8	21
			22.9	2280	21.0	92	8.9	40	22.2	89	6.2	50	22.2	91	7.7	48
			22.7	2460	21.2	85	6.9	39	22.8	88	4.7	60	23.1	87	6.7	43
			23.3	2350	21.1	89	9.8	35	22.9	90	5.8	36	22.5	93	7.0	40
FeCrAlY:	12.6	78	21.9	2070	22.7	84	5.3	75	21.0	81	10.2	29	20.6	83	10.5	27
			22.3	2010	20.9	88	13.4	24	20.8	85	10.6	23	20.8	82	18.7	21
			23.1	2100	22.4	85	8.4	36	20.5	84	7.4	35	21.7	86	10.6	29
			22.8	1920	22.3	85	16.5	20	22.0	87	9.4	29	22.6	87	12.7	27
Haynes 188:	7.7	80	18.5	1660	21.4	80	14.1	26	21.1	80	18.0	20	21.0	76	31.5	12
			18.4	1360	21.1	77	17.9	21	21.3	76	15.8	21	21.4	82	19.9	19

(1) Test Conditions:

7° Impingement Angle, Velocity - Mach 0.35
2#20 min. particulate feed in 5 min. intervals
-200 + 325 mesh quartz particulate

(2) Based on weight losses in last 15 minutes of test

(3) Based on thickness lost at center of samples

* Based on weight losses in last 10 minutes of test

TABLE XXVI

HOT PARTICULATE EROSION REGRESSION ANALYSIS

X_1 = Fiber Diameter, μm

X_2 = Hardness, R_{5Z}

X_3 = Test Temperature, °F

X_4 = L/D

X_5 = UTS

X_6 = % Density

X_7 = Wt. % Preoxidation

Y = Erosion Rate (cc/min x 10^{-3})

	% Variation Explain. $(R^2) \times 100$	Mult. Correlation Coeff. (R)	Significance Level %
FeCrAlY			
$Y = 31.3-0.77X_1-0.25X_2+0.0077X_3$	$X_1 = 52$ $X_2 = 16$ $X_3 = 8$ 76	0.87	$X_1 = 100$ X_2 100 $X_3 = 99.9$ X_4 = insign. X_5 = X_6 = X_7 =
FeNiCrAlY (16.6 μm fiber dia.)			
$Y = 99.6-1.20X_2+0.0102X_3$	$X_2 = 72$ $X_3 = 4$ 76	0.87	$X_2 = 100$ $X_3 = 87.4$ X_5 = insign. X_6 X_7
NiCrAlY (11.1 μm fiber dia.)			
$Y = 44.6-0.52X_2+0.0071X_3$	$X_2 = 82$ $X_3 = 11$ 93	0.96	$X_2 = 98.9$ $X_3 = 87.3$ X_5 = insign. X_6 =
Haynes 188			
$Y = 31.8-0.97X_1-0.28X_2+0.0123X_3$	$X_1 = 61$ $X_2 = 7$ $X_3 = 8$ 76	0.87	$X_1 = 100$ $X_2 = 95.2$ $X_3 = 95.6$ X_5 = insign. X_6 = insign.

TABLE XXVII

CALCULATED EROSION RATES(1)

A. Calculated Erosion Rates at Constant Hardness

Alloy	D_f = 16.6 μm Temp = 1250°F Hardness = 80 R_{5Z}	D_f = 11.1μm Temp. = 1250°F Hardness = 80 R_{5Z}
FeCrAlY	8.1	12.4
Haynes 188	8.7	14.0
FeNiCrAlY	16.4	-
NiCrAlY	-	11.9

B. Calculated Erosion Rates at Constant Density & Tensile Strength

Temp. = 1250°F
Density = 20%
UTS = 1800 psi

Material	Calculated Hardness(2) R_{5Z}	Calculated Erosion Rate
12.6 μm FeCrAlY	78.1	11.7
7.7 μm Hs 188 (FM-521)	77.4	18.0
16.6 μm FeNiCrAlY	85.0	10.4
11.1 μm NiCrAlY	81.6	11.0

(1) cc/min. x 10^{-3} units
(2) From Table XIV

Alloy Evaluation

The evaluation of the erosion resistance of the four alloys tested in the program relative to each other is shown in Table XXVII. Part A shows the erosion rates calculated from the derived linear regression equations at a constant hardness and at two fiber diameters. On this basis, the NiCrAlY is the most erosion resistant while the FeNiCrAlY was the least resistant. To compare the systems on a more realistic basis, Part B shows the calculated erosion rates for the four best abradable candidates from the rub rig testing at a constant density and tensile strength. To do this, the hardnesses were calculated from the linear equations derived in Table XIV. On this basis, the 16.6 micron FeNiCrAlY system was the most erosion resistant fiber metal tested and significantly better than the baseline material, FM-521. This appears to be the combined result of the larger fiber diameter and the higher hardness of the FeNiCrAlY fiber metal at constant density and tensile strength.

Abradability

Introduction

Communications with P & WA have indicated that typical interactions of blades with abradables in either military or commercial engine compressors occur at about 800 ft/sec at either the acceleration or deceleration pinch points. The typical interaction rates are in the range of 0.0001 to 0.001 inch/sec. A surge-induced deflection can cause interactions at a significantly higher rate. Typically, interference rates of 0.010 inch/sec are used in rub rigs to simulate this type of rub. Typical single blade tip penetrations into seals occur over arcs of less than 180° to depths as much as 0.030"; however, a used abradable seal could show rubs through a 360° arc as a result of multiple rubs.

A high speed rub rig is essential to simulate engine operating tip speeds and penetration rates to obtain equivalent energy input rates and heat losses. Brunswick has operated such a rig since 1970 for evaluation of fiber metal and alternative abradable seal materials.

A rub test study and product improvement program[1] was completed in 1976. In this study, the base line material for this program, FM-521, was tested using severe 360° rubs to simulate rubs expected with advanced engines with close clearance seals.

(1) Technetics Div. Engineering Report #377, Blade Tip and Knife Edge Rub Testing of FELTMETAL® Seals, R. T. Frank and A. R. Erickson

Operating conditions used were:

	Blade Tips	Knife Edges
Temperature, °F	70	70
Rub Arc, degrees	360	360
Depth of rub, inches	0.020	0.020
Interaction rate, in/sec	0.001	0.005
Tip Speed, ft/sec	710-755	800
Rotor Materials	Incoloy 901	Waspaloy

Good rubs were obtained with the 7.7 micron Haynes 188 fiber metal to tensile strengths of 2400 psi for blade tip rubs and to 2100 psi for knife edge rubs. The maximum strength specification for the FM-521B was reduced from 2650 to 1900 psi to assure that no blade wear would be encountered on the F100 high compressor seals. No compressor blade wear problems have been reported with the FM-521B material, so this was chosen as the baseline material for this program.

Equipment, Procedures, and Calculations

Details of the high speed rub rig, operating conditions, and calculations are described in Appendex D.

Triplicate 3 x 5 in. fiber metal specimens of each material variant were brazed to 0.090 in. thick Waspaloy backing plates, machined, and rubbed at each of three operating conditions:

Blade Tip Material	Titanium AISI 811	Waspaloy	Waspaloy
Temperature, °F	600	1250	1250
Penetration rate, in/sec	0.001	0.001	0.010

Constant conditions used for all three test types were:

Wheel Speed, rpm	42,000
Tip Speed, ft/sec	710 - 802
Blade Tip Dimensions, in.	0.020 x 0.250
No. of Blades	2
O.D. of Rub Groove, in.	4.375
Max. Depth of Rub, in.	0.030

The flat seal specimens were mounted at a slight angle to the plane of the rotor so that a 180° rub arc was achieved after the blades had penetrated to a depth of 0.030 in. at the center of the arc.

The data obtained included rotor speed loss, normal force, torque, blade wear, abradable wear, and subjective observations of the heat discoloration and appearance of the blades and abradable specimens. The rub energy was calculated by graphical integration of data recorded on high speed strip charts by multiplying speed x torque x time. Hardnesses were measured after rub testing in three spots in the machined areas adjacent to the rub grooves. The hardnesses were averaged and recorded in the data tables for each test.

In Task II, specimens representing extremes of density and tensile strengths were prepared in an attempt to obtain both good and bad rubs with each material variant. After selecting the best materials in Task II, three specimens of each material variant were prepared of each material covering narrower ranges of density and tensile strength in order to evaluate the effect of fiber diameter and aspect ratio (L/D) with the FeCrAlY system. After selecting the best FeCrAlY system in Task III to compare with the 16.6 micron FeNiCrAlY (which was found to be the best abradable in both Tasks II and III) in Task IV, four specimens of each of the two best materials were prepared over narrow ranges of strength and density but at a higher strength level than used in Task III. Since the oxidation data generated in Tasks II and III indicated that improved resistance to oxidation by theFeNiCrAlY could be achieved with a high temperature preoxidation, it was decided to preoxidize the FeNiCrAlY and FeCrAlY specimens used for erosion, dynamic oxidation, and rub testing in Task IV. The FeNiCrAlY specimens were preoxidized to the 4.0% weight gain level at 1800°F for 1 hour. The finer FeCrAlY specimens were preoxidized to the 1.9% level at 1600°F for 1 hour.

Results

Data

The data and results are presented in separate tables, Tables XXVIII, XXIX and XXX, for the three types of rub tests employed. Photographs of typical rubbed specimens with 100X scanning electron micrographs (SEM) of the rubbed surfaces are shown in Figures 32 to 35 for three good rubs and one bad rub. Corresponding photomicrographs of the rub grooves and photographs of the blades are shown in Figures 36 to 39 for the same rub tests. S.E.M. photomicrographs of some typical blade tip surfaces are presented in Figures 40 and 41 for good and bad rubs, respectively.

Data Evaluation Methods

In the evaluation of the rub test results, the primary criterion of a bad rub is blade wear which increases blade tip operating clearances and decreases engine performance. For those rub tests which resulted in blade tip wear greater than 0.0005 in., these lead rubs are indicated in the data tables with an underlining of the blade wear measurements. This blade wear is almost always accompanied by heavy heat discoloration of the blade tip and moderate to heavy burnishing of the rubbed abradable surface. The exception to this which was an anomaly in the program was 20.8 μm Haynes material rubbed with titanium blades in tests 293 and 294 which had non-burnished, fiberous rub grooves and light discoloration of the blades.

As the strengths of these materials are reduced below the strength levels at which blade wear is encountered, moderate discoloration of blades and some burnishing of the rubbed surfaces is normally observed. At still lower abradable strength levels, good fibrous rub zones with minimal heat discoloration are observed.

TABLE XXVIII
WASPALOY BLADE RUB TEST DATA - 0.010 IN/SEC

Material	Seal Specimen Data: Fiber L/D	Fiber Dia. (μ)	Dens. (%)	UTS (psi)	Hardness R_{5Z}	Wt. Loss (g)	Calc. Vol.(1) Loss (in^3)	Max. Rub Depth (in)	Rub Groove Appear. ance(2)	Rub Rig Measurements: Max. Norm. Force (lb)	Max. Torque (in-lb)	Speed Loss (rpm/mil)	Rub Energy in-lb/in^2 x10	Blade Tip Data: Blade #1 Weight Change (g)	Blade #1 Height Change (in)	Blade #1 Discoloration(2)	Blade #2 Weight Change (g)	Blade #2 Height Change (in)	Blade #2 Discoloration(2)	Test No.
TASK II																				
FeNiCrAlY	64	16.6	23.9	1180	88	0.36	0.011	0.016	30% G	1.10	0.56	22	239	+0.0011	+0.0040	S	+0.0012	+0.0024	S	304
			25.7	2690	89	0.54	0.016	0.020	50% G	2.60	1.05	52	536	-0.0001	+0.0014	M	+0.0023	+0.0047	S	305
FeCrAlY	50	16.5	18.7	610	71	0.74	0.024	0.026	F, SG	0.25	0.24	12	111	+0.0007	+0.0011	M	-0.0013	+0.0024	M	301
			26.8	1380	80	1.45	0.045	0.038	10% G	0.33	0.30	9	111	-0.0002	+0.0010	M	(Broken during removal)			302
	40	23.4	19.1	610	66	1.05	0.035	0.033	F, SG	0.60	0.42	18	194	+0.0001	+0.0016	M-H	-0.0001	+0.0013	O	303
			29.9	2170	90	0.25	0.004	0.009	90% G	1.05	0.48	117	1481	-0.0122	-0.0207	H	-0.0123	-0.0225	H	306
NiCrAlY	47	11.1	19.2	1550	85	1.25	0.037	0.034	F	0.95	0.96	38	284	+0.0017	+0.0076	M	+0.0015	+0.0032	S	399
			29.0	2990	95	0.24	0.019	0.022	HG	2.45	1.26	53	546	+0.0147	-0.0015	H	+0.0017	-0.0027	H	300
Haynes 188	68	20.8	17.6	980	73	1.15	0.030	0.030	F, SG	0.60	0.48	19	176	-0.0001	+0.0013	H	+0.0008	+0.0013	S	307
			27.9	3240	91	0.84	0.019	0.022	30% G	1.08	0.72	55	707	-0.0082	-0.0134	H	-0.0088	-0.0146	H	308
FM-521	80	7.7	18.3	1240	78	1.68	0.054	0.043	F	0.45	0.78	16	131	+0.0002	+0.0020	M	+0.0005	+0.0012	O	310
			18.7	1620	78	1.47	0.033	0.033	5% G	0.58	0.51	24	197	+0.0012	+0.0029	M	+0.0009	+0.0010	O	309
TASK III																				
FeNiCrAlY	64	16.6	22.5	640	76	1.26	0.037	0.034	F, VSG	0.25	0.15	9	57	-0.0002	0	VS	-0.0010	+0.0011	O	354
			20.4	1410	79	2.10	0.076	0.056	F, SG	0.35	0.33	7	60	-0.0006	+0.0003	O	-0.0001	+0.0011	VS	353
			18.7	1440	81	0.83	0.029	0.029	F, SG	0.50	0.39	17	119	-0.0005	+0.0005	O	+0.0003	+0.0007	VS	352
FeCrAlY	78	12.6	21.9	1090	74	1.33	0.041	0.036	25% G	0.50	0.39	10	106	-0.0020	+0.0013	M	-0.0006	+0.0001	M	348
			18.5	1150	72	1.26	0.052	0.042	50% G	0.85	0.57	18	139	-0.0110	+0.0005	H	-0.0003	+0.0006	S	346
			21.0	1500	80	0.96	0.028	0.029	35% G	0.70	0.57	28	143	-0.0032	-0.0023	H	-0.0014	-0.0006	H	347
	45		19.0	1070	71	0.88	0.030	0.030	40% G	0.80	0.63	30	217	-0.0037	-0.0015	H	-0.0023	+0.0006	H	349
			22.2	1150	76	1.25	0.033	0.032	20% G	0.35	0.30	14	115	-0.0006	+0.0010	M-H	-0.0005	+0.0005	VS	351
			20.4	1260	78	1.42	0.046	0.039	35% G	0.80	0.54	27	157	-0.0006	+0.0006	M	-0.0021	-0.0010	H	350
	50	16.5	21.3	1120	75	1.43	0.052	0.042	35% G	1.20	0.60	24	155	-0.0027	-0.0002	H	-0.0012	+0.0020	H	343
			23.1	1380	80	1.01	0.034	0.033	25% G	0.95	0.66	29	262	-0.0398	-0.0062	H	-0.0067	-0.0067	H	344
			25.5	1460	82	1.93	0.050	0.041	30% G	0.90	0.48	22	121	-0.0013	+0.0006	H	0	+0.0003	S	345
TASK IV																				
FeNiCrAlY	64	16.6	20.8	1940	86	0.87	0.033	0.033	30% G	0.90	0.60	6	71	+0.0006	+0.0017	S	+0.0012	+0.0019	M	377
(Preoxidized, 4.0%)			22.6	2280	86	1.05	0.048	0.040	20% G	0.90	0.45	14	131	+0.0015	+0.0008	VS	+0.0008	+0.0014	H	378
			22.8	2350	86	0.63	0.023	0.025	30% G	0.45	0.30	8	130	+0.0010	+0.0015	H	+0.0018	+0.0019	S	380
			22.3	2470	85	0.79	0.024	0.027	25% G	1.10	0.51	19	207	+0.0009	+0.0019	M-H	+0.0009	+0.0016	VS	379
FeCrAlY	78	12.6	22.7	1920	81	0.56	0.019	0.023	40% G	0.45	0.45	17	231	-0.0023	-0.0065	H	-0.0013	-0.0036	H	384
(Preoxidized, 1.9%)			22.2	2010	84	1.29	0.045	0.038	40% G	0.55	0.48	17	135	-0.0001	+0.0007	H	+0.0003	+0.0010	S	382
			22.1	2070	87	0.54	0.022	0.026	50% G	0.85	0.51	19	202	0	+0.0012	H	-0.0004	+0.0012	H	381
			23.1	2100	87	0.60	0.023	0.025	50% G	0.80	0.48	20	165	+0.0004	+0.0007	H	0	+0.0010	H	383
FM-521	80	7.7	20.8	1660	82	1.18	0.043	0.037	50% G	0.55	0.66	24	168	+0.0005	+0.0009	S	+0.0006	+0.0032	H	385
			20.6	1360	79	0.73	0.027	0.029	F, SG	0.30	0.54	17	169	+0.0017	+0.0017	M	+0.0009	+0.0009	S	386

(1) Calc. vol. loss based on rub depth measurements.
(2) Description Code: F - Fibrous, G - Glaze, H - Heavy, M - Moderate, O - None, S - Slight, V - Very

TABLE XXIX
WASPALOY BLADE RUB TEST DATA - 0.001 IN/SEC

Material	Seal Specimen Data: Fiber L/D	Fiber Dia. (μ)	Dens. (%)	UTS (psi)	Hardness R_{5Z}	Wt. Loss (g)	Calc. Vol.(1) Loss (in^3)	Max. Rub Depth (in)	Rub Groove Appearance(2)	Rub Rig Measurements: Max. Norm. Force (lb)	Max. Torque (in-lb)	Speed Loss (rpm/mil)	Rub Energy $\frac{in\text{-}lb}{in^2} \times 10^3$	Blade Tip Data: Blade #1 Weight Change (g)	Blade #1 Height Change (in)	Blade #1 Discoloration(2)	Blade #2 Weight Change (g)	Blade #2 Height Change (in)	Blade #2 Discoloration(2)	Test No.
A. TASK II																				
FeNiCrAlY	64	16.6	23.6	1180	86	1.22	0.035	0.034	F,SG	1.90	-	44	-	-0.0003	+0.0005	S	+0.0005	+0.0009	M	320
FeNiCrAlY	64		26.2	2690	93	1.40	0.041	0.038	75% G	1.80	0.54	66	936	+0.0011	+0.0015	H	Broken	Blade	S	321
FeCrAlY	50	16.5	18.4	610	69	1.06	0.039	0.036	F,SG	0.10	0.09	31	139	-0.0008	+0.0014	VS	-0.0002	+0.0013	VS	313
FeCrAlY	50		26.8	1380	84	1.62	0.039	0.038	20% G	0.50	0.18	36	428	-0.0008	+0.0026	S	-0.0007	+0.0007	M	314
FeCrAlY	40	23.4	17.9	610	63	0.91	0.024	0.034	F,SG	0.10	0.21	32	420	-0.0008	+0.0013	O	+0.0002	+0.0005	O	315
FeCrAlY	40		29.2	2170	87	1.54	0.030	0.031	50% G	1.70	-	60	-	-0.0004	+0.0005	S	-0.0004	+0.0016	H	316
NiCrAlY	47	11.1	19.4	1550	86	1.10	0.028	0.031	F,VSG	0.20	0.24	52	567	-0.0003	+0.0002	O	-0.0003	+0.0020	M	311
NiCrAlY	47		30.3	2990	95	1.60	0.035	0.034	75% G	3.10	1.02	115	1,949	+0.0007	+0.0004	H	+0.0011	+0.0062	H	312
Haynes 188	68	20.8	19.2	980	77	1.60	0.043	0.040	F,SG	0.25	0.24	38	377	-0.0003	+0.0010	S	-0.0001	+0.0003	M	317
Haynes 188	68		30.0	3240	93	1.37	0.023	0.030	60% G	1.40	0.60	108	1,794	-0.0024	-0.0002	H	-0.0017	-0.0002	H	318
FM-521	80	7.7	18.9	1240	79	1.25	0.033	0.033	F, SG	0.25	0.30	44	455	-0.0002	+0.0001	VS	-0.0001	0	M	323
FM-521	80		18.9	1620	83	1.56	0.043	0.039	30% G	0.30	0.24	37	330	+0.0004	+0.0006	S	-0.0007	+0.0002	M	319
B. TASK III																				
FeNiCrAlY	64	16.6	22.2	640	76		DATA N.G.													366
	64		20.3	1410	80	0.98	0.033	0.032	F	0.20	0.18	31	252	0	+0.0011	O	-0.0003	+0.0006	O	365
	64		19.0	1440	84	1.08	0.041	0.037	F	0.20	0.18	39	316	-0.0005	+0.0008	O	-0.0003	+0.0008	S	364
FeCrAlY	78	12.6	22.7	1090	80	1.16	0.031	0.031	F, SG	0.40	0.18	81	372	-0.0006	0	O	-0.0006	+0.0005	M	360
	78		18.4	1150	75	1.33	0.046	0.039	F, SG	0.40	0.24	35	332	-0.0001	-0.0001	VS	-0.0002	+0.0011	M	358
	78		20.5	1500	78	1.19	0.035	0.034	F, SG	0.40	0.18	32	455	-0.0004	-0.0002	O	-0.0002	+0.0005	M-H	359
	45		18.9	1070	72	1.14	0.037	0.035	F, SG	0.30	0.24	41	441	-0.0001	+0.0006	O	-0.0002	+0.0013	VS	361
	45		22.9	1150	79	1.31	0.030	0.030	F, SG	0.35	0.18	20	523	-0.0008	-0.0004	O	-0.0006	+0.0005	M	363
	45		21.2	1260	80	1.33	0.035	0.033	F, SG	0.40	0.18	39	549	-0.0001	+0.0022	S	-0.0004	+0.0007	O	362
	50	16.5	20.8	1120	74	1.18	0.031	0.032	F, SG	0.40	0.18	34	485	0	+0.0011	S	-0.0002	+0.0008	VS	355
	50		24.2	1380	85	1.39	0.039	0.035	F, SG	0.70	0.30	41	398	+0.0001	+0.0009	VS	0	+0.0021	S-M	356
	50		24.8	1460	87	1.37	0.033	0.032	F, SG	0.50	0.18	41	504	-0.0002	+0.0008	M	-0.0004	0	VS	357
C. TASK IV																				
FeNiCrAlY	64	16.6	20.8	1940	86	1.23	0.041	0.036	F,20% G	0.15	0.15	15	333	+0.0013	+0.0011	S	+0.0006	+0.0009	M	387
(Preoxidized,	64		22.6	2280	89	0.96	0.026	0.027	F, SG	0.35	0.12	33	293	+0.0005	+0.0001	S	+0.0009	+0.0005	M-H	388
4.0%)	64		22.8	2350	87	1.10	0.033	0.033	F, SG	0.10	0.12	11	288	-0.0004	+0.0009	S	+0.0009	+0.0011	S	390
	64		22.3	2470	87	1.23	0.045	0.038	F, SG	0.10	0.06	13	221	+0.0009	+0.0009	S	+0.0007	+0.0005	S	389
FeCrAlY	78	12.6	22.7	1920	83	1.02	-	0.028	F,20%G	0.20	-	11	-	+0.0008	+0.0004	VS	+0.0006	+0.0008	M-H	394
(Preoxidized,	78		22.2	2010	81	0.81	0.024	0.027	F, SG	0.15	0.18	14	439	+0.0006	+0.0008	M	+0.0007	+0.0003	S	392
1.9%)	78		22.1	2070	83	0.66	0.024	0.027	30% G	0.30	0.24	41	531	+0.0011	+0.0014	S	+0.0007	+0.0008	M-H	391
	78		23.1	2100	84	0.95	0.024	0.027	F, SG	0.15	0.12	26	339	+0.0011	+0.0006	S	+0.0007	+0.0005	H	393
FM-521	80	7.7	20.9	1660	82	1.13	0.035	0.034	30% G	0.35	0.30	51	867	+0.0011	+0.0007	VS	+0.0013	+0.0010		396
	80		20.6	1360	79	3.94	0.138	0.089	-	0.15	0.27	20	181(3)	+0.0005	-	BENT	+0.0010	-	BENT	395

(1) Calc. vol. loss based on rub depth measurements
(2) Description Code: F - Fibrous, G - Glaze, H - Heavy, M - Moderate, O - None, S - Slight, V - Very
(3) Very high plunge rate - Blades bent, rig out of control.

AD-A072 171 BRUNSWICK CORP DELAND FL TECHNETICS DIV F/G 21/5
DEVELOPMENT OF IMPROVED ABRADABLE COMPRESSOR GAS PATH SEAL.(U)
JUL 78 W P JARVI, A R ERICKSON F33615-76-C-5302
UNCLASSIFIED ER-382 AFML-TR-78-101 NL

2 OF 2
AD A072171

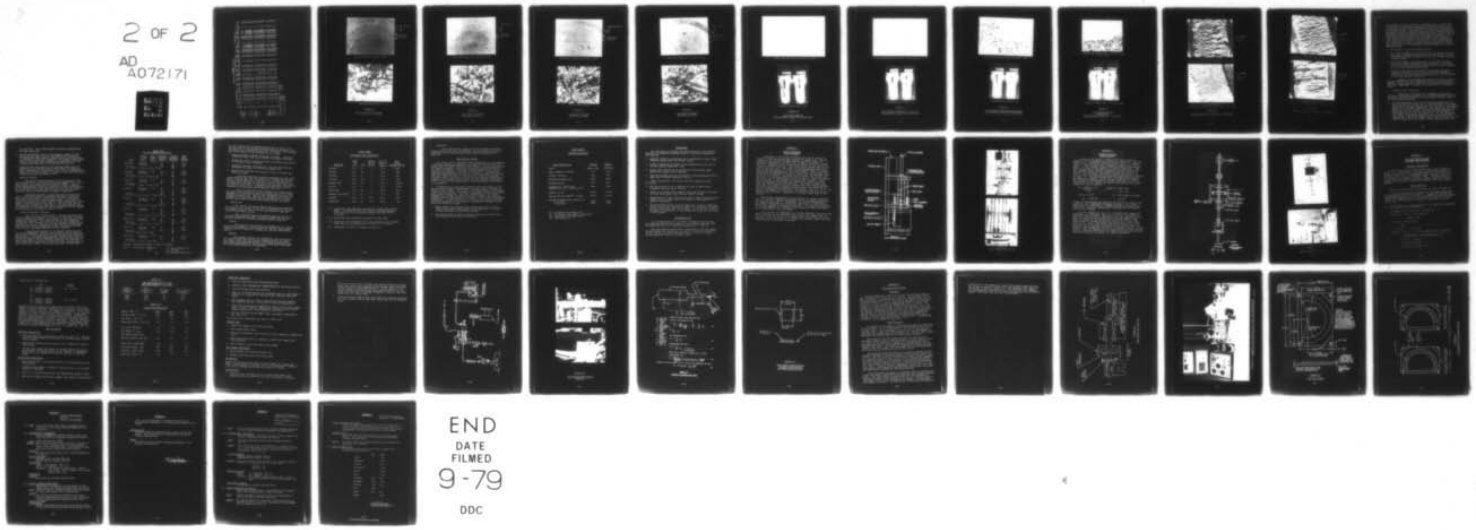

END
DATE FILMED
9-79
DDC

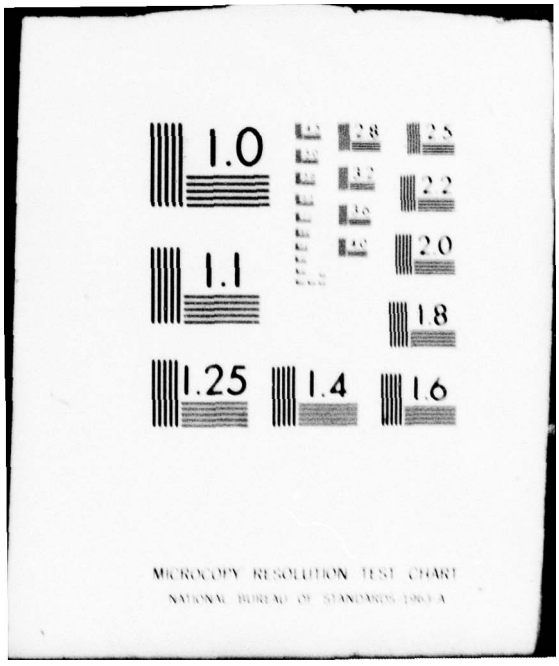
1.0
1.1
1.25
1.4
1.6
2.2
2.0
1.8
MICROCOPY RESOLUTION TEST CHART
NATIONAL BUREAU OF STANDARDS 1963-A

TABLE XXX

TITANIUM BLADE RUB TEST DATA - 0.001 IN/SEC

Material	Seal Specimen Data: Fiber L/D	Fiber Dia. (μ)	Dens. (%)	UTS (psi)	Hardness R_{5Z}	Wt. Loss (g)	Calc. Vol.(1) Loss (in³)	Max. Rub Depth (in)	Rub Groove Appearance(2)	Rub Rig Measurements: Max. Norm. Force (lb)	Max. Torque (in-lb)	Speed Loss (rpm/mil)	Rub Energy in-lb/in³ x10³	Blade Tip Data: Weight Change (g)	Height Change (in)	Discoloration(2)	Weight Change (g)	Height Change (in)	Discoloration(2)	Test No.
A. TASK II																				
FeNiCrAlY	64	16.6	24.2	1180	89	1.66	0.041	0.036	F	0.70	0.24	58	482	-0.0006	0	0	-0.0002	+0.0006	M	297
	64		25.6	2690	89	1.62	0.041	0.036	<10% G	1.40	0.35	64	801	+0.0001	+0.0002	0	+0.0024	+0.0014	M-H	298
FeCrAlY	50	16.5	18.7	610	72	1.02	0.043	0.037	F	0.30	0.12	24	272	+0.0002	-0.0001	0	+0.0002	0	S	289
	50		26.1	1380	78	1.52	0.030	0.030	F	0.15	0.12	33	242	+0.0004	-0.0001	S	+0.0023	0	0	290
	40	23.4	17.7	610	66	1.06	0.041	0.035	F	0.80	0.36	14	253	+0.0018	+0.0017	S	+0.0022	+0.0010	S	291
	40		28.7	2170	94	1.56	0.048	0.041	50% G	2.30	0.60	77	682	+0.0007	-0.0014	H	+0.0016	-0.0019	H	292
NiCrAlY	47	11.1	19.2	1550	85	1.41	0.048	0.041	F	0.50	0.30	27	245	+0.0005	+0.0021	0	+0.0004	+0.0021	0	287
	47		29.1	2990	95	0.64	0.017	0.023	90% G	4.00	1.08	139	1906	-0.0029	-0.0096	H	-0.0026	-0.0110	H	288
Haynes 188	68	20.8	17.9	980	76	1.43	0.035	0.034	F	0.20	0.18	32	239	+0.0003	-0.0022	S	+0.0004	-0.0011	0	293
	68		28.8	3240	95	1.29	0.021	0.024	F	1.20	0.30	85	1203	-0.0032	-0.0143	M	-0.0030	-0.0150	M	294
FM-521	80	7.7	19.0	1240	78	1.74	0.048	0.040	F	0.30	0.18	25	261	+0.0037	-0.0001	0	+0.0016	-0.0001	S	296
	80		19.0	1620	83	1.61	0.035	0.033	F	0.50	0.24	46	252	+0.0018	+0.0014	S	+0.0017	+0.0015	0	295
B. TASK III																				
FeNiCrAlY	64	16.6	21.8	640	75	1.23	0.030	0.031	F	0.20	0.12	23	52	-0.0003	+0.0006	0	-0.0003	+0.0001	0	342
	64		19.8	1410	75	0.95	0.027	0.029	F	0.10	0.09	24	251	+0.0003	+0.0008	0	-0.0001	+0.0006	0	341
	64		19.0	1440	80	0.88	0.030	0.030	F	0.20	0.12	47	329	+0.0003	+0.0007	0	-0.0002	+0.0003	0	340
FeCrAlY	78	12.6	22.1	1090	77	0.67	0.017	0.022	F	0.15	0.12	27	540	-0.0004	+0.0002	VS	-0.0004	-0.0001	VS	336
	78		18.9	1150	74	0.90	0.026	0.027	F, SG	0.25	0.21	31	604	-0.0003	-0.0004	0	-0.0007	+0.0012	S	333
	78		21.2	1500	80	0.89	0.024	0.027	F, SG	0.20	0.18	22	502	-0.0001	-0.0001	0	-0.0001	+0.0008	M	335
	45		18.9	1070	69	0.95	0.027	0.029	F, SG	0.25	0.18	50	621	+0.0001	+0.0014	S	-0.0001	+0.0006	0	337
	45		22.1	1150	75	1.24	0.033	0.032	F	0.20	0.12	41	323	-0.0001	-0.0005	0	-0.0002	-0.0008	S	339
	45		20.4	1260	76	2.17	0.071	0.052	F, SG	0.35	0.15	21	306	+0.0002	+0.0004	S	-0.0001	+0.0004	M	338
	50	16.5	21.8	1120	83	1.57	0.046	0.039	F, SG	0.30	0.24	18	501	-0.0003	+0.0002	0	-0.0005	+0.0006	M	331
	50		23.1	1380	85	1.01	0.029	0.029	F, SG	0.30	0.18	29	405	-0.0002	+0.0012	M	+0.0002	-0.0001	0	332
	50		25.1	1460	82	1.35	0.033	0.032	F, SG	0.25	0.18	25	442	-0.0003	+0.0002	0	-0.0003	+0.0003	M	334
C. TASK IV																				
FeNiCrAlY	64	16.6	20.8	1940	82	1.30	0.048	0.040	F, SG	0.30	0.18	28	389	+0.0008	+0.0011	S	+0.0007	+0.0009	S-M	367
(Preoxidized, 4.0%)	64		22.6	2280	92	1.07	0.033	0.033	F, SG	0.25	0.18	39	343	+0.0013	+0.0009	M	+0.0010	+0.0003	S	368
	64		22.8	2350	87	0.73	0.024	0.026	F	0.10	0.06	15	385	+0.0005	-0.0001	S	+0.0009	+0.0004	S	370
	64		22.3	2470	90	0.63	0.024	0.026	F, SG	0.35	0.15	58	442	+0.0009	0	S	+0.0012	+0.0005	S-M	369
FeCrAlY	78	12.6	22.7	1920	83	0.68	0.024	0.026	F	0.10	0.06	19	218	+0.0001	-0.0008	M	+0.0004	+0.0001	S	374
(Preoxidized, 1.9%)	78		22.2	2010	82	0.60	0.020	0.023	F	0.20	0.12	39	770	+0.0010	+0.0002	S	+0.0007	-0.0001	M	372
	78		22.1	2070	85	0.69	0.024	0.026	F	0.20	0.12	46	441	+0.0011	+0.0002	M	+0.0012	+0.0002	S	371
	78		23.1	2100	81	0.42	0.016	0.021	F, SG	0.20	0.12	45	778	+0.0016	+0.0012	M-H	+0.0015	+0.0006	S	373
FM-521	80	7.7	21.1	1660	80	0.97	0.033	0.033	F, SG	0.40	0.33	23	793	+0.0012	+0.0008	S	+0.0006	+0.0003	H	375
	80		20.6	1360	78	0.59	0.026	0.027	F	0.10	0.21	22	629	+0.0016	-0.0009	S	+0.0009	+0.0005	M	376

(1) Calc. volume loss based on rub depth measurements.

(2) Description Code: F - Fibrous, G - Glaze, H - Heavy, M - Moderate, O - None, S - Slight, V - Very

(3) Plunge rate was 0.010 in/sec.

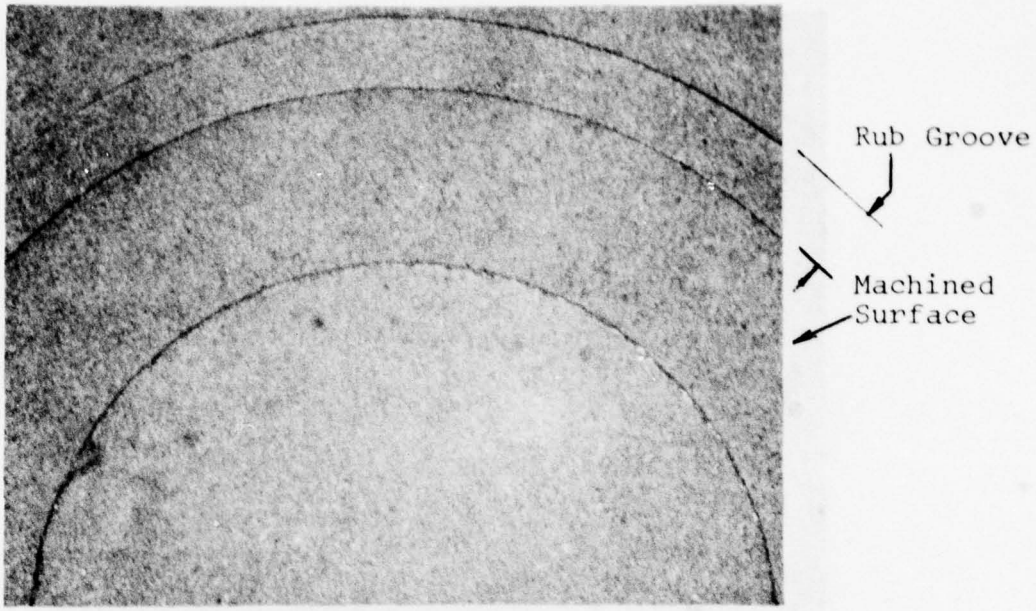

Rub Test #395, FM-521, 1.5X

SEM 100X Rub Groove

FIGURE 32

FM-521 RUB TEST SPECIMEN

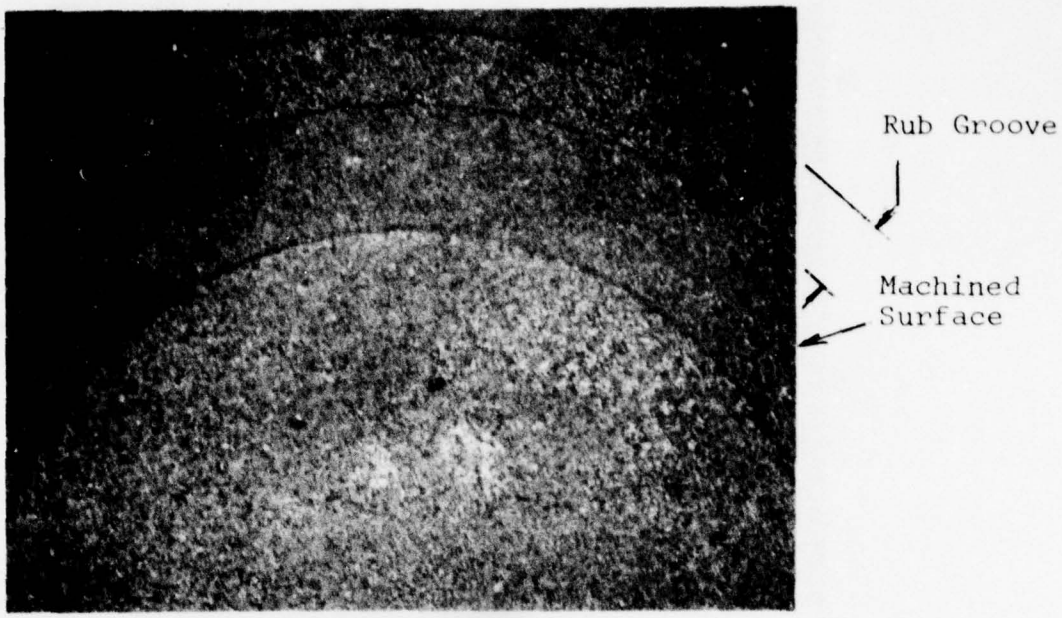

Test #365, Typical Good Rub, 1.5X

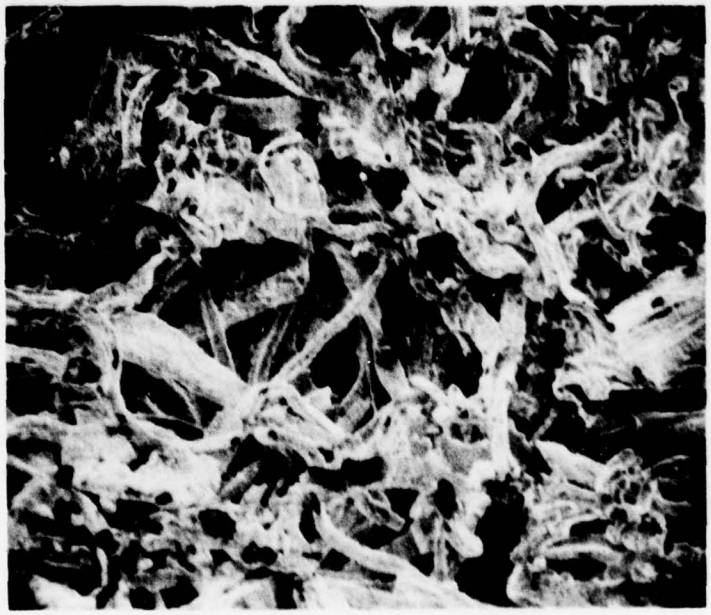

SEM 100X Rub Groove

FIGURE 33

16.6 MICRON FeNiCrAlY
RUB TEST SPECIMEN

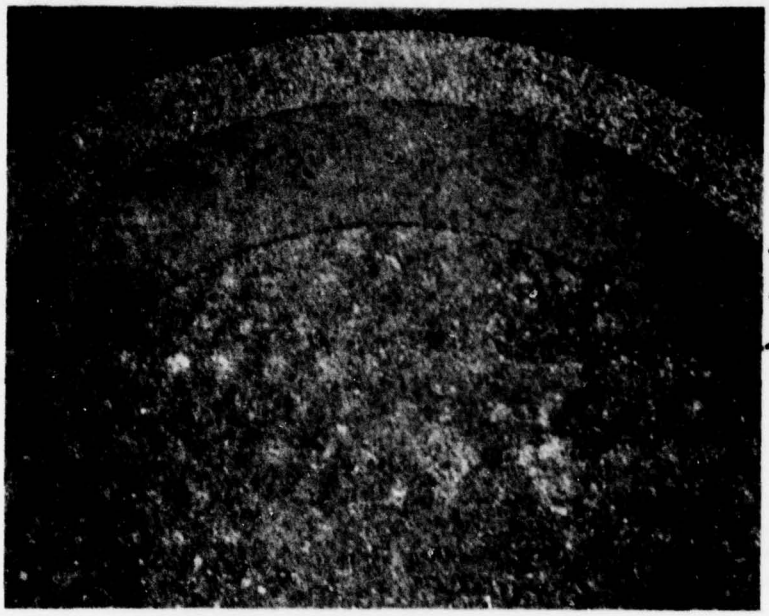

Test #360, Typical Good Rub, 1.5X

SEM 100X Rub Groove

FIGURE 34

12.6 MICRON FeCrAlY
RUB TEST SPECIMEN

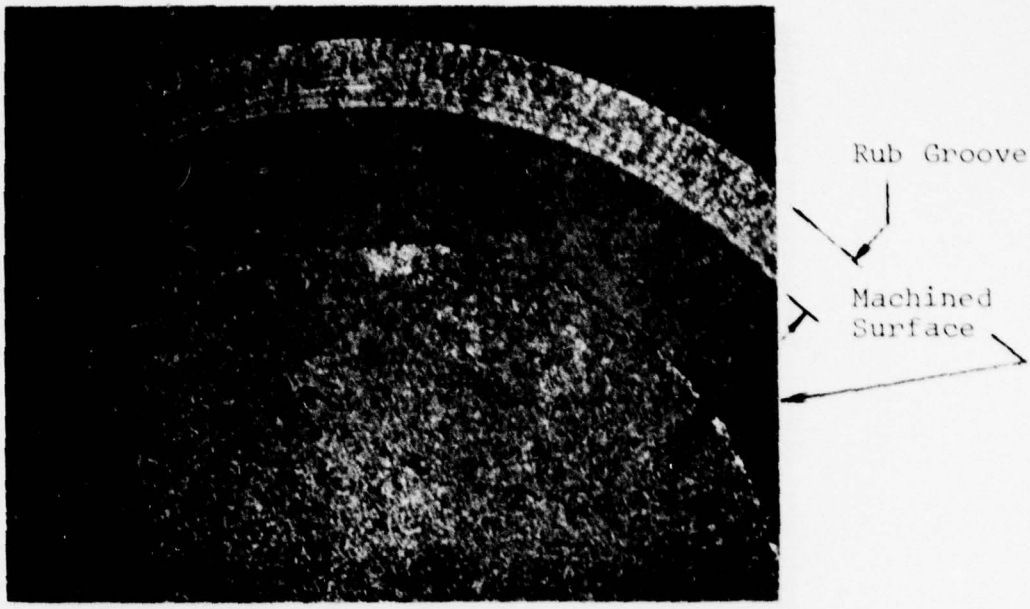

Test #306, Typical Poor Rub, 1.5X

SEM 100X Rub Groove, Test 306

FIGURE 35

23.4 MICRON FeCrAlY
RUB TEST SPECIMEN

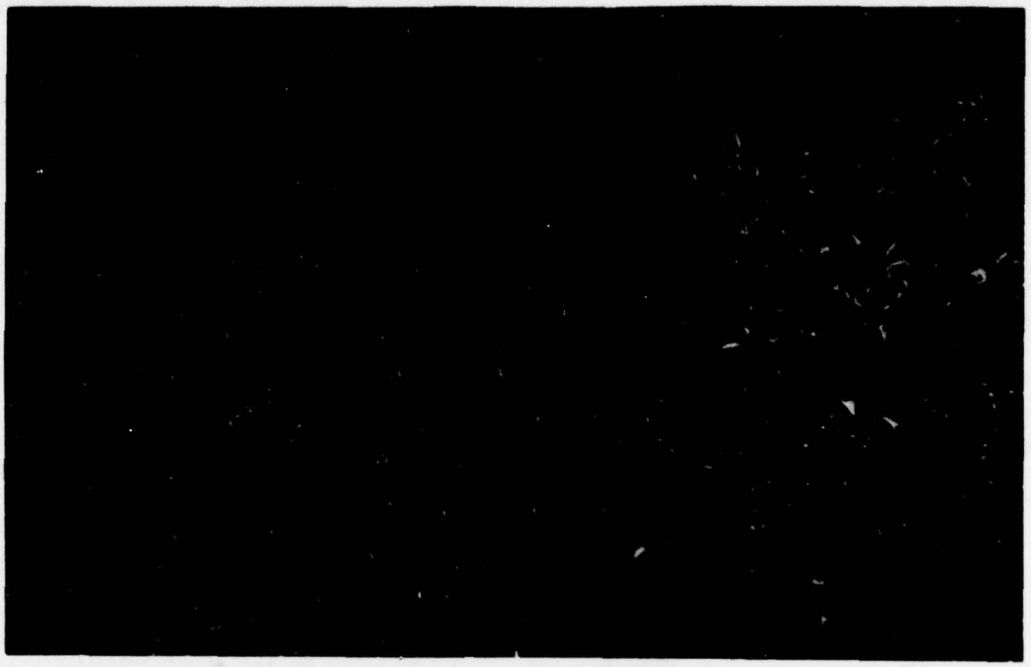

FM-521 Rub Groove Cross Section - 50X

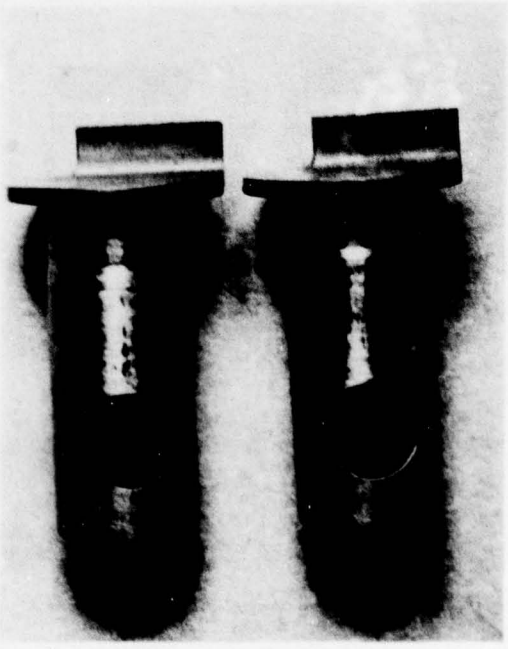

Waspaloy Blade Tips - 3X

FIGURE 36

FM-521 RUB GROOVE
WITH WASPALOY BLADE TIPS (GOOD RUB)

16.6 μm FeNiCrAlY Rub Groove Cross Section - 50X

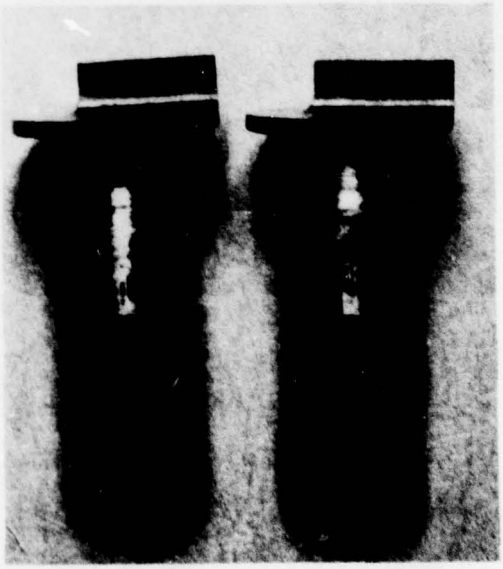

Waspaloy Blade Tips - 3X

FIGURE 37

16.6 MICRON FeNiCrAlY RUB GROOVE
WITH WASPALOY BLADE TIPS (GOOD RUB)

FeCrAlY Rub Groove Cross Section - 50X

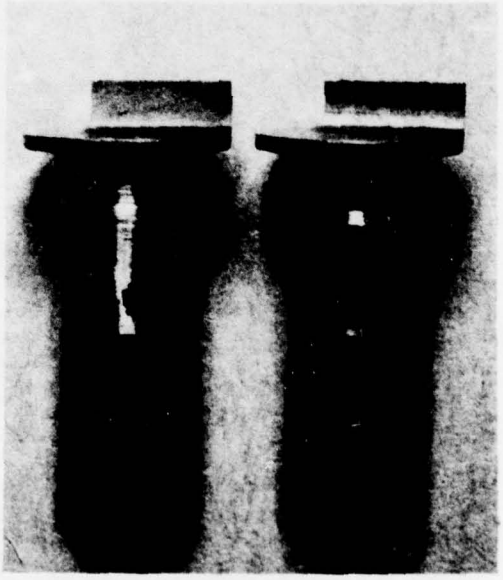

Waspaloy Blade Tips - 3X

FIGURE 38

12.6 MICRON FeCrAlY (RUB GROOVE)
WITH WASPALOY BLADE TIPS (GOOD RUB)

FeCrAlY Rub Groove Cross Section - 50X
Test #306

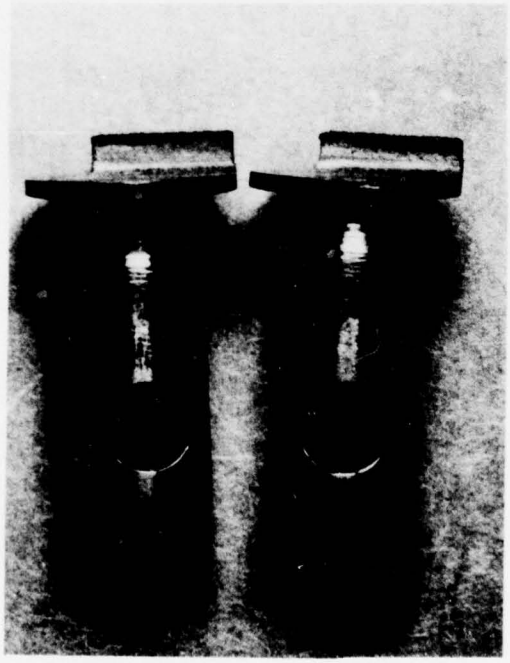

Waspaloy Blade Tips - 3X, Test #306

FIGURE 39

23.4 MICRON FeCrAlY
RUB GROOVE
WITH WASPALOY BLADE TIPS (BAD RUB)

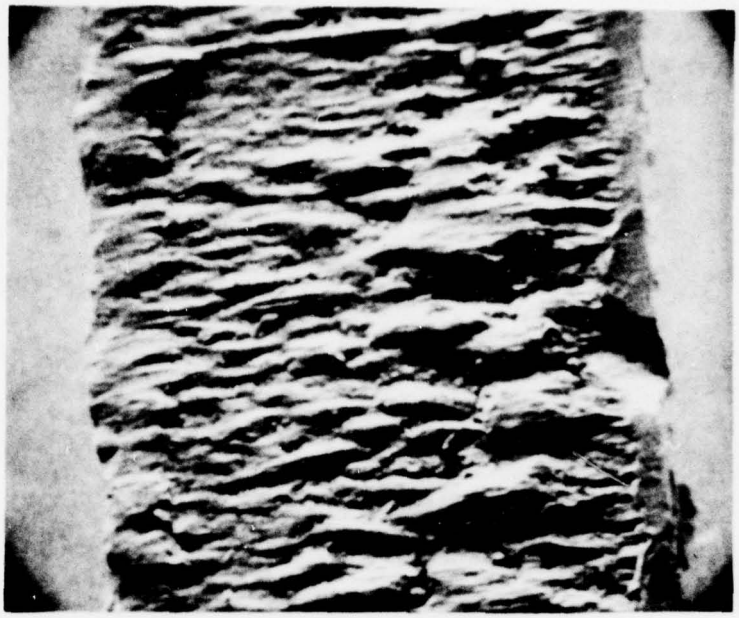

Direction of Rub

180X SEM, Test #389
FeNiCrAlY Test, Waspaloy Blade Tip, Good Rub

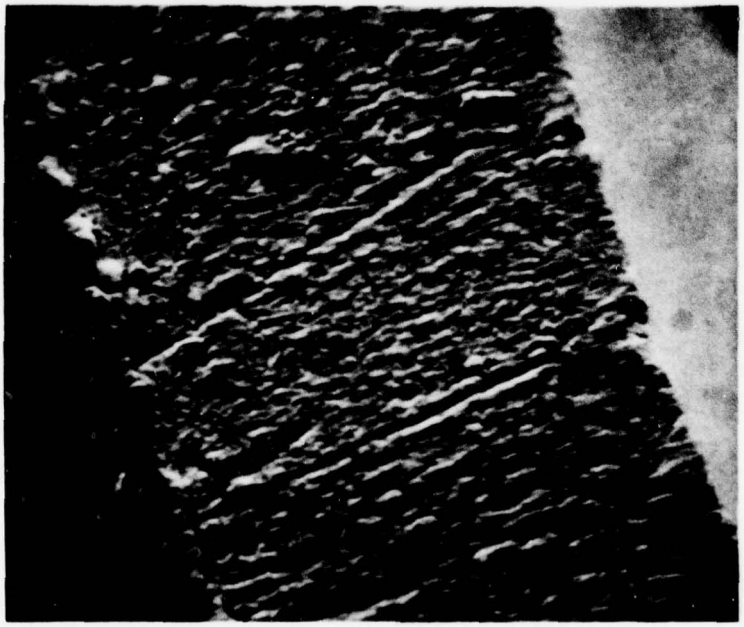

Direction of Rub

180X SEM, Test #392
FeCrAlY Test, Waspaloy Blade Tip, Good Rub

FIGURE 40

TYPICAL BLADE TIP SURFACES - GOOD RUBS

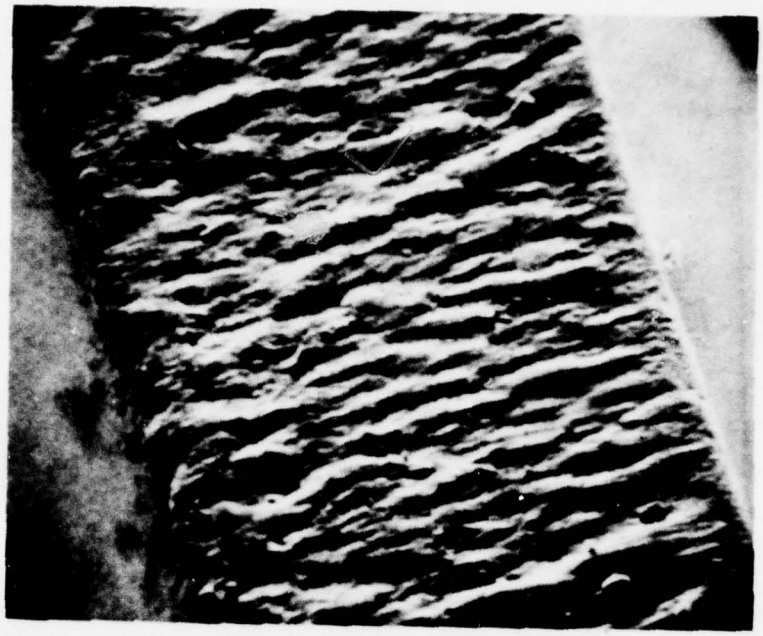

Direction of Rub

180X SEM, Test #292
FeCrAlY Test, Titanium Blade Tip, Poor Rub

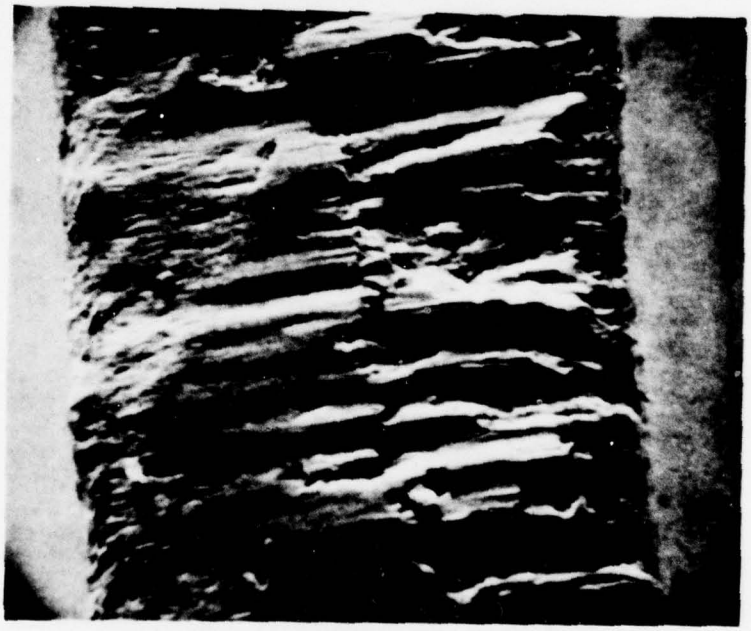

Direction of Rub

180X SEM, Test #306
FeCrAlY Test, Waspaloy Blade Tip, Poor Rub

FIGURE 41

TYPICAL BLADE TIP SURFACES - BAD RUBS

These observations are difficult to quantify when no blade wear is observed, so rub energy measurements have been used in order to evaluate the effects of different materials and properties on rub characteristics. Unfortunately, no satisfactory mathematical model of the effect of material properties on rub energy has been developed to date so empirical methods have been used to correlate rub energy from these rub tests with material properties. Previous studies have indicated the rub energy to be a function of fiber metal tensile strength and the alloy tested with considerable unexplained variance. Consideration of the transformation and conservation of the rotational rub energy measured in these tests with the use of the Bernoulli equation leads to the following conclusions:

1. The change in potential energy is zero.

2. The fracture energy of the fiber metal (see modulus of toughness data in Mechanical Properties section) is very low and considered negligible compared with the rub energies measured in the program.

3. If the rub debris were accelerated to the blade tip speed, the kinetic energy acquired by the rub debris is only about 5×10^3 in-lb/in^3 of abraded material which is small compared with the rub energies measured here.

4. The major portion of the rotational rub energy measured is converted into heat to heat up the blade tips, abradable material and rub debris which transfer heat to the air pumped by the high velocity blade tips.

Lacking a good mathematical model with which to explain the wide variation in rub energies measured, it was decided to attempt a linear regression analysis to correlate rub energy with the known independent variables. The results will be discussed below.

Effect of Test Conditions

Inspection of the data and averaging of the results in each of the three data tables for the three different test conditions on triplicated samples of each material variant leads to the following conclusions:

1. The high penetration rate rub with Waspaloy blades at 0.010 in/sec was the most severe test. More specimens caused blade wear than in the lower penetration rate rub tests. The maximum normal force measured averaged 50 - 57% higher than the slower speed rubs at 0.001 in/sec. The maximum torque measured at the end of the rub over the full 180° rub arc averaged 124 - 154% higher than for the low speed rubs. The rub energy per unit volume of abradable removed for the 0.010 in/sec rubs averaged 38 - 39% of the energy used for low rate rubs but the rate of energy input was almost 4 times higher than for the

low rate rubs. This caused higher interfacial temperatures and more blade wear.

2. The low penetration rate rub with Waspaloy blades at 0.001 in/sec was the least severe of the three test conditions. No significant blade wear was measured with any of the material variants at this test condition. The maximum normal force, torque, and energy input averaged about the same as for the titanium blade tip rubs at the same penetration rate.

3. Blade wear was more severe on the titanium blades than for Waspaloy at the same penetration rate despite the lower ambient temperature of the titanium rubs. This is probably the result of the lower strength of titanium at the high interfacial temperatures generated during a rub.

Material Transfer

The heavily burnished areas of the rub grooves of the seal specimens which caused blade wear were examined with a microprobe using X-ray energy dispersive analysis (EDAX). None of these samples showed evidence of transfer of blade tip material to the abradable and it was concluded that the worn blade material was thrown off of the blade tips at the exit of the rub groove where the blade tip would reach its highest temperature.

Microprobe analyses of the blade tips (see Figures 40 and 41) indicated deposits of abradable materials on both worn and non-worn blade tips including some of the best rubs where there were small deposits on the leading edges. The blade tip height measurements (see Tables XXVIII - XXX) indicated that these deposits were typically of the order of 0.001 inch high and not serious enough to generate large gaps in an engine sealing system in comparison with the gaps that can be generated with the longest blade relative to the shortest blade in a set.

Multiple Regression Analyses

The rub data in Tables XXVIII - XXX were evaluated with a linear regression analysis in an attempt to determine the significant variables and develop a correlation of rub energy with the independent variables. Rub energy was used as the independent variable and fiber diameter, L/D, tensile strength, hardness, percent density, and wt. % preoxidation were treated as independent variables even though strength and hardness are related to each other and both are highly dependent on the % density.

A preliminary analysis of the FeCrAlY system (on which all of the independent variables were changed in the program) indicated that % density and fiber L/D were insignificant variables. The analysis of the remaining independent variables gave mixed results with these variables appearing significant for one test type and not the others. It was decided to treat all the remaining four variables as significant to generate linear equations for the other three alloy system. The results are shown in Table XXXI.

TABLE XXXI

RUB TEST REGRESSION ANALYSES

ALLOY	BLADE TIP RUB TEST	MULT. CORREL. COEFF.	INDEPEND. VARIABLES USED(1)	PERCENT VARIATION EXPLAINED	SIGN. LEVEL PERCENT
FeNiCrAlY	Waspaloy 1 mil/sec	0.95	X_2	0	22.7
			X_3	50	80.3
Equation:			X_4	40	94.6
$Y = -3449 + 0.074X_2 + 44.5X_3 - 79.7X_4$				90	
FeNiCrAlY	Waspaloy 10 mil/sec	0.94	X_2	19	96.1
			X_3	42	89.8
Equation:			X_4	27	99.2
$Y = -1310 + 0.16X_2 + 15.5X_3 - 60.0X_4$				88	
FeNiCrAlY	Titanium 1 mil/sec	0.93	X_2	51	97.4
			X_3	8	85.0
Equation:			X_4	27	97.7
$Y = -1007 + 0.24X_2 + 12.7X_3 - 65.3X_4$				86	
FeCrAlY	Waspaloy 1 mil/sec	0.59	X_1	1	39.0
			X_2	1	89.6
			X_3	13	56.8
Equation:			X_4	19	88.5
$Y = 440 + 5.5X_1 + 0.39X_2 - 7.13X_3 - 150.7X_4$				34	
FeCrAlY	Waspaloy 10 mil/sec	0.89	X_1	36	99.8
			X_2	29	98.4
			X_3	3	78.2
Equation:			X_4	11	98.4
$Y = 511 + 51.8X_1 + 1.0X_2 - 30.5X_3 - 252.1X_4$				79	
FeCrAlY	Titanium 1 mil/sec	0.48	X_1	0	14.6
			X_2	17	83.0
			X_3	2	55.1
Equation:			X_4	4	41.4
$Y = 1029 + 5.2X_1 + 0.38X_2 - 14.6X_3 - 61.4X_4$				23	
Haynes 188	Waspaloy 1 mil/sec	0.996	X_1	0	26.0
			X_2	89	84.7
Equation:			X_3	10	81.0
$Y = 23{,}459 - 4.2X_1 + 3.0X_2 - 337.3X_3$				99	
Haynes 188	Waspaloy 10 mil/sec	0.995	X_1	8	88.7
			X_2	91	88.1
Equation:			X_3	0	24.3
$Y = 77 + 7.5X_1 + 0.21X_2 - 3.6X_3$				99	
Haynes 188	Titanium 1 mil/sec	0.991	X_1	0	18.4
			X_2	75	97.9
Equation:			X_3	23	96.6
$Y = 11{,}032 + 1.6X_1 + 1.8X_2 - 166X_3$				98	

NiCrAlY: Insufficient number of cases to analyze

(1) Y = Rub Energy, $\frac{\text{in-lb}}{\text{in}^3} \times 10^3$

X_1 = Fiber Diameter, μm
X_2 = UTS, psi
X_3 = Hardness, R_{57}
X_4 = pre-oxid. wt. gain, %

The most significant correlations accounting for most of the variance with all alloys were developed using the Waspaloy blade tip rub data at a penetration rate of 0.010 in/sec. The indicated qualitative effect of the variables was as follows:

1. Decreasing fiber diameter decreases rub energy. Fiber diameter was varied only on the FeCrAlY and Haynes 188 alloys.

2. Decreasing tensile strength decreases rub energy consistently on all three alloys evaluated.

3. Decreasing hardness decreases rub energy for FeNiCrAlY but increases rub energy for FeCrAlY and Haynes 188.

4. Preoxidation decreases rub energy for both the FeCrAlY and FeNiCrAlY alloys.

Using the regression equations generated for the 0.010 in/sec Waspaloy rubs, the rub energies for all material variants tested in the program were calculated at a constant density of 20% and tensile strength of 1800 psi to permit a ranking of the alternatives in the order of decreasing rub energies. The results are shown in Table XXXII. Hardnesses used were the hardnesses calculated from the equations presented in Table XIV.

With the exception of the anomalous 20.8 micron Haynes 188 system, this ranking of material variants tested was in fair agreement with the blade tip wear seal burnishing, and blade discoloration observations. The best two abradables were the preoxidized 16.6 micron FeNiCrAlY and the preoxidized 12.6 micron FeCrAlY fiber metals with the former being clearly the better.

Haynes 188

The coarse, 20.8 micron Haynes 188 system was abandoned after Task II as a result of the poor titanium blade tip rub at a low strength level as well as for the low oxidation resistance relative to the MCrAlY alloys.

The 7.7 micron Haynes 188 baseline material was one of the better abradables but had rub energies higher than the preoxidized FeCrAlY and FeNiCrAlY materials tested in Task IV.

NiCrAlY

This material demonstrated good abradability at a reasonable tensile strength but was abandoned for further testing after Task II primarily because of a higher cost than the other MCrAlY alloys.

FeCrAlY

This material showed poor abradability with the coarsest 23.4 micron fibers and fair to good abradability with the finer 12.6 micron fibers when preoxidized. One anomalous high wear rub (Test #384) was experienced during Task IV which makes this material a poor second choice to the FeNiCrAlY.

TABLE XXXII

CALCULATED RUB ENERGIES(1)

Material	Fiber Dia. μm	L/D	Preoxidation Wt. %	Calc.(2) Hardness R_{5Z}	Rub Energy in-lb/in^3 x 10^3
FeCrAlY	23.4	40	0	73.4	1284
FeCrAlY	16.4	50	0	74.6	890
FeCrAlY	12.6	45	0	74.0	707
FeCrAlY	12.6	78	0	78.1	582
Hayness 188	20.8	68	0	71.8	353(3)
NiCrAlY	11.1	47	0	81.6	315(4)
FeNiCrAlY	16.6	64	0	85.0	296
Hayness 188 (FM521)	7.7	80	0	77.4	234
FeCrAlY	12.6	78	1.9	78.1	103
FeNiCrAlY	16.6	64	4.0	85.0	56

(1) Calculated from regression equations in Table XXXI 1250°F Basis: 20% Density; 1800 psi Tensile Strength; Waspaloy blade tip rubs at 0.010 in/sec plunge rate, 800 ft/sec tip speed.

(2) Calculated from regression analysis in Table XIV.

(3) Blade wear was experienced with this material with titanium blade tips at low energy level of 289 x 10^3 in-lb/in^3.

(4) Estimated for tensile strength of 1800 psi.

FeNiCrAlY

This material was clearly the best abradable material tested particularly when preoxidized. No blade wear was encountered with any of the rub tests with tensile strengths up to 2700 psi.

Seal Specifications

As a result of the improved testing performed on this program, a new high temperature abradable seal material, FM-537, was defined using 17 micron FeNiCrAlY fiber metal. The new specification is shown in Appendix E along with the specification FM-521B for the baseline material. The same strength limitations of 1100 to 1900 psi were defined for FM-537 as for FM-521B. Although the FeNiCrAlY demonstrated good rubs to a tensile strength of 2700 psi with 180° blade tip rubs, it was decided to place the maximum strength limit at 1900 psi to allow for the improved abradability required for shrouded blade tips in advanced turbine seals where a 360° rub may be encountered when close installation clearances are specified.

A comparison of properties and estimated performance of the two products at their average densities and tensile strengths is shown in Table XXXIII. The FM-537 is an improvement over the baseline material in terms of oxidation resistance, erosion resistance, weight and abradability. The only disadvantage is the higher permeability of newly installed material; however, the pores get plugged with fine particulates in service so that this disadvantage disappears. In cases where this is critical for meeting performance specifications on new engines, alternative materials can be made with FeNiCrAlY fibers:

1. Make a denser and stronger fiber metal with the 17 micron fibers while sacrificing weight and abradability to increase erosion resistance and decrease leakage.

2. Use finer fibers in the 8-10 micron range while sacrificing some erosion and oxidation resistance.

TABLE XXXIII

PRODUCT PROPERTIES

Specification No.	FM-521B	FM-537
Alloy	Haynes 188	FeNiCrAlY
Fiber Diameter, microns	7.7	16.6
Density, percent	19.0	20.5
Tensile Strength, psi	1500	1500
Hardness R_{5Z} (1)	74.4	84.2
Permeability Coefficient (CFH/ft^2-in. H_2O - 1/16 in.) (2)	1850	6905
Weight, lb/in^3	0.0627	0.0520
Erosion Rate @ 1400°F (3), cc/min	0.0172	0.0128
Oxidation Temperature Limits, °F		
@ 1000 hr	1280	1610
@ 10,000 hr	1210	1520

(1) Calculated from Table XIV
(2) Calculated from Table V, Equation 2
(3) Calculated from Table XXVI
(4) From Figure 22

CONCLUSIONS

The following conclusions are made relative to the baseline material for improved abradable seals for advanced compressors and turbines.

1. Improved oxidation resistance can be achieved by using larger diameter fibers made from MCrAlY alloys.

2. A small reduction in weight can be achieved with the use of the low density FeNiCrAlY alloy.

3. Particulate erosion can be reduced by using harder fiber metals and larger fiber diameters.

4. Improved abradability can be achieved using preoxidized FM-537 made from 17 micron FeNiCrAlY fibers.

Other significant conclusions from the program are the following:

1. Hot gas erosion is not a problem as long as fiber metal strengths are held above 700 psi.

2. There is no problem with thermal shock and fatigue resistance of fiber metal seals made from the MCrAlY alloys.

3. Abradability of fiber metal seals can be improved with smaller fibers and with lower tensile strengths at the expense of erosion resistance.

4. The preoxidized FM-537 material made from 17 micron FeNiCrAlY fibers can provide improved abradability, oxidation resistance, erosion resistance, and lower weight. It is the best overall abradable seal material of the alternative materials evaluated in the program.

RECOMMENDATIONS

It is recommended that the FM-537 abradable seal material be engine tested for both compressor and turbine blade tip seals and labyrinth seals for operating temperatures to 1600°F.

More theoretical work should be performed to develop mathematical models for explaining the effects of material properties on the friction and wear characteristics of the low strength porous materials used for abradable seals.

APPENDIX A

STATIC OXIDATION TEST EQUIPMENT

A schematic of the cyclic oxidation test rig is shown in Figure A-1 and photographs are presented in Figure A-2. The rig consists of an electric paragon furnace currently capable of operating temperatures to 1700°F and a sample holder with a capacity of 12 specimens which automatically cycles in and out of the furnace at preset intervals. The cycle can be varied from one (1) to 60 cycles per hour. The cycle on this program was set at one hour in and one minute out of the furnace which lowers the sample temperature to approximately 300°F from 1600°F. Quartz tubes are inserted in the furnace to catch any spall from the specimens that occurs in the furnace. The tubes are 14 inches long, closed one end, with a 25 mm nominal bore and a 27.4 mm O.D. When the samples are cycled out of the furnace, a rotating disc indexes a high purity alumina crucible under the sample and collects any spall from the specimen in the out position. The sample holding rods that carry the samples into the furnaces are 1/4" diameter Hoskins Alloy 875 rods which are highly oxidation and spall resistant at the test temperatures (1200, 1400, and 1600°F). The 6" x .5" x .125" tensile bar samples are attached to the holding rods with 12 mil Hoskins Alloy 875 wire. This wire is replaced after each 20 hour exposure.

The furnace temperature is controlled by an Inconel shielded Type "K" (chromel-alumel) thermocouple while the sample temperature is indicated by a Type "R" (platinum, 13% rhodium) thermocouple. The sample temperature is continuously recorded on an ACCO Bristol, Series 64A, dynamaster controller-recorder. The sample thermocouple is located adjacent to a sample in the furnace and does not cycle out of the furnace with the samples.

Cycle control is regulated by a Lincoln Pneumatic Control System which controls the air cylinders that actuate the sample rods in and out of the furnace and the rotating disc which moves the alumina crucibles under the samples. The Kunke air operated timers are also controlled by the Lincoln controller.

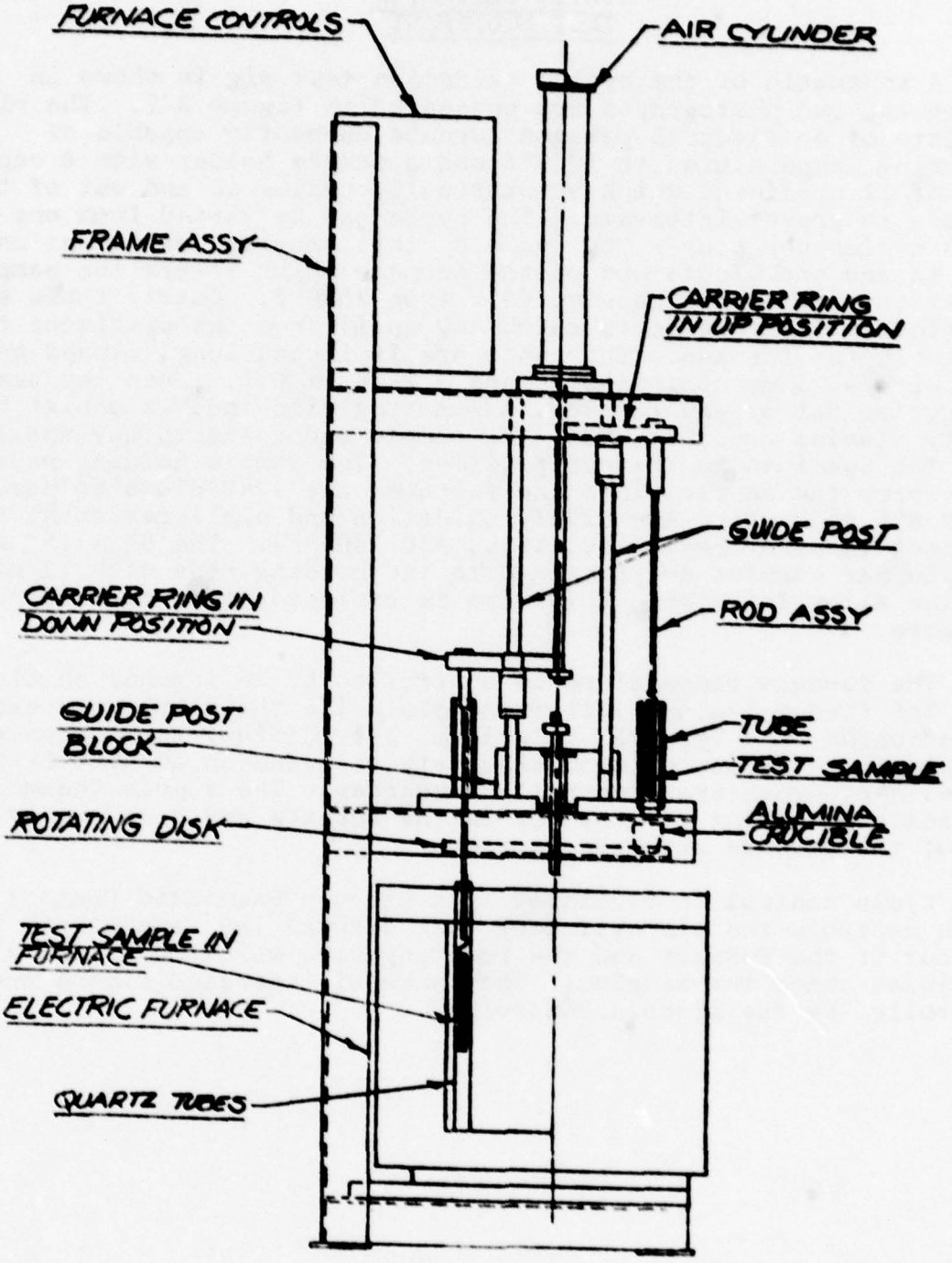

FIGURE A-1
STATIC OXIDATION TEST STAND

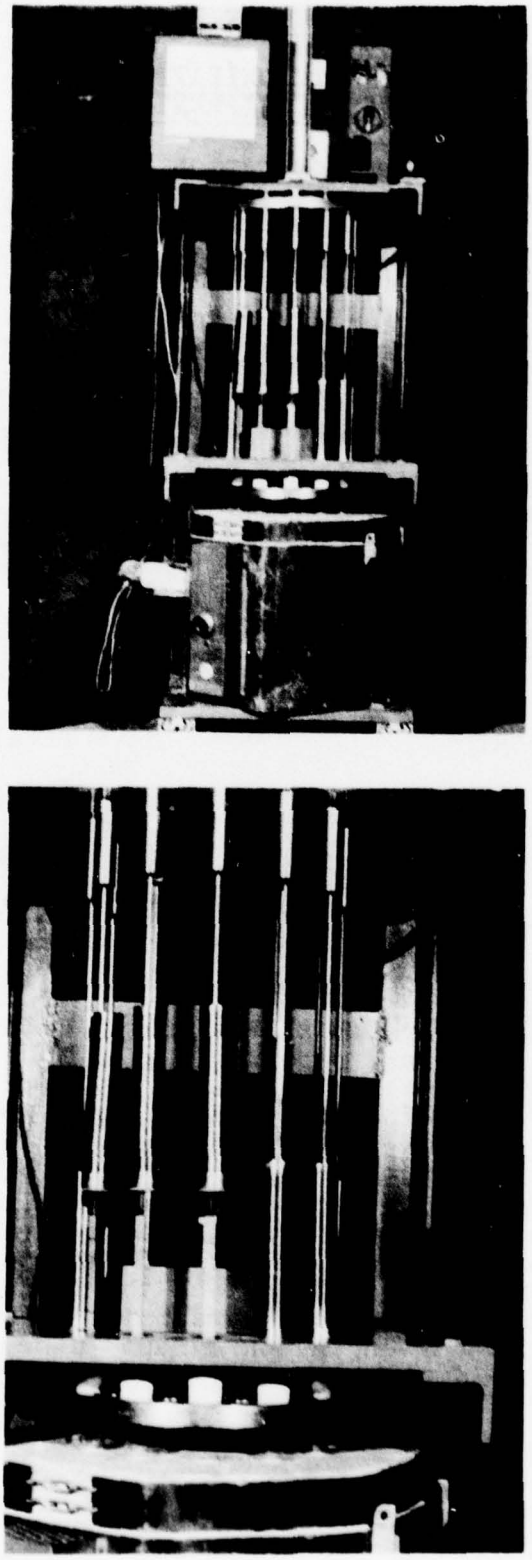

FIGURE A-2
STATIC OXIDATION TEST RIG

APPENDIX B

DYNAMIC OXIDATION TEST EQUIPMENT

A sketch of the dynamic oxidation test rig is shown in Figure B-1 and photographs are presented in Figure B-2. The rig consists of a cylindrical clamshell furnace, 8-1/2" in diameter with a 6" deep hot zone with a temperature capability of up to 1500°F. A high pressure propane combustor directs high velocity (Mach = 0.8) gas at the samples at a pre-set temperature. The test temperatures of both the furnace and jet exit were 1400°F. The resultant sample surface temperature was also measured at 1400°F. The jet burned a mixture of propane and oxygen at an 8:1 ratio and flow that would produce the calculated exit velocity of Mach = 0.8. Air was injected into the burner downstream of the combustion chamber to lower the exit temperature to 1400°F. The cooling air was included in the mass flow rate calculation. Calculations used to obtain the correct exit velocity at a given temperature are as follows:

$$M_E = \frac{\sqrt{T_E}\, M_T}{1440} = 0.8$$

Where T_E = Exit Temp. (°F + 460)

M_T = Total Mass Flow Rate (lb/hr)

For T_E = 1400°F

$$M_E = .02995\ M_T$$

A type "K" thermocouple was placed at the jet exit to monitor and record the exit temperature throughout the test. The furnace temperature was controlled by a Barber-Coleman controller, model #297C, with a Type "K" thermocouple, which was also recorded on the dual pen recorder.

The test samples are 1" x 1" x .125" which are brazed with Nicrobraze LM 3 mil braze tape to 1" x 1.25" x 0.90" Waspaloy (AMS 5544) backing plates. The twelve (12) test samples for each task are mounted on the periphery of a circular sample holder which is rotated in the furnace past the jet at 175 rpm. The sample holder is rotated in the furnace on a water cooled shaft by a 1/2 H.P. motor. The samples are cycled in and out of the furnace by an air cylinder controlled by a 60 minute timer. The cycle for this program was 60 minutes in and one minute out of the furnace. When the samples are out of the furnace, a high velocity cool air stream is directed on the samples to simulate the thermal shock experienced in an engine on a rapid deceleration.

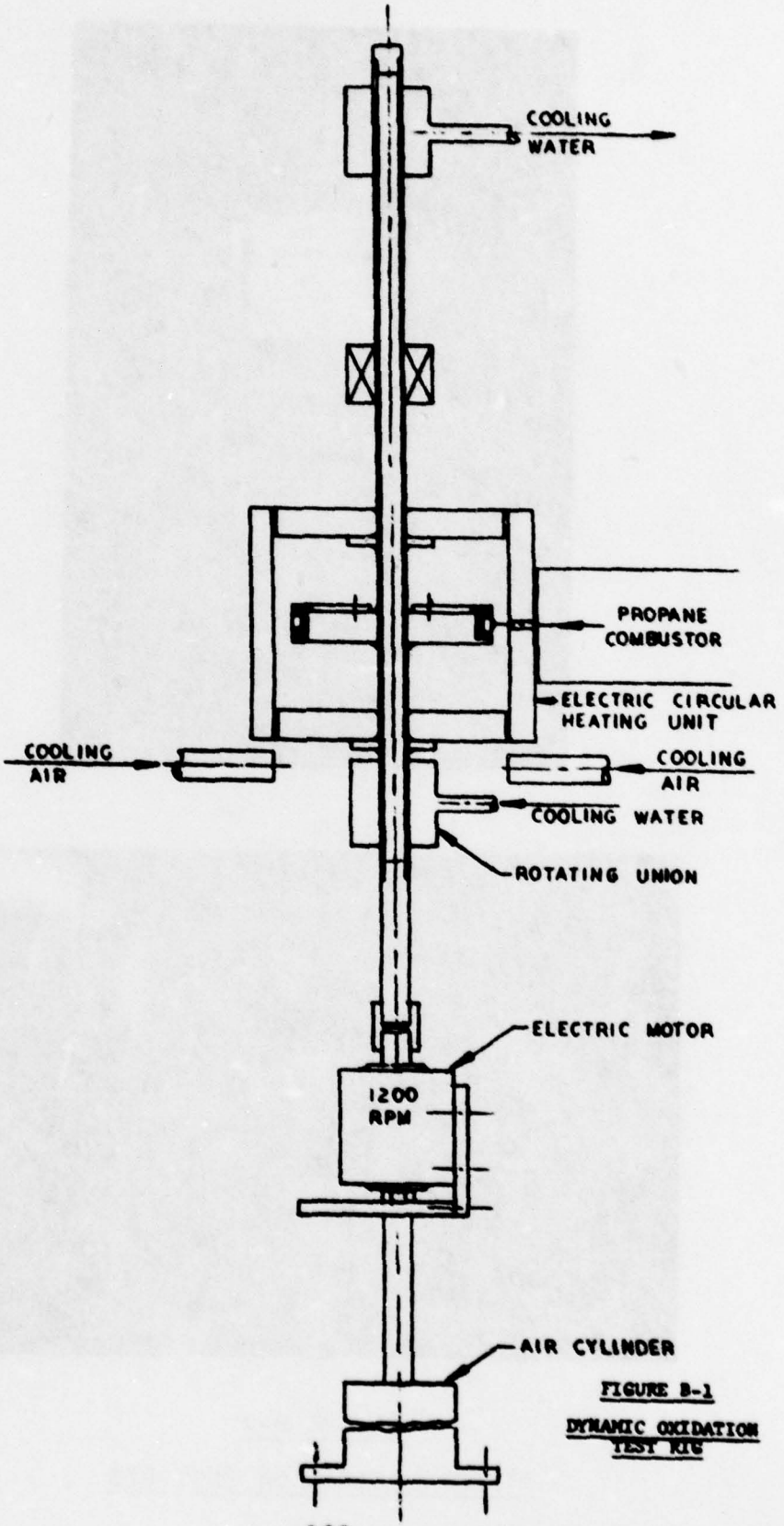

FIGURE B-1

DYNAMIC OXIDATION
TEST RIG

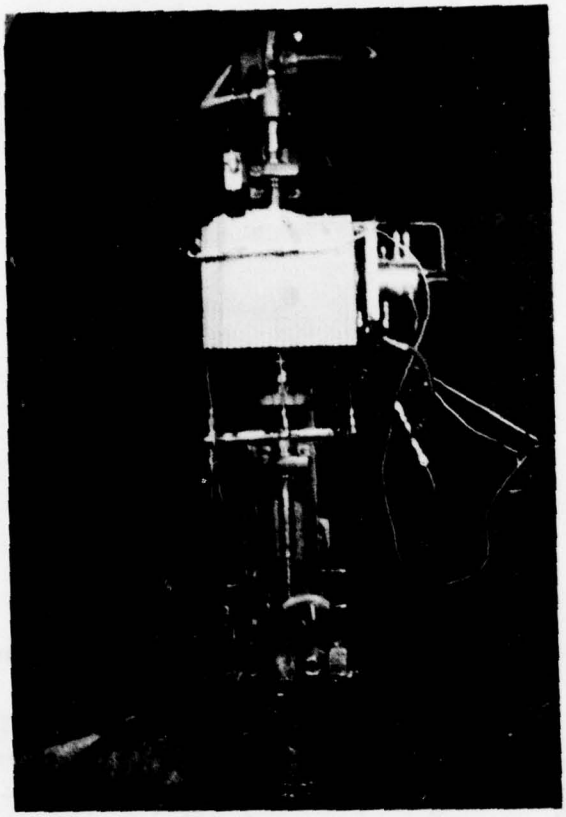

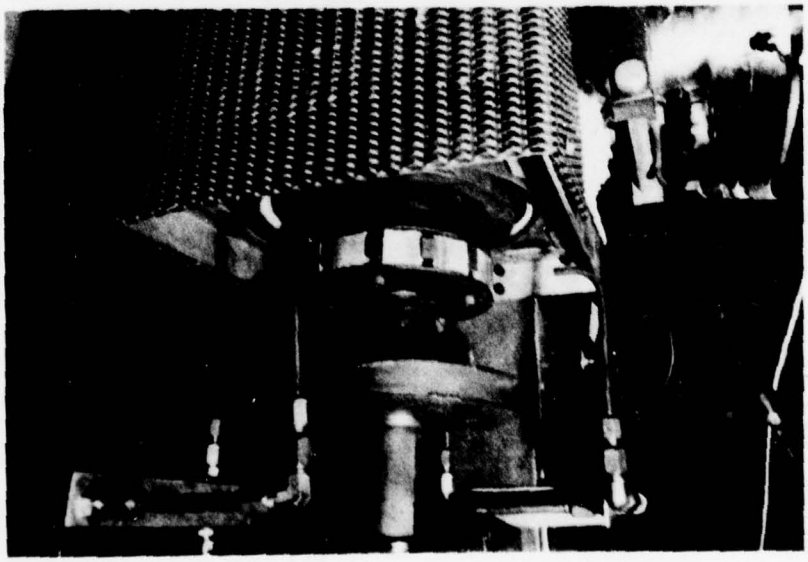

FIGURE B-2

DYNAMIC OXIDATION TEST RIG

APPENDIX C

HOT PARTICULATE EROSION EQUIPMENT AND PROCEDURE

Equipment Description

A schematic of the hot particulate erosion rig is shown in Figure C-1. A photograph of the rig is shown in the top part of Figure C-2 while the lower photograph shows the nozzle and a test specimen mounted at a 7° impingement angle. Details of the rig are available on Brunswick drawing, D-1291. The rig consists of a fuel system, air system, combustion chamber, ignition system, particulate feed system, sample positioning system, and a control system.

Test Conditions

The test conditions were established as shown in Figure C-3.

A surface thermocouple indicated that the sample temperature was approximately 250°F cooler than T_1. Therefore, the test procedure that was used was to set T_1 as required to obtain the desired sample test temperature (T_2 = 1200, 1400, or 1600°F). The thru flow (Q_a) is then adjusted accordingly to equation (6) to set M_1 = 0.35.

The following is a rough estimate of the actual flow condition in the vicinity of the test sample:

$$\text{in general, } V^2 + (2/k-1)\, C^2 = (2/k-1)\, C_o^2$$

$$\text{and } (V/C)^2 + 2/k-1 = (2/k-1)(C_o/C)^2$$

$$\text{since } M = V/C$$

$$M^2 + 2/k-1 = 2/k-1\ (C_o/C)^2$$

and

$$M^2 = [(C_o/C_1)^2 - 1]\ (2/k-1)$$

$$M_1^2/M_2^2 = [C_o/C_1)^2 - 1]\ (2/k-1)/[(C_o/C_2)^2 - 1]\ (2/k-1)$$

$$= 49\sqrt{T_o}/49\sqrt{T_1})^2 - 1]/[(49\sqrt{T_o}/49\sqrt{T_2})^2 - 1]$$

$$= T_o/T_1 - 1/\ T_o/T_2 - 1$$

$$= T_o - T_1/T_1 \times T_2/T_o - T_2$$

$$= (T_2/T_1)\ (T_o - T_1/T_o - T_2)$$

Evaluation of equation (6)

At	Yields
T_o = 2000°F = 2460°R T_1 = 1650°F = 2110°R T_2 = 1400°F = 1860°R	M_2 = 1.36 M
and	
T_o = 4000°F = 4500°R T_1 = 1650°F = 2110°R T_2 = 1400°F = 1860°R	M_2 = 1.12 M

Assuming that the combustion temperature is between 2000°F and 4000°F, the above analyses indicates that the actual surface Mach number is likely to be 15 - 25% higher than desired. It is felt, however, that for purposes of uniformity, control of the flow conditions at station 1 was the best test procedure. Furthermore, the air flow rate used to set Mach number was the indicated flow which is approximately 7% higher (by virtue of delivery temperature and pressure) than the actual flow rate. This has the effect of partially compensating the 15 - 25% excess in the sample Mach number due to the temperature differential. Therefore, the best estimate of sample Mach number is 0.35 + 8 to 18%, i.e. .38 →.41.

Test Procedure

Specimen Preparation

1. Test specimens were fabricated as shown in Fig. C-4. The test materials were weighed and measured to determine exact density before brazing.

2. Measure and record pretest weight of test sample and leading edge shield.

3. Install test sample and shield in holding fixture so that it is presented to the gas stream at the desired 7° impingement angle and at the appropriate location relative to the exit plane.

Particulate Preparation

1. Sieve silica sand to the required 200 x 325 mesh particle size distribution.

2. Calibrate belt feeder to achieve a feed rate of .5 lb of particulate in 5 minutes.

3. Place .5 lb of particulate over the appropriate length of belt.

4. Record belt speed, particulate weight, and length of particulate.

TABLE C-I

FLOW CONDITIONS FOR M = 0.35
AND EXIT PRESSURE 14.7 PSIA

Sample Temperature (°F)	Exit Temperature (°F)	Air Flow (SCFM)	Fuel Flow (ref) (cc/min)
1200	1525	42	66.4
1400	1725	40	62.7
1600	1825	38	59.6

TABLE C-II

ACTUAL FLOW CONDITIONS

Sample Temp., °F	1200	1400	1600
Gas Exit Temp., °F (T_1)	1525	1725	1825
Gas Press., psi (P_1)	.25	.25	.25
Combustion Press., psi (P_o)	2.0	2.0	2.0
Air Flow, SCFM (W_a)	42	40	38
Air Temp., °F (T_a)	130	130	130
Air Supply Press, psi	4	4	4
Air Del. Press., psi (P_a)	2.5	2.5	2.5
Fuel Flow, cc/min (W_a)	58	62	64
Fuel Sup. Press., psi	160	195	215
Fuel Del. Press., psi	160	195	215
Fuel Del. Temp., °F	74	74	74

Combustion Apparatus

1. Turn on electrical power and cooling water.

2. Calibrate exit temperature thermocouple and indicating device.

3. Place discharge duct into position.

4. Turn on air blower and set its discharge valve so that supply pressure is 5 psig at 45 SCFM air flow. Maintain this air flow.

5. Set hydrogen ignitor flow as required and energize ignitor. Note ignition by 200 - 400°F rise in exit gas temperature.

6. Start fuel flow and note ignition by rapid rise in exit temperature to 1500 - 2000°F. Adjust fuel flow to achieve desired sample temperature. Allow system to stabilize.

7. Set air flow for desired Mach number and sample temperature per Table C-I.

The actual flow conditions are shown in Table C-II.

Erosion Test

1. Bring test sample to the test position.

2. Start particulate feed.

3. Record all pertinent test conditions (flow, pressure, temperature, etc.)

4. When particulate feed is complete, retract test sample from test position.

5. Allow sample to cool and remove from holder.

Test Sample Evaluation

1. Weigh sample and calculate weight loss.

2. Measure depth and width of erosion path.

Reiteration

Repeat the previous steps three (3) more times for a total test time of approximately 20 minutes and a total particulate charge of 2 lbs for an average particulate feed rate of 6 lb/hr.

Calculations

1. Calculate rate of volume loss in cc/min from weight loss, sample density, and time for the last 15 minutes of testing.

The data for the first 5 minutes are ignored because of weight gains that result from plugging of the largest pores with some of the smallest particulates present. If the rates for the second 5 minutes of testing are also unrealistically low compared with the final 15 minutes of testing, these too are eliminated from the calculation.

2. Calculate erosion time in sec. per 0.001 in. eroded by dividing the total erosion time by the total depth loss at the specimen center.

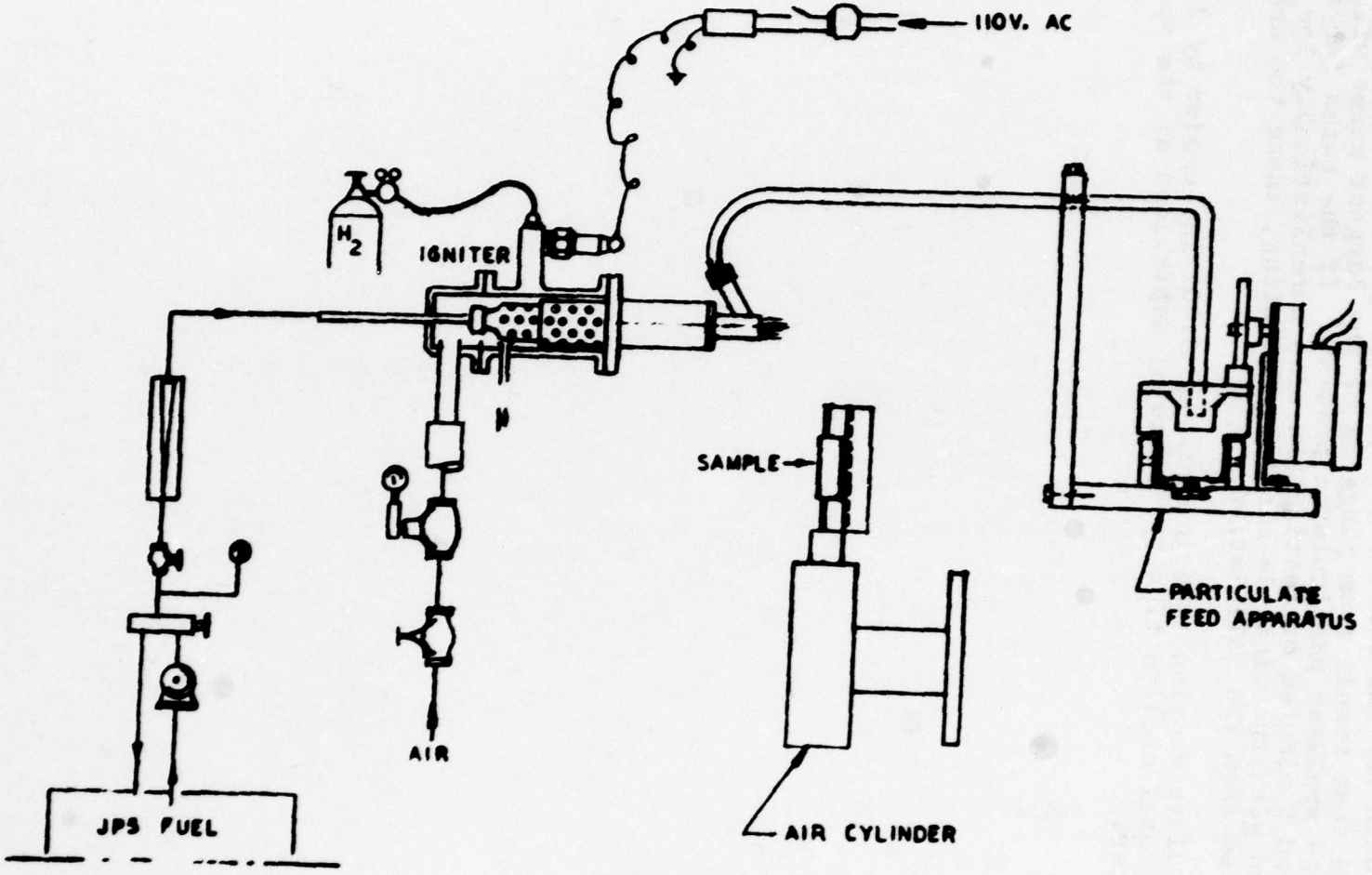

FIGURE C-1
HOT PARTICULATE EROSION
TEST RIG

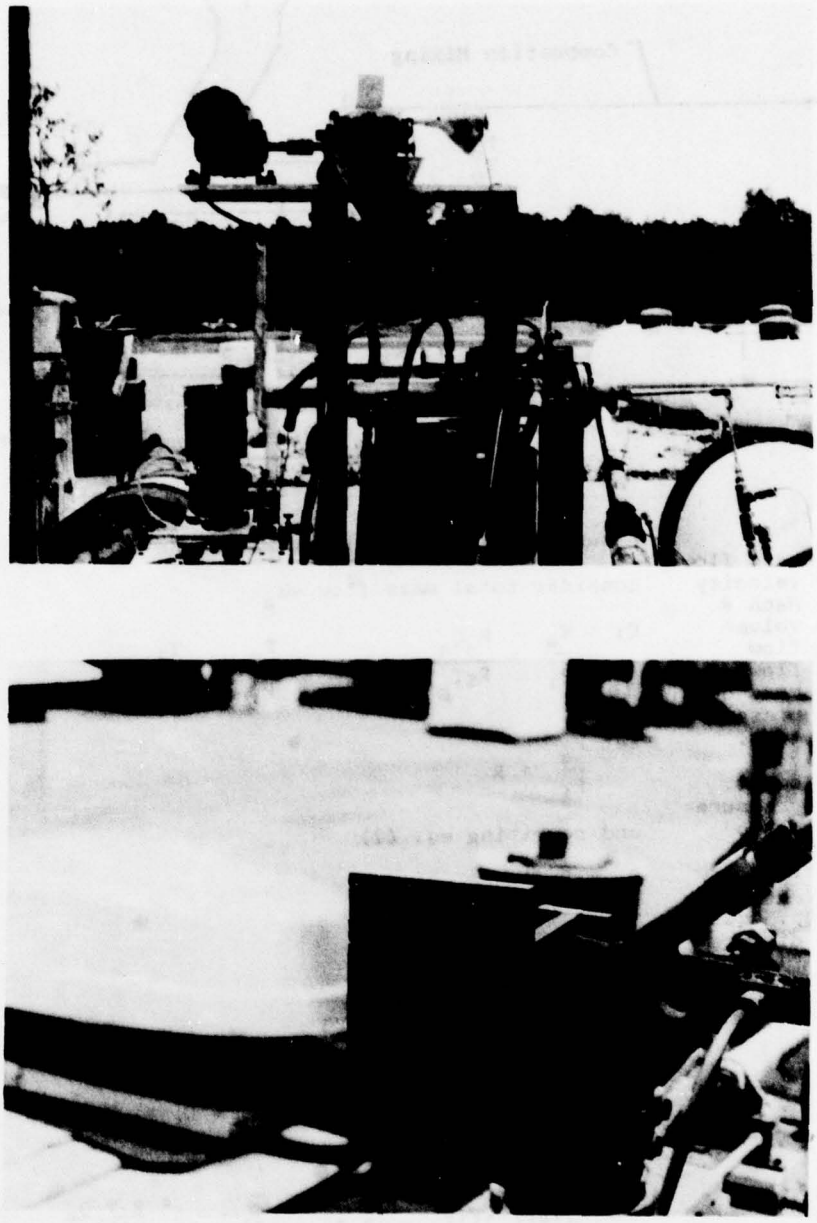

FIGURE C-2

HOT PARTICULATE EROSION
TEST RIG

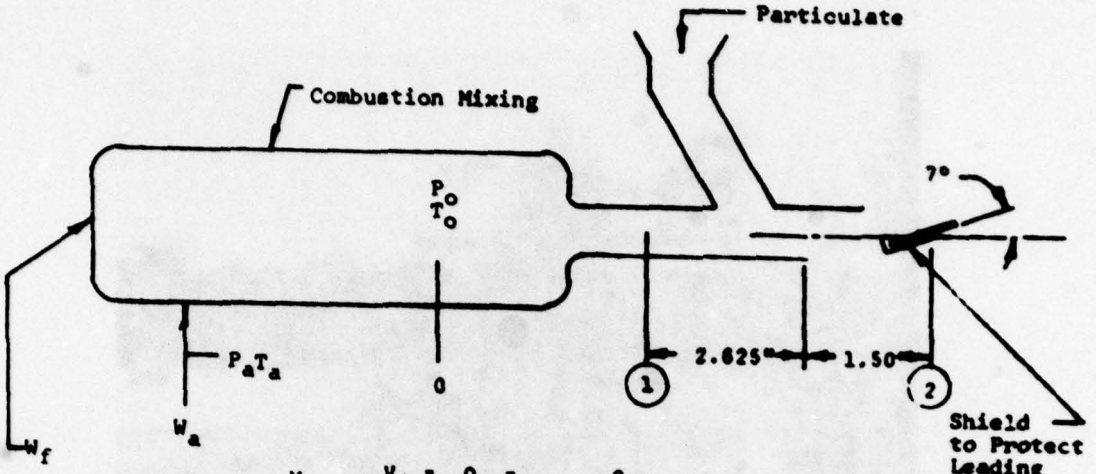

$$M = \frac{V_1}{C_1} = \frac{Q_1}{A_1 C_1} = \frac{Q_1}{A_1\ 49.02\sqrt{T_1}} \qquad (1)$$

W = mass flow
V = velocity
M = Mach #
Q = volume flow
A = flow area
= mass density
P = pressure
T = temp.
Rg = gas const.
R = pressure ratio
C = sonic velocity
k = ratio sp. heats
D = diameter
a = air
f = fuel

Assume (30 air/1 fuel) wgt ratio and consider total mass flow $\approx W_a$

$$Q_1 = \frac{W_a}{S_1} = \frac{P_a Q_a}{RgT_a \frac{P_1}{RgT}} = \frac{P_a}{P_1} \frac{T_1}{T_a} Q_a \qquad (2)$$

set $\frac{P_a}{P_1} = R$

and rewriting eq. (2)

$$Q_1 = R \frac{T_1}{T_a} Q_a \qquad (3)$$

substituting (3) → (1)

$$M_1 = R \frac{T_1}{Ta} Q_a \frac{1}{A_1\ 49.02\ \sqrt{T_1}} \qquad (4)$$

and for Q_a = SCFM, $T_a = 520°R$, & $D_1 = .75$ in

rewriting eq. (4)

$$M_1 = \frac{R\sqrt{T_1}\ Q_a}{\frac{.785(.75)^2}{144} \times 49.02 \times 520 \times 60} = \frac{R\sqrt{T_1}Q_a}{4690} \qquad (5)$$

Subsequent testing showed .95 <R <1.05 for all conditions so that

$$M_1 = \sqrt{T_1}\ Q_a/4690 \ ; \ \begin{matrix} Q_a = \text{SCFM} \\ T_1 = °R \end{matrix} \qquad (6)$$

FIGURE C-3

SCHEMATIC OF EROSION TEST SETUP

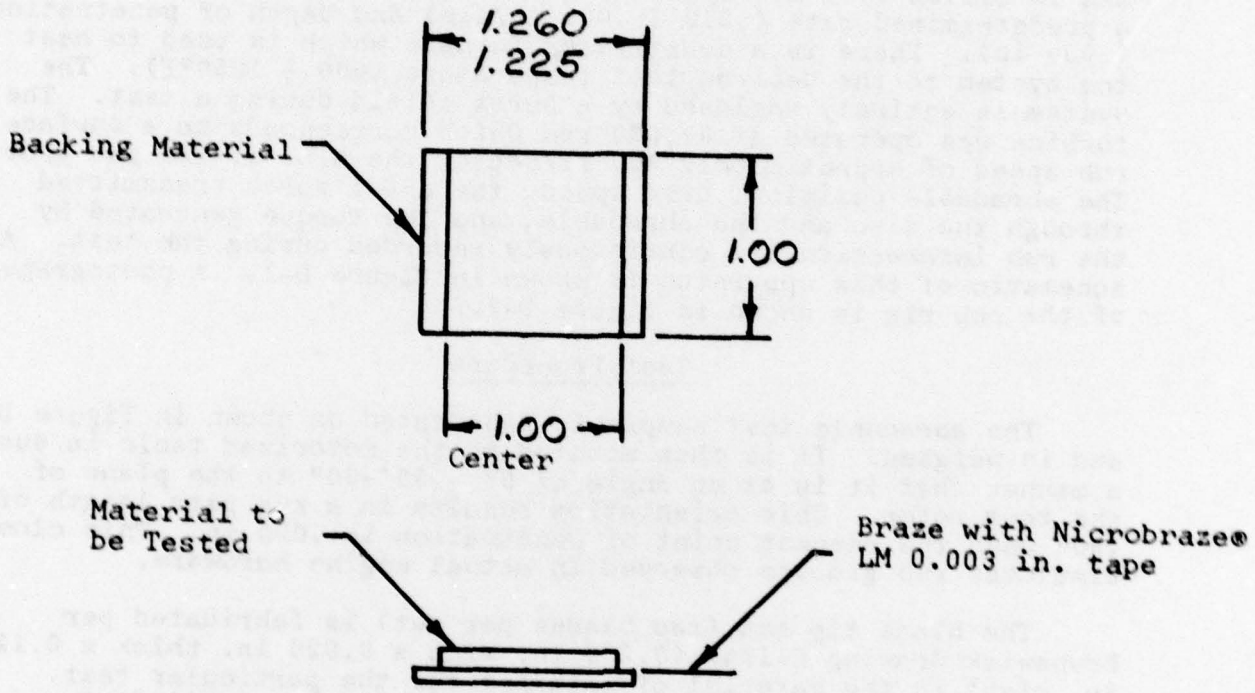

FIGURE C-4

TEST SAMPLE CONFIGURATION
DYNAMIC OXIDATION AND
HOT PARTICULATE EROSION

APPENDIX D

HIGH SPEED RUB TESTING

Equipment

The test apparatus consists of an air turbine which drives a disc containing the blade tip to be tested. The abradable specimen is driven by a motorized table into the rotating blade tips at a predetermined rate (.010 & .001 in/sec) and depth of penetration (.030 in). There is a quartz lamp furnace which is used to heat the system to the desired test temperature (600 & 1250°F). The system is entirely enclosed by a burst shield during a test. The turbine was operated at 42,000 rpm which corresponds to a surface rub speed of approximately 800 ft/sec at the O.D. of the rub groove. The abradable position, disc speed, the axial force transmitted through the disc and the abradable, and the torque generated by the rub interaction are continuously recorded during the test. A schematic of this apparatus is shown in Figure D-1. A photograph of the rub rig is shown in Figure D-2.

Test Procedure

The abradable test sample is fabricated as shown in Figure D-3 and is weighed. It is then mounted on the motorized table in such a manner that it is at an angle of 0° - 50'-00" to the plane of the test rotor. This orientation results in a rub path length of 180° when the deepest point of penetration is .030 in. This closely simulates rub grooves observed in actual engine hardware.

The blade tip set (two blades per set) is fabricated per Brunswick drawing C-1047 (0.250 in. wide x 0.020 in. thick x 0.125 in. high) in the material of interest for the particular test. The materials used for this program were titanium (AISI 811) and Waspaloy (AMS 5544). The blades are individually weighed and measured so that wear weight loss and height loss can be determined. The blade tips are installed into the test rotor.

The motorized table is brought to a position leaving .010 in. clearance between the abradable sample surface and the blade tip surface. The rotor speed is increased to 42,000 rpm which results in a surface velocity of 800 ft/sec at the blade outside diameter. The motorized table is then advanced at the desired penetration rate for a total travel of 0.040 in. This results in penetration into the abradable surface to a nominal depth of 0.030 in. (0.040 in. travel - 0.010 in. initial clearance). During this time, the rotor speed, table position, axially transmitted force, and torque are continually recorded on a pen chart recorder.

After the test, the amount of blade tip wear is determined by weight and height measurements and comparison with pretest measurements. The actual depth of penetration into the abradable is measured at three places (deepest point and 45° on either side of the deepest point) on the abradable test sample. The abradable test sample is weighed. The rub energy is calculated by graphical

integration of the speed and torque traces made during the test. The volume of material removed from the abradable test sample is calculated as shown in Figure D-4. The abradable test samples are photographed, examined with SEM, and sectioned for photomicrographs. The blade tips are also photographed.

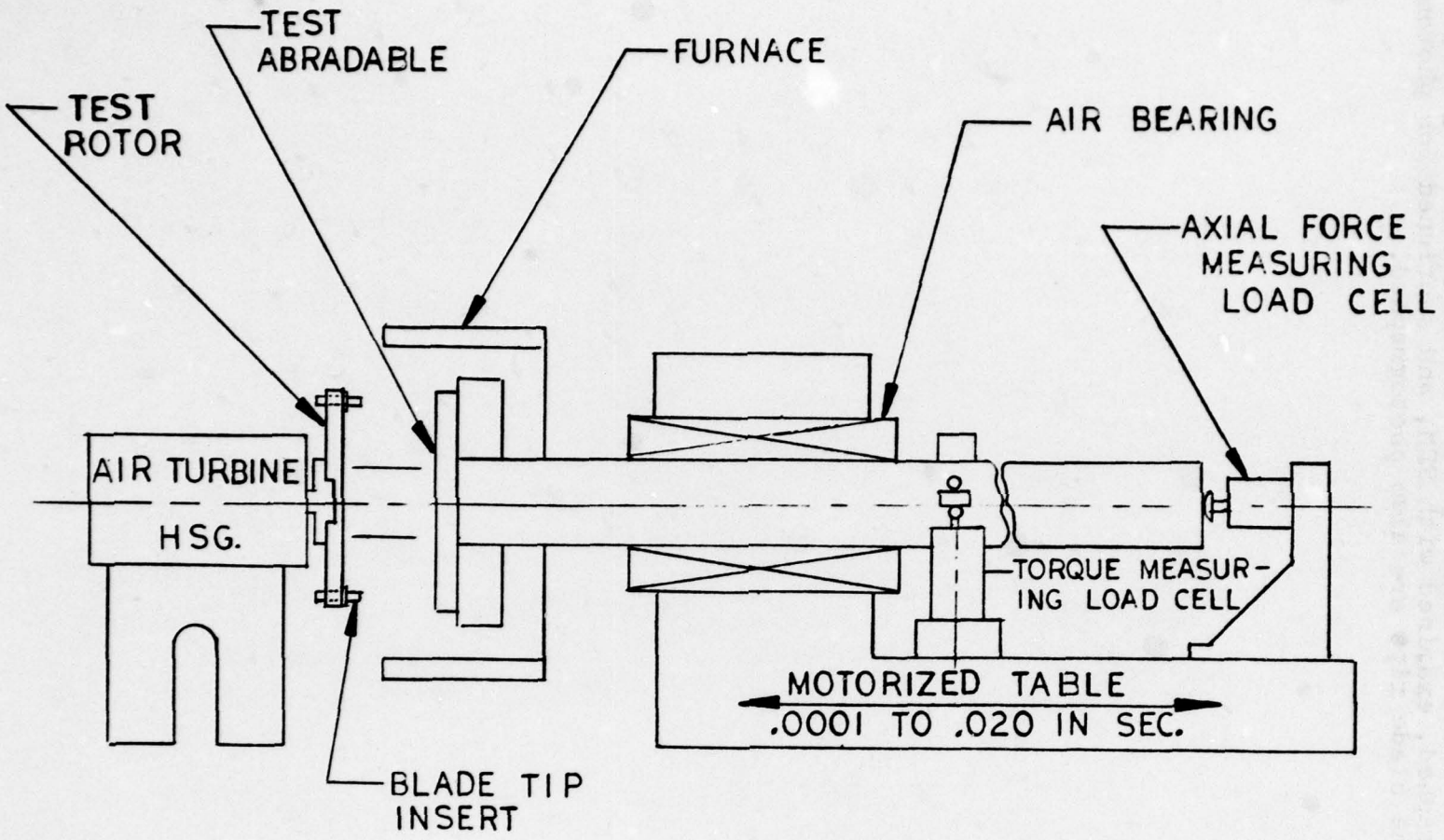

FIGURE D-1

HIGH SPEED RUB TEST RIG

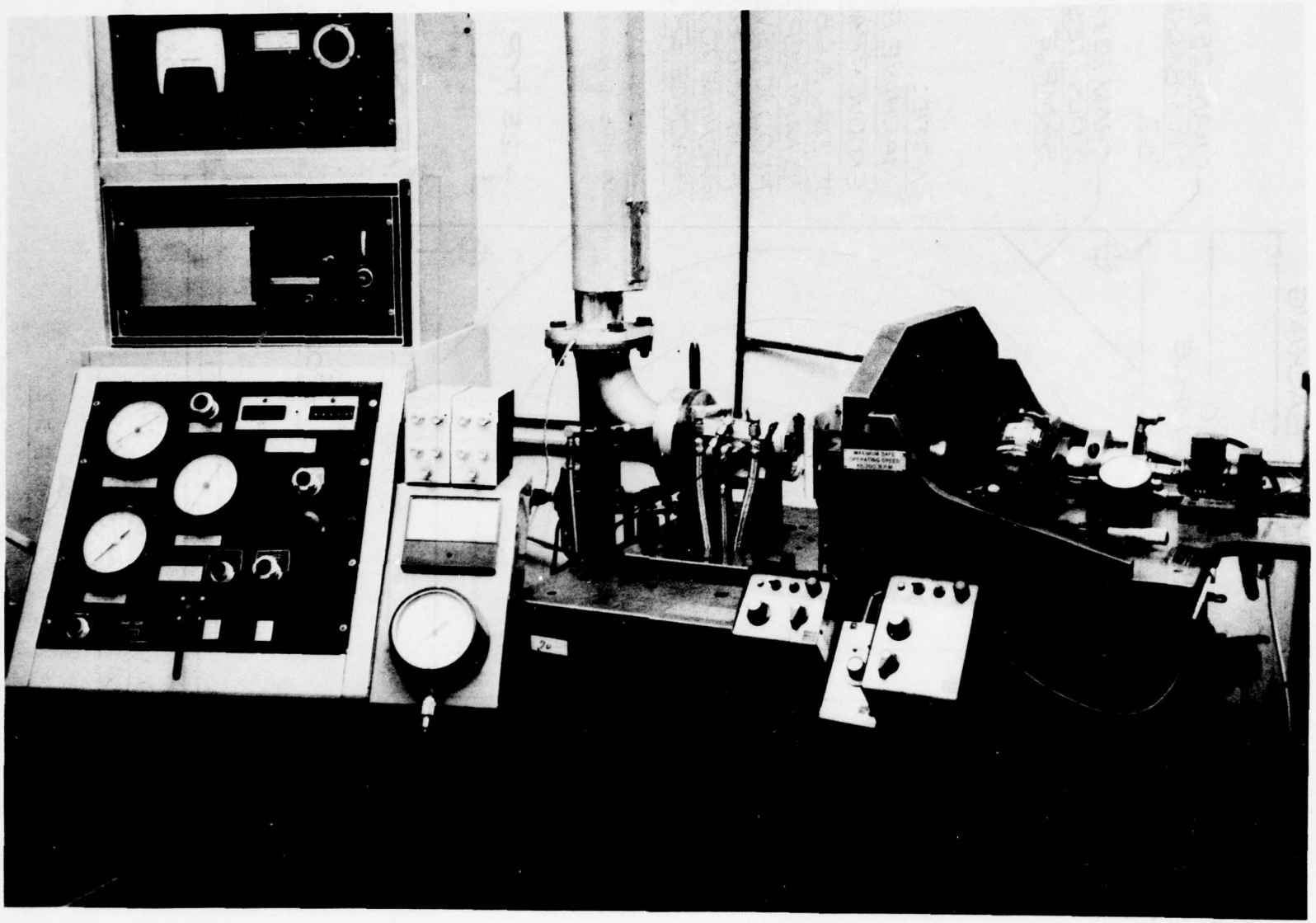

FIGURE D-2 - BRUNSWICK HIGH SPEED RUB RIG - 360° RUB CONFIGURATION
(Disc with one knife edge shown with furnace and shield removed)

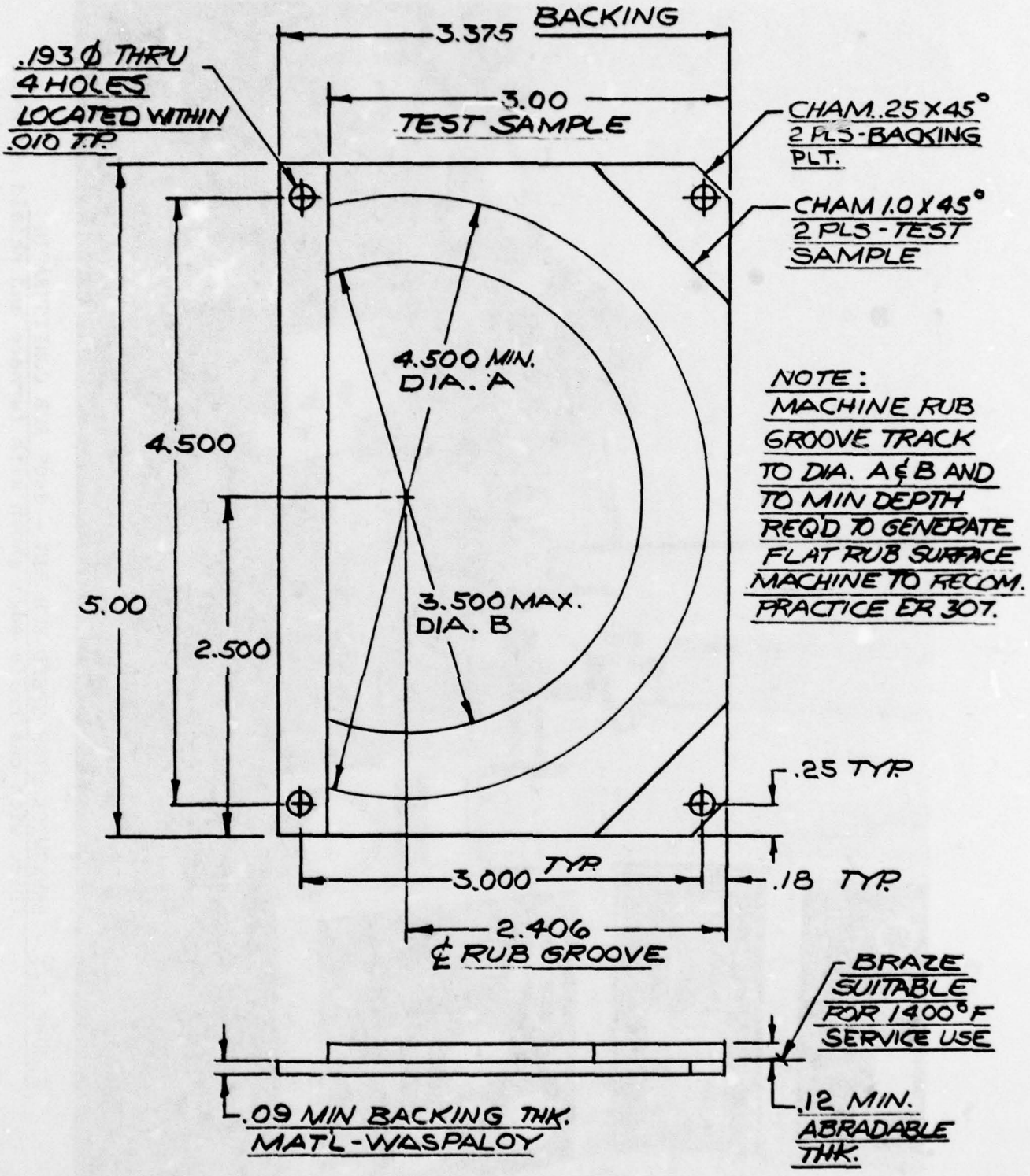

FIGURE D-3

RUB TEST SAMPLE

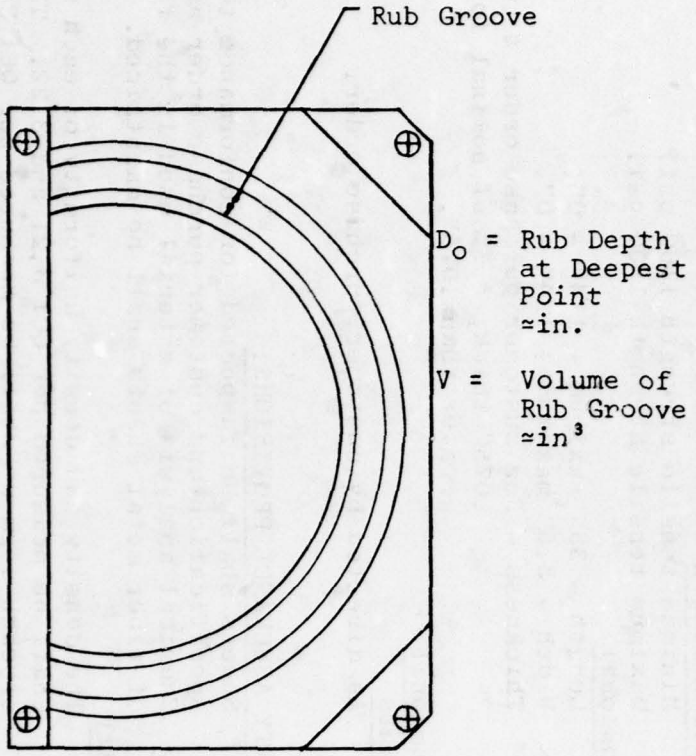

(a)

Rub groove extends beyond the edge of test sample.

$V = 1.8719\ D_o - .026137$

D_o = Rub Depth at Deepest Point ≈in.

V = Volume of Rub Groove ≈in^3

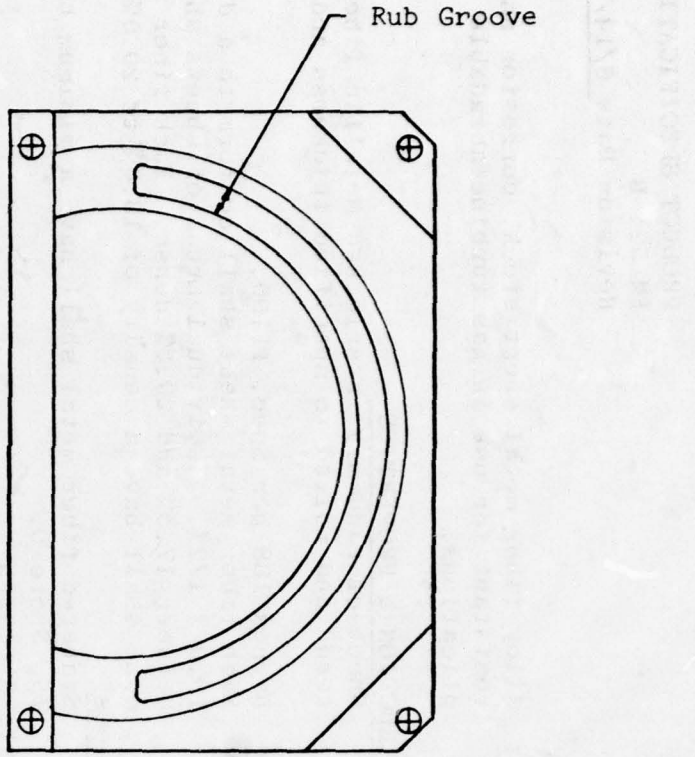

(b)

Rub groove ends before the edge of test sample.

$$V = 1.03125\left[(D_o-.03)\ \cos^{-1}\left(1-\frac{100}{3}\ D_o\right) + .03\sqrt{1-\left(1-\frac{100}{3}\ D_o\right)^2}\right]$$

FIGURE D-4

CALCULATION OF RUB GROOVE VOLUME

APPENDIX F

PRODUCT SPECIFICATION
FM 521 B
Revision Date 6/14/76

1.0 FORM: Alloy fiber metal sheet stock, corrosion and heat resistant for use in gas turbine abradable seal applications.

2.0 CONSTRUCTION & PROPERTIES:

Sheet of randomly interlocked metallic fibers, sintered and rolled to specified thickness and density.

Fiber — Haynes 188 per Spec. FF100.

*Density — Each fiber metal sheet shall conform to a density of 19.0 ± 1/2%. Individual areas of sheets shall be between 17.5% and 20.5% dense. Each fiber metal segment shall have a density of 18.0% to 20.0%.

Hardness

Sintered fiber metal shall have a minimum hardness of 75, Shore D.

Tensile Strength

Minimum tensile strength 1100 psi.
Maximum tensile strength 1900 psi.

Dimensional

Length - 33" maximum + 1/4" - 0".
Width - 3.5" maximum + 1/4" - 0".
Thickness - Per customer purchase order ± .005" to .075" thick, ± 7% of nominal for thickness greater than .075".

Dimensional Segments

As directed by customer purchase order.

3.0 QUALITY ASSURANCE PROVISIONS:

Sheets shall be inspected for conformance to this specification and customer purchase order as follows:

Alloy — Chemical analysis of material used in the fabrication of fiber metal sheets shall be maintained.

Density

The density and density uniformity of each sheet shall be measured per QCI 3.21 and 3.22. The density of each segment shall be measured per QCI 3.23.

Tensile Strength and Hardness

Tensile and hardness tests shall be conducted on 25% of the sheets from each sintered batch per QCI 3.2 and

APPENDIX E

3.24. If any single physical property does not meet specification requirements, all sheets in the batch will be tested.

Identification

Each sheet shall be identified with a serial and FM spec. number. Each segment will be identified as dire by the customer purchase order.

Visual

All sheets shall be visually inspected uniformity of appearance and condition.

D H Ingraham
QUALITY ASSURANCE

APPENDIX E

PRODUCT SPECIFICATION
BRUNSLLOY 537 FIBER METAL

DATE 6/24/77

REVISED _____

1.0 FORM: Alloy fiber metal sheet stock, corrosion and heat resistant for use in high temperature abradable seal applications.

2.0 CONSTRUCTION & PROPERTIES:
Sheet of randomly interlocked metallic fibers, sintered and rolled to specified thickness and density.

Fiber — FeNiCrAlY (Brunswick Alloy #5) per attached chemistry Type Al3.

Density — Each fiber metal sheet shall conform to a density of 20.5 ±.5%. Individual areas of sheets shall be between 19.0 and 22.0% dense. Each fiber metal segment shall conform to a density of 19.0% to 22.0%.

Tensile Strength
Minimum tensile strength 1100 psi
Maximum tensile strength 1900 psi

Hardness — Fiber metal sheets shall conform to the following hardness, Rockwell 5Z (5 Kg load with a 3/4" dia. ball).

Minimum - 78
Maximum - 88

Dimensional Sheets

Length	11.5" maximum + 1/2" -0
Width	3.5" maximum + 1/4" -0"
Thickness	per customer purchase order, ±.005" to .075" thick, 7% of nominal for thickness greather than .075".

Dimensional Segments
As directed by customer purchase order.

3.0 QUALITY ASSURANCE PROVISIONS:
Sheets shall be inspected for conformance to this specification and customer purchase order as follows:

Alloy — Chemical analysis of material used in the fabrication of fiber metal sheets shall be maintained.

Density — The density and density uniformity of each sheet shall be measured per QCI 3.1 and 3.39. The density of each segment shall be measured per QCI 3.21.

APPENDIX E

PRODUCT SPECIFICATION
BRUNSLLOY 537 FIBER METAL

Tensile Strength and Hardness

Tensile strength and hardness tests shall be conducted on 25% of the sheets from each sintered batch per QCI 3.2. If any single physical property does not meet specification requirements, all sheets in the batch will be tested.

Identification

Each sheet shall be identified with a serial and spec. number. Each segment will be identified as directed by customer purchase order.

Visual — All sheets shall be visually inspected for uniformity of appearance and condition.

4.0 CHEMICAL COMPOSITION:

All sintered fiber metal sheets shall conform to the following chemical analysis:

	Min.	Max.
Carbon	-	0.04
Manganese	-	0.50
Silicon	-	0.10
Phosphorus	-	0.015
Sulfur	-	0.015
Boron	-	0.003
Chromium	18.0	19.0
Aluminum	8.50	9.25
Yttrium	0.01	0.03
Iron	Bal.	
Nickel	24.0	26.0
Cobalt		0.50

R V Adams
Quality Assurance

*U.S.Government Printing Office: 1979 — 657-002/879